

Multitargeting in cardioprotection: An example of biaromatic compounds

Grigory V. Mokrov 

FSBI "Zakusov Institute of Pharmacology",
Moscow, Russia

Correspondence

Grigory V. Mokrov, FSBI "Zakusov Institute of
Pharmacology", Baltiyskaya 8, Moscow
125315, Russia.
Email: g.mokrov@gmail.com

Funding information

State task of the Zakusov Research Institute
of Pharmacology for 2022–2024,
Grant/Award Number: FGFG-2022-0005

Abstract

A multitarget drug design approach is actively developing in modern medicinal chemistry and pharmacology, especially with regard to multifactorial diseases such as cardiovascular diseases, cancer, and neurodegenerative diseases. A detailed study of many well-known drugs developed within the single-target approach also often reveals additional mechanisms of their real pharmacological action. One of the multitarget drug design approaches can be the identification of the basic pharmacophore models corresponding to a wide range of the required target ligands. Among such models in the group of cardioprotectors is the linked biaromatic system. This review develops the concept of a "basic pharmacophore" using the biaromatic pharmacophore of cardioprotectors as an example. It presents an analysis of possible biological targets for compounds corresponding to the biaromatic pharmacophore and an analysis of the spectrum of biological targets for the five most known and most studied cardioprotective drugs corresponding to this model, and their involvement in the biological effects of these drugs.

KEYWORDS

cardioprotectors, linked biaromatic compounds, multitarget drugs, network pharmacology

Abbreviations: $[Ca^{2+}]_i$, intracellular calcium; B_{max} , total density of receptors in a sample of tissue; C_{max} , the maximum plasma concentration of a drug; $I_{Ca,L}$, L-type calcium current; $I_{Ca,T}$, T-type calcium current; I_{Ca} , calcium current; I_f , "funny" current, electric current in the heart that flows through the HCN channel; I_h , retinal current; I_K , delayed rectifier potassium current; I_{KAcH} , the cardiac acetylcholine activated inwardly rectifying potassium current; I_{Kr} , rapidly activating component of the delayed rectifier potassium current; I_{Ks} , slowly activating component of the delayed rectifier potassium current; I_{Kur} , ultra-rapid delayed rectifier potassium currents; $I_{Na,L}$, late sodium current; I_{Na} , sodium current; I_{Na-Ca} , inward sodium-calcium exchange current; I_{to} , transient outward potassium current; K_d , dissociation constant; K_i , inhibition constant; T_{max} , time of peak plasma concentration; 5-HT_x, serotonin receptors subtype x; AF, atrial fibrillation; AP, action potential; APD, action potential duration; AR, adrenoceptor; ATX-2, sea anemone toxin; AUC, area under the pharmacokinetic curve; AVN, atrioventricular node; cAMP, cyclic adenosine monophosphate; Cavx.y, voltage-gated calcium channel isoform x.y; CHF, chronic heart failure; CHO, Chinese hamster ovary; CNS, central nervous system; CPVT, catecholaminergic polymorphic ventricular tachycardia; CVD, cardiovascular diseases; D_x, dopamine receptor subtype x; DAD, delayed afterdepolarization; EAD, early afterdepolarization; EC₅₀, the half maximal effective concentration; EMA, European Medicines Agency; eNOS, endothelial nitric oxide synthase; EPC, endothelial progenitor cells; ERP, effective refractory period; FDA, Food and Drug Administration; GABA_A, γ -aminobutyric acid receptor type A; H_x, histamine receptors subtype x; HCN, hyperpolarization-activated cyclic nucleotide-gated channel; HEK293, human embryonic kidney 293 cells; hERG, human ether-a-go-go-related gene that codes Kv11.1 ion channel; HF, heart failure; HMG-CoA, 3-hydroxy-3-methylglutaryl coenzyme A; HR, heart rate; IC₅₀, the half maximal inhibitory concentration; IHC, inner hair cells; IWB, IonWorks Barracuda automated patch clamp platform; IWW, IonWorks Quattro automated patch clamp platform; K_{ATP}, ATP-sensitive potassium channel; K2P, two-pore-domain potassium channel; Kirx.y, inward-rectifier potassium ion channel isoform x.y; Kv_x.y, voltage-gated potassium channel isoform x.y; LQT, long QT syndrome; LQT1, long QT syndrome with mutation of *KCNQ1* gene; LQT2, long QT syndrome with mutation of *KCNH2* gene; LQT3, long QT syndrome with mutation of *SCN5A* gene; LV, left ventricular; M_x, muscarinic receptors subtype x; MAP, mean arterial pressure; minK, minimal potassium channel subunit encoded by *KCNE1* gene; NADH, reduced nicotinamide adenine dinucleotide; Nav1.x, voltage-gated sodium channel isoform 1.x; NMDA, N-methyl-D-aspartate; NOS, nitric oxide synthase; PIP2, phospholipid phosphatidylinositol 4,5-bisphosphate; PKA, protein kinase A; PMC, paramyotonia congenital; PRP, platelet-rich plasma; QNB, quinuclidinyl benzilate; RyR_x, ryanodine receptor type x; SAN, sinoatrial node; SERT, serotonin transporter; SOICR, suppresses store overload-induced Ca²⁺ release; SR, sarcoplasmic reticulum; TASK-1, two-pore domain K⁺ channel (K2P3.1); TdP, torsade de Pointes; TEM, effector memory T-cells; TSP0, translocator protein; VM, ventricular myocytes; VT, ventricular tachycardia; WHO, World Health Organization; WT, wild type.

1 | INTRODUCTION

The single-target approach dominated in drug design and medicinal chemistry in the 20th century.^[1] Since the beginning of the 21st century, there was the intensive development of a “multitarget” approach in drug-design, primarily aimed for the treatment of such multifactorial diseases as cardiovascular diseases (CVD), cancer, and neurodegenerative diseases with multiple signaling pathways in their pathogenesis.^[2]

The dynamics of using “multitargeting” in drug design is clearly illustrated by the diagrams of search results in pubmed.org. At the end of 2022s for the query “multitarget,” this search engine returns 10,459 results, and almost half of them (4302 results) are from 2020 to 2022s. A similar dynamic is observed when searching for the closely related query “network pharmacology,” which is an emerging discipline useful in drug discovery, which combines genomic technologies and system biology through computational biological tool. Of the 47,647 total search results for “network pharmacology,” 2020–2022 accounts for over 30% (14,875) of results.

Undoubtedly, the active development of the “multitarget” approach in modern research is due to the explosive progress in information technologies, which made it possible to process huge arrays of data and predict various biochemical interactions in silico with high accuracy. Among the resources of this type are continuously updated databases such as ChEMBL (<https://www.ebi.ac.uk/chembl/>), BindingDB (<https://www.bindingdb.org/rwd/bind/index.jsp>), ZINC (<https://zinc.docking.org/>), and similar; structural databases PDB (<https://www.rcsb.org/>) and Alpha Fold DB (<https://alphafold.ebi.ac.uk/>). There are numerous docking programs that allow calculation of ligand-protein interactions, for example: Glide Schrödinger (<https://www.schrodinger.com/>) and AutoDock (<https://autodock.scripps.edu/>); molecular target prediction programs such as SwissTarget (<http://www.swisstargetprediction.ch>), SEA (<http://sea.bkslab.org>), and PASS (<http://www.way2drug.com/PASSonline>).

In addition to the “multitarget approach to the design of new drugs,” numerous studies are being carried out to identify the spectrum of biological targets of well known drugs used in clinical practice. For the majority of such substances, many of which were created as part of a single-target approach or were discovered by chance, an extensive set of biotargets is revealed. Thus, the biological effect of such drugs is an integral effect of interactions with all these targets.

According to the novel network pharmacology paradigm the selective compounds, compared with multitarget drugs, may exhibit lower than desired clinical efficacy.^[3] Moreover, in modern works one can often read the phrase that “selective drugs do not exist.”^[4] So the “selective” drugs can in practice be only “understudied” that means that not enough potential targets have yet been assessed. Meanwhile, the most complete information about the spectrum of biological targets of drugs seems to be extremely important, since the integral effect of a molecule on several targets can radically differ from that when exposed to only one of them.

Despite the obvious advantages of multitarget drugs, their development is a serious challenge and often faces a number of problems. One of the main ones is the choice of the right combination of targets for the selected disease. This requires a deep understanding of the associations between targets and diseases, as well as the relationships between pathways, targets, drugs, and adverse events. Additionally, the selection process should consider whether modulating the chosen targets would result in additive or synergistic effects. Additive effects occur when the targets are part of the same pathway, while synergism is only achievable if the selected targets are located on functionally complementary pathways. In both cases, lower doses can produce the desired effect, potentially leading to a better safety profile compared to single-target drugs. The rational drug design is also not an easy task since it requires combining the several different scaffolds into a single chemical entity starting from compounds with the desired affinity towards the selected targets. In this case, the most commonly used approach is the imposition of pharmacophore elements or their conjugation with cleavable or noncleavable linkers. Despite numerous challenges in multitarget drug design, a number of successful implementations prove that these efforts are worth it.^[5,6]

2 | CVD AND MULTITARGETING

According to the World Health Organization (WHO), CVD are the leading cause of death worldwide. In 2019, about 17.9 million people died from CVD, primarily from heart attacks and strokes, which is 32% of the total number of deaths. Of the 17 million premature deaths from noncommunicable diseases in 2019 in people under 70, 38% were due to CVD.^[7,8]

The COVID-19 pandemic has made a significant additional contribution in prevalence and severity of CVD. Patients with concomitant CVD belong to a more vulnerable cohort characterized by a severe course of COVID-19 and high hospital mortality. There is evidence of de novo formation of a COVID-19-induced cardiovascular pathology, called acute COVID-19-associated cardiovascular syndrome, expressed in various types of arrhythmias, myocarditis, acute cardiac injuries and thrombotic disorders.^[9]

There is currently a growing conviction among researchers that effective and safe cardioprotective agents should have a multitarget mechanism of action.^[10–13] This is fully consistent with the “multitarget approach to cardioprotection” being developed in the modern cardiology community.^[10,14,15]

The need to consider a significant number of biotargets in the design of potential cardioprotective agents is due to the multifactorial nature of cardiovascular disorders and the involvement of a large number of systems and mechanisms in their pathogenesis. For example, angiotensin-converting enzyme inhibitors, α - and β -adrenoreceptor (AR) inhibitors, angiotensin II receptor antagonists, calcium channel blockers, diuretics, direct renin inhibitors or glyceryltrinitrates may be involved in the treatment of hypertension.^[16] A variety of ion channels and receptor systems and

transcription factors are involved in the pathogenesis of various types of arrhythmias.^[17,18] A good example of using the multitargeting analysis of drugs in relation to the cardiovascular system is the CiPA (Comprehensive in vitro Proarrhythmia Assay) approach created for proarrhythmia risk prediction. This approach postulates the considering a comprehensive assessment of the interaction of potential drugs with an extensive set of cardiac ion channels to assess its safety and ability to initiate arrhythmias.^[19,20] Neuropsychiatric disorders may be a special factor in the development of CVD, which makes an additional contribution to the range of biological targets that can be considered in the drug design of such comorbid diseases.^[21,22] For example, anxiety is one of the triggers for atrial fibrillation (AF).^[23] The link between depression and CVD mortality also has been established.^[24]

The main issue that arises in the design or analysis of the drugs with a multitarget mechanism of action is the ratio of single mechanisms, in particular the ratio of the affinity of the drug molecule to various biotargets. This raises the following questions:

- (1) How do the affinity parameters of a molecule for various biotargets correlate? Is the concept of "selectivity" universal or is it rather relative?
- (2) How to determine the pharmacological significance of any target based on the data of the molecule affinity and the pharmacokinetic parameters of the drug?

In response to the first question, literature data indicate that the "selectivity" of compounds with respect to various biotargets is a rather relative concept. This is evidenced by the following facts:

1. Affinities determined in vitro in different experiments using different displacing ligands can differ by up to 3–4 orders of magnitude. For example, according to the Guide to Pharmacology database,^[25] the affinity of the hERG-blocker dofetilide for hERG (human ether-a-go-go-related gene that codes Kv11.1 ion channel) varies from 4 to 44.000 nM, and the affinity of haloperidol for D₂ receptors varies from 0.12 to 6400 nM. Such a difference can be explained by the difference in the methods used to determine the affinity (manual or automated patch clamp, radioligand binding method, fluorescence polarization assay, etc.), the difference in tissues or cell cultures used for analysis.
2. In addition to the values of the affinity of a molecule for a biotarget, the density of this biotarget (B_{\max}) is also important. For example, it was found that adenine sulfate shows its cardioprotective effects by significant increasing of muscarinic M₂-receptors B_{\max} value in the damaged heart tissues.^[26]
3. Despite remarkable in vitro affinity for a biological target, a drug is often unable to exert pharmacological and therapeutic effects in vivo. Often this can be explained by the fact that a drug does not bind its biological target long enough. In particular, the time a drug spends in contact with its biological target (so-called residence time) is now considered a key parameter for optimization because there is some evidence that it can predict drug efficacy in vivo and

thus demonstrate the pharmacological significance of the biotarget.^[27–29]

4. Some biotargets are species-specific. For example, it was found that binding of translocator protein (TSPO) ligands with TSPO occurs with different efficiencies. Studies have divided the human population into three types: high-affinity binders (with high affinity for TSPO), low-affinity binders (with low affinity for TSPO) and mixed-affinity binders. The differences in the TSPO affinity of its ligands for high-affinity binders and low-affinity binders turned out to be very significant up to two orders of magnitude.^[30]
5. The affinity of a compound for a biotarget can correlate very differently with its pharmacokinetic characteristics, including metabolism. The latter may be of decisive importance in the pharmacological significance of the target biotarget.^[31,32]

Here we should also explain the very concept of affinity, its types and relationships since different studies use various binding parameters. One of the most common parameters describing affinity is the inhibition constant (K_i) or dissociation constant (K_d). K_d is a type of equilibrium constant that measures the dissociation of any complex into components. K_i is a term used to describe the binding affinity between an inhibitor and its corresponding biotarget. The difference between K_d and K_i is that K_d is a more general term for various dissociation processes, whilst K_i is more narrowly used to indicate the dissociation equilibrium constant of the protein-inhibitor complex. Another common affinity parameter is the half maximal inhibitory concentration (IC_{50}). IC_{50} quantifies the concentration of inhibitor necessary to halve the reaction rate of a protein-provided process observed under specified assay conditions. While K_i is a constant value for a given compound with an biotarget, an IC_{50} is a relative value, whose magnitude depends upon the concentration of substrate used in the assay. The relationship between IC_{50} and K_i is calculated by the Cheng-Prusoff equation.^[33] For competitive inhibitors, which inhibit the protein-catalyzed reaction by binding to free protein it looks as follows:

$$IC_{50} = K_i \left(1 + \frac{[S]}{K_M} \right).$$

For uncompetitive inhibitors, which bind only to the protein-substrate complex, Cheng-Prusoff equation looks as follows:

$$IC_{50} = K_i \left(1 + \frac{K_M}{[S]} \right).$$

In these equations $[S]$ is the substrate concentration used in the assay, and K_M is the Michaelis constant of the substrate. Thus, to transform IC_{50} to K_i or vice versa, additional parameters are required, which are usually not available in publications. Nevertheless, in a large number of works in which both values are given, they differ insignificantly, within the same order of magnitude. Thus, in this paper, we make the assumption that $IC_{50} = K_i$.

The EC_{50} parameter is the drug concentration that produces a half-maximal response. This parameter is very similar to IC_{50} . The

EC_{50}/IC_{50} ratio is most often around 1.^[34] All of the listed parameters are often given in the form of their negative decimal logarithms (pK_i , pK_d , pIC_{50} , and pEC_{50}), which makes them easier to represent and compare.

To answer the second question regarding the clinical significance of different affinity values for biotargets, we compared the values of pharmacokinetic parameter C_{max} (the maximum plasma concentration) for various drugs with different activities and their correlations with the affinity for their main biotargets (Table 1). These data were collected from pubmed publications and clinical trial reports. It has been established that the values of pC_{max} and pK_i for drugs can differ by more than 2, and pC_{max} can be either greater or less than pK_i . Of particular interest are those cases where pK_i is less than pC_{max} . The presence of such examples indicates that even those biotargets for which the drug affinity is at least two orders of magnitude lower than its plasma concentration are of clinical significance.

One explanation for the fact that in many cases, the IC_{50} values of compounds against different biological targets *in vitro* are greater than their therapeutic, is that the local high levels of these chemicals may be achieved *in vivo*, due to their high solubility in the lipids and tissue accumulations, to enable their action. On the other hand, the lipophilic compounds may change membrane structure by

partitioning through the lipid bilayers, exerting for example a higher impact on membrane channels.^[35–38]

One of the approaches to the drug design of multitarget compounds and the prediction of the biotarget spectrum of molecules can be the identification of basic pharmacophore models.^[39,40] Previously, we published a review that describes a large set of different cardioprotective agents with different mechanisms of action, corresponding to a single pharmacophore model.^[41] This model contains two aromatic cycles (marked violet) connected by a linker (indicated by green) with the length of about 5–15 bonds and with at least one heteroatom in it (Figure 1).

There are cardioprotectors of all main mechanisms of action among the compounds corresponding to this pharmacophore model: hyperpolarization-activated cyclic nucleotide-gated (HCN) channel blockers, sodium and potassium channel blockers and activators, β -adrenergic receptor (β -AR) inhibitors, calcium channel blockers, ryanodine receptor (RyR) inhibitors, and a number of others. Many of these compounds, as expected, had a multitarget mechanism of action, having an affinity for several of the listed biotargets at once.

Based on the literature analysis, we hypothesized the universality of the identified biaromatic pharmacophore for compounds with cardioprotective activity and the possibility of using it as a “basic pharmacophore” for designing new potential cardioprotective agents.

TABLE 1 Correlation of the pharmacokinetic parameter C_{max} of various drugs with their affinity for the main biotargets.

Drug	Action	pK_i	Main target	Dose (mg)	pC_{max}	$pK_i - pC_{max}$
Atorvastatin	Lipid-lowering medication	8.09	3-Hydroxy-3-methylglutaryl coenzyme A (HMG-CoA) reductase inhibitor	40	7.67	0.42
Cediranib	Anticancer agent	9.30	Tyrosine kinase inhibitor of vascular endothelial growth factor receptors	30	7.03	2.27
CP-778875	Drug for treatment of atherosclerosis and dyslipidaemia	8.15	Peroxisome proliferator-activated receptor α agonist	0.3	7.50	0.66
Diazepam	Anxiolytic	8.31	γ -aminobutyric acid receptor type A (GABA _A) positive allosteric modulator	10	6.28	2.03
Digoxin	Cardiotonic	6.60	Na ⁺ , K ⁺ -ATPase inhibitor	0.2	8.614	-2.01
Diltiazem	Antiarrhythmic	6.95	Cav1.2 blocker	120	6.44	0.51
Dofetilide	Antiarrhythmic	7.52	hERG blocker	1.5	8.28	-0.76
Everolimus	Immunosuppressant and anticancer	8.70	mTOR inhibitor	10	7.20	1.50
Flecainide	Antiarrhythmic	5.22	Nav1.5 blocker	100	6.39	-1.17
Ivabradine	Antianginal	5.67	HCN-channels blocker	10	7.28	-1.71
Linagliptin	Antidiabetic	9.11	DPP ₄ inhibitor	5	8.05	1.06
Mibefradil	Antianginal	5.57	T-type Ca ²⁺ channel blocker	200	5.54	0.03
Nifedipine	Hipotensive	6.70	L-type Ca ²⁺ channel blocker	10	6.46	0.24
Quinidine	Antiarrhythmic	4.41	Nav1.5 blocker	300	4.75	-0.34
Simvastatin	Lipid-lowering medication	7.95	HMG-CoA reductase inhibitor	40	7.88	0.07
Tiagabine	Anticonvulsant	6.19	GABA transporter type 1 inhibitor	8	6.40	-0.20

Note: Data collected from Pubmed publications and clinical trial reports.

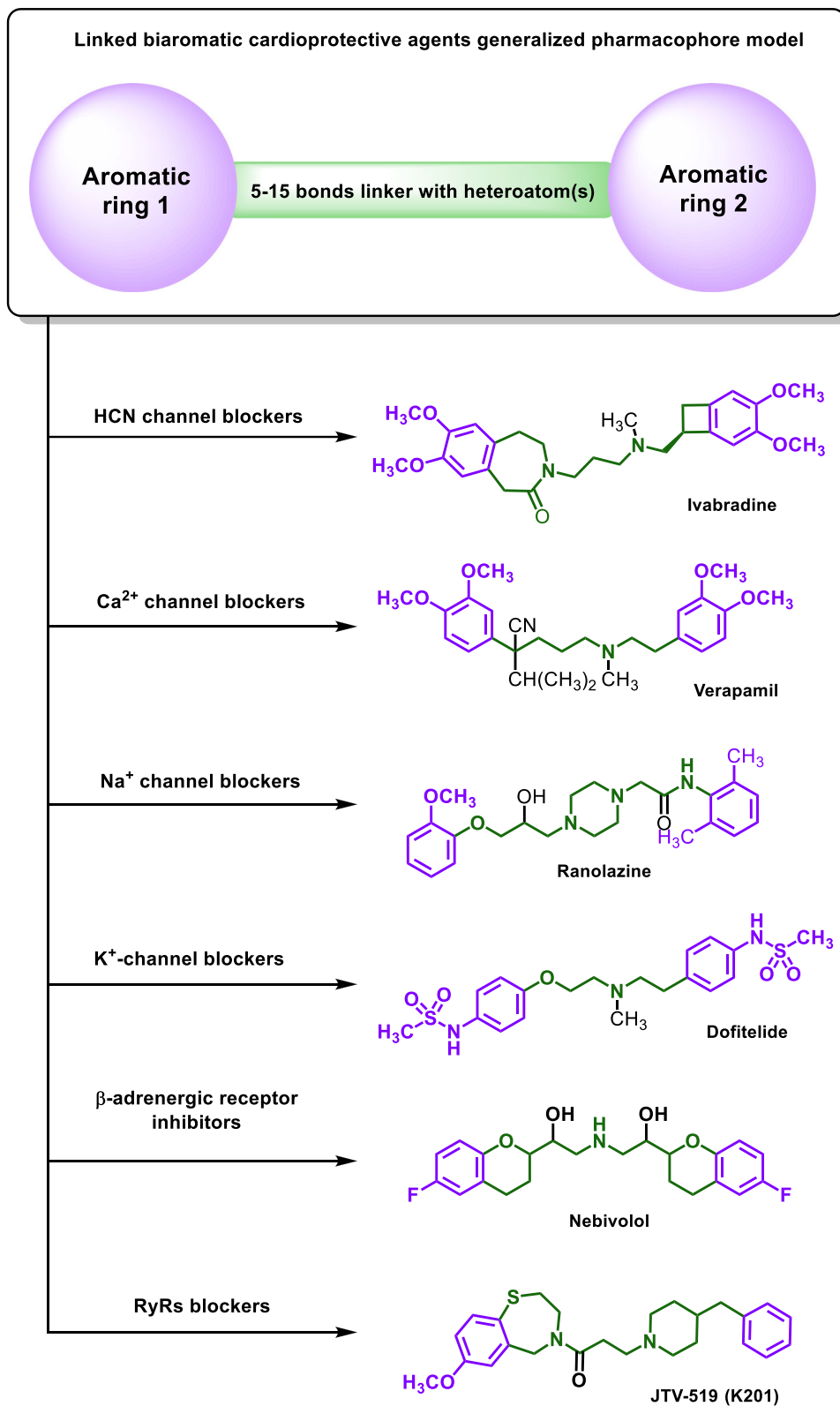


FIGURE 1 Generalized pharmacophore model of linked biaromatic compounds with cardioprotective activity. Examples of compounds with cardioprotective activity with different mechanisms of action are shown.

This review is an attempt to develop the concept of "basic pharmacophore" and additionally confirm the absence of "single-targeted" drugs using the biaromatic pharmacophore as an example. The objectives of this review are:

1. Analysis of possible biological targets for compounds corresponding to the biaromatic pharmacophore.
2. Analysis of the spectrum of biological targets for the five most known and most studied cardioprotective drugs corresponding to the biaromatic pharmacophore, and their involvement in the biological effects of these drugs. Carvedilol, ivabradine, nebivolol, ranolazine and verapamil were chosen as these drugs.

3 | THE TARGETS FOR LINKED BIAROMATIC COMPOUNDS

To analyze possible biological targets of compounds that correspond to the biaromatic pharmacophore model presented in Figure 1, we have selected examples of such structures with different mechanisms of action which are presented in the Table 2. Among these targets are a number of ion channels: HCN-channels (HCN1–HCN4); sodium channels (Nav1.1–Nav1.8); potassium channels (Kv1.3–Kv1.8; Kv2.1; Kv3.1; Kv4.3; Kv7.1; Kv10.1; Kv11.1; Kir2.1; Kir2.3; K_{ATP} ; K2P3.1); calcium channels (Cav1.1–Cav1.3; Cav2.1, Cav2.2; Cav3.1, Cav3.2; RyR2); α -ARs (α 1A– α 1D; α 2A– α 2C); β -ARs (β 1– β 3); serotonin receptors (5-HT₁–5-HT₇); serotonin transporter (SERT); muscarinic receptors (M_1 – M_3); dopamine receptors (D_1 – D_3); histamine receptors (H_1 , H_2); σ_1 -receptor. Table 2 also presents the localization of listed biotargets and the possible involvement of their ligands in therapeutic effects in the cardiovascular system and biological effects of these ligands. Examples of molecules are shown in the coloring corresponding to Figure 1: aromatic substituents are highlighted in violet, and the linker that binds them is in green.

4 | THE ROLE OF THE LINKED BIAROMATIC COMPOUNDS MAIN TARGETS IN THE CARDIOVASCULAR SYSTEM

4.1 | Calcium channels

Calcium channels are important regulators of the electrical and contractile activity of the cardiovascular system. They play a crucial role in the depolarization and contraction of cardiac myocytes, as well as the release of neurotransmitters from sympathetic nerve terminals. There are several types of calcium channels expressed in the heart, each with distinct functions.^[123]

L-type Ca^{2+} channels, including the family of voltage-gated Cav1.1–Cav1.4 calcium channels, are predominantly expressed in cardiac myocytes and are responsible for the influx of Ca^{2+} ions that trigger muscle contraction. These channels are activated by

membrane depolarization, which occurs during the AP of the cardiac myocyte. In addition to their role in contractility, L-type Ca^{2+} channels also contribute to the regulation of the HR by modulating the APD and AP frequency. Dysfunction of L-type Ca^{2+} channels has been linked to various cardiovascular disorders, including arrhythmias and HF.^[124] For example, mutations in the CACNA1C gene, which encodes for the α -1C subunit of the L-type Ca^{2+} channel, have been associated with long QT syndrome (LQT), which is characterized by a prolonged QT interval on the electrocardiogram and an increased risk of ventricular arrhythmias and sudden cardiac death, and the similar Brugada syndrome.^[125]

T-type Ca^{2+} channels, including the family of Cav3.1–Cav3.3 channels, are expressed in the SAN and the AVN and are involved in the pacemaker activity of the heart. These channels are activated at more negative membrane potentials than L-type channels and contribute to the spontaneous depolarization of the cardiac myocytes in these specialized regions of the heart. Inactivation of T-type Ca^{2+} channels leads to bradycardia and atrioventricular conduction delay, which underlines the importance of this channel in maintaining a normal heart rhythm.^[126]

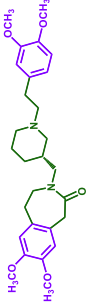
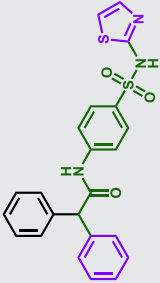
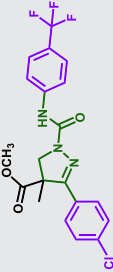
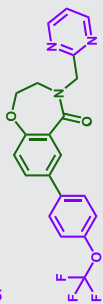
RyRs are a family of ion channels that play a critical role in Ca^{2+} signaling in the cardiovascular system. These channels are found primarily in the sarcoplasmic reticulum (SR) of cardiac and skeletal muscle cells, where they mediate the release of Ca^{2+} ions from the SR into the cytoplasm in response to an AP. This Ca^{2+} release triggers muscle contraction and plays an important role in the regulation of cardiac function.^[127] There are three isoforms of RyRs, with RyR2 being the predominant isoform in the heart. Mutations in the RYR2 gene have been linked to various inherited cardiac disorders, including catecholaminergic polymorphic ventricular tachycardia (CPVT) and arrhythmogenic right ventricular dysplasia.^[128] In these disorders, abnormal Ca^{2+} release from RyRs leads to ventricular arrhythmias, which can cause sudden cardiac death. Pharmacological agents that modulate RyR activity have been investigated as potential therapies for specified CVD.^[129]

4.2 | Sodium channels

Voltage-gated sodium channels (Nav) are essential in the initiation and propagation of the AP in the cardiac tissues. These channels are responsible for the rapid influx of Na^+ ions into the cell during depolarization, which triggers the opening of Ca^{2+} channels and subsequent muscle contraction. In cardiac myocytes, sodium channels are predominantly composed of the voltage-gated Nav1.5 isoform, which is responsible for the AP upstroke. Nav1.5 is preferentially expressed in the atria, Purkinje fibers, and ventricles.^[130,131] Mutations in the SCN5A gene that encodes for Nav1.5 have been linked to various inherited cardiac disorders, including LQT and Brugada syndrome.^[132]

Pharmacological agents that modulate sodium channel activity have been investigated as potential therapies for these disorders. For example, the drug mexiletine, a class I antiarrhythmic agent, can block

TABLE 2 Examples of biaromatic structures with affinities to different biotargets, their effects; localization of biotargets and the possible involvement of their ligands in therapeutic effects in the cardiovascular system.

Bio-target	Sytype	Type of action	Localization	Therapeutic effect in the cardiovascular system	Name of example	Structure of biaromatic compound	K _i /IC ₅₀	Effect	Reference
Hyperpolarization-activated cyclic nucleotide-gated channel (HCN)	HCN1	Blocking	Central nervous system (CNS); dorsal root ganglion; and heart	Reducing HR, action potential duration (APD) prolongation.	Cilobradine		IC ₅₀ = 1.15 μM IC ₅₀ = 0.9 μM IC ₅₀ = 0.99 μM IC ₅₀ = 0.92 μM	Cilobradine was found to significantly decrease the pacemaker diastolic depolarization rate and the rate of cell firing. Studies also showed a reduction of heart rate (HR), an elongation of diastole, and a decrease in myocardial oxygen demand in animal models.	[42–44]
	Nav1.1	Blocking	CNS, cardiac myocytes	Nav1.1-originated late sodium current (I _{Na,L}) blocking is physiologically relevant to controlling AP shape and duration, as well as to cell Ca ²⁺ dynamics.	ICA-121431		IC ₅₀ = 13 nM	Potential CNS agent	[45, 46]
	Nav1.2	Blocking	Central neurons, peripheral neurons	?			IC ₅₀ = 240 nM		
	Nav1.3	Blocking	Central neurons, peripheral neurons and cardiac myocytes	?			IC ₅₀ = 23 nM		
Nav1.4	Blocking	Skeletal muscle	?		RH 3421		IC ₅₀ = 2.05 μM	Insecticide	[47]
Nav1.5	Blocking	Cardiac myocytes, skeletal muscle, central neurons	Reducing ischemic Na ⁺ loading and preserving cardiac energy status.		Eleclazine		IC ₅₀ = 0.62 μM	Eleclazine demonstrated a 93% reduction in ischemic burden in a rabbit ST segment in vivo at 500 nM, and it completely protected against a Torsade de Pointes (TdP) ventricular arrhythmia model at 2.4 μM.	[48]

(Continues)

TABLE 2 (Continued)

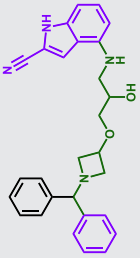
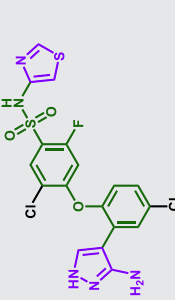
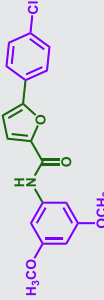
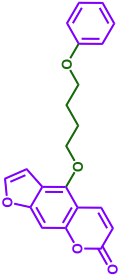
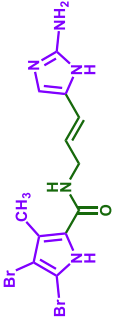
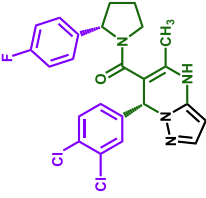
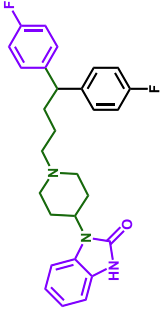
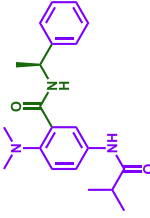
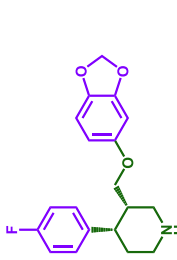

Bio-target	Sybytype	Type of action	Localization	Therapeutic effect in the cardiovascular system	Name of example	Structure of biaromatic compound	K _i /IC ₅₀	Effect	Reference
		Activation		Increasing the APD	BDF 9198		EC ₅₀ = 0.03–0.26 μM	A concentration-dependent increase in action potential duration (APD) at 50% repolarization was observed when BDF 9198 was tested on guinea-pig isolated ventricular muscle strips at a concentration of 10 ⁻⁹ M or higher. In addition, BDF 9198 was found to increase force of contraction in both nonfailing and failing human myocardium in the same way as calcium.	[49, 50]
	Nav1.7	Blocking	Dorsal root ganglia, sympathetic neurons, Schwann cells, and neuroendocrine cells	?	PF-05089771		IC ₅₀ = 11 nM	PF-05089771 reduces coughing by affecting the electrical activity in nerve endings in the airways.	[51]
	Nav1.8	Blocking	Dorsal root ganglia, cardiac myocytes	Reducing late Na ⁺ current and shortening APD.	A-803467		IC ₅₀ = 8 nM	A 803467 at small doses specifically blocks I _{Na,L} and decreases the APD in mouse and rabbit heart cells.	[52, 53]
Potassium channels	Kv1.3	Blocking	lymphocytes, macrophages, fibroblasts, platelets, osteoclasts, microglia, oligodendrocytes, brain, lung, thymus, spleen, lymph nodes, and testis	Kv1.3 is involved in coronary metabolic dilation.	PAP-1		IC ₅₀ = 2 nM	The administration of PAP-1 significantly decreases the multiplication of human effector memory T-cells (TEM) cells and curbs the delayed type hypersensitivity reaction, which is a TEM cell-mediated response, in rats.	[54, 55]

TABLE 2 (Continued)

Bio-target	Sybtpe	Type of action	Localization	Therapeutic effect in the cardiovascular system	Name of example	Structure of biomimetic compound	K _i /IC ₅₀	Effect	Reference
Kv1.4	Blocking	Brain, testis, lung, kidney, colon, heart and adrenal tissue	Kv1.4 contributes to I _{to} , the main contributing current to the repolarizing phase 1 of the cardiac AP.	CHEMBL4208517			IC ₅₀ = 230 nM	-	[56, 57]
Kv1.5	Blocking	Cardiac myocytes	Prolonged atrial AP recovery, increased effective refractory period (ERP), and reduced repolarization reserve.	BMS-394136			IC ₅₀ = 50 nM	At a dose of 3 mg/kg, BMS-394136 increased the duration of the atrial ERP by more than 20% in a rabbit model. Furthermore, due to its selectivity for Kv1.5 over ventricular ion channels, the highest dose of 10 mg/kg had no impact on the ventricular ERP.	[58]
Kv1.8	Blocking	Renal blood vessels, aorta, and heart	Kv1.8 may be involved in regulating the tone of renal vascular smooth muscle and may also participate in the AP.	Pimozide			IC ₅₀ = 300 nM	Pimozide is an antipsychotic drug of the diphenylbutylpiperidine class with multitarget action.	[59]
Kv2.1	Blocking	Brain neurons and heart, β-cells	Control of falling phase of physiological action potentials (AP), cardiac beat and rate synchronicity.	RY-796			IC ₅₀ = 250 nM	Administration of RY796 increased the secretion of somatostatin from human and mouse islets in vitro, as well as from pancreas of wild type and Kv2.1 ^{-/-} mice in situ.	[60, 61]
Kv3.1	Blocking	Brain neurons	?	Paroxetine			IC ₅₀ = 9.4 μM	Paroxetine blocks the open state of Kv3.1 channels.	[62]
Kv4.3	Blocking	Heart muscle, brain	Regulating resting membrane potential and basal tone in vascular smooth muscles.	Dapoxetine			IC ₅₀ = 5.3 μM	Dapoxetine is associated with vasovagal-mediated (neurocardiogenic) syncope.	[63, 64]

(Continues)

TABLE 2 (Continued)

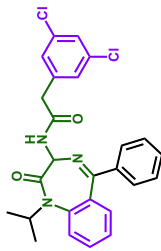
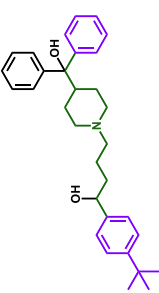
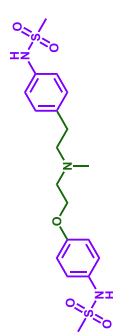
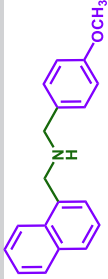
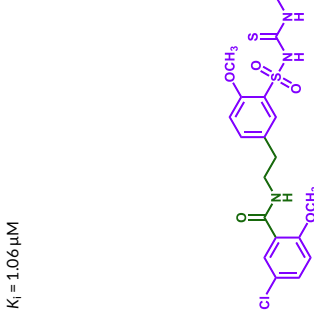
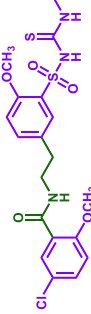
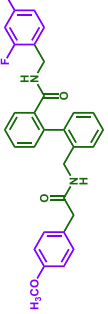
Bio-target	Sybytype	Type of action	Localization	Therapeutic effect in the cardiovascular system	Name of example	Structure of biomimetic compound	K _i /IC ₅₀	Effect	Reference
Kv7.1	Blocking	Epithelia, brain, heart, and inner ear organs	Increase in AP recovery time Increase in refractor period with decreased reentrant tendency.	L-761710			IC ₅₀ = 10 nM	L-761710 increase ventricular refractoriness and increase QTc interval, decreases sinus HR. L-761710 caused a notable prolongation of the atrioventricular nodal (AVN) conduction, marked by a 40.7% stretch in the atrial-to-His interval, and augmented the functional refractory period of the AVN conduction system by 19.9%.	[65]
Kv10.1	Blocking	CNS	?	Terfenadine			pIC ₅₀ = 7.8	Terfenadine is an antihistamine that used for the treatment of allergic conditions. It is also acts as a potassium channel blocker.	[66]
Kv11.1 (hERG)	Blocking	Cardiac myocytes	Increase in AP recovery time. Increase in refractor period with decreased reentrant tendency.	Dofetilide			IC ₅₀ = 7 nM	Dofetilide, which was approved by the Food and Drug Administration (FDA) for the treatment of AF and atrial flutter lasting over one week, was found to increase both the atrial and ventricular ERP in pentobarbitone anesthetized dogs. It has been successfully used off-label for patients with paroxysmal AF, atrial flutter, atrial tachycardia, and ventricular tachycardia (VT).	[67, 68]

TABLE 2 (Continued)

Bio-target	Sybyte	Type of action	Localization	Therapeutic effect in the cardiovascular system	Name of example	Structure of biomimetic compound	K _i /IC ₅₀	Effect	Reference
Kir2.1	Blocking	Heart, endothelial cells, kidney	Control of terminal cardiac repolarization and resting membrane stability.	ML-133			IC ₅₀ = 290 nM	Administration of ML133 induced endothelial progenitor cells (EPC) polarization and enhanced EPC activities such as movement, adhesion and vascularization in a laboratory setting. Implantation of ML133-treated or Kir2.1 diminished EPCs hastened re-endothelialization in a rat arterial injury and blocked neointima formation in vivo.	[69]
Kir2.3	Blocking			Terfenadine	See above		K _i = 1.06 μM	Terfenadine blocked Kir2.3 channels much more effectively than Kir2.1 channels, with an IC ₅₀ of 1.06 μM.	[70]
K _{ATP}	Blocking	Cardiac myocytes, pancreas	Potential decrease in AP recovery time.	HMR1098			K _i = 0.4 μM	HMR1098 decreased the incidence of VT and fibrillation in animal models. It was demonstrate that a selective sarcolemmal K _{ATP} blockade by HMR1098 can induce cardioprotection in Langendorff-perfused rat heart.	[71, 72]
K2P3.1 (TASK-1)	Blocking	Cardiac tissue, pulmonary artery smooth muscle cells	Modulate cardiac conduction, repolarization, and HR.	A1899			IC ₅₀ = 40 nM	A1899 showed antiarrhythmic effects in a pig model.	[73, 74]

(Continues)

TABLE 2 (Continued)

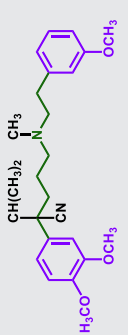
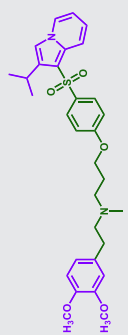
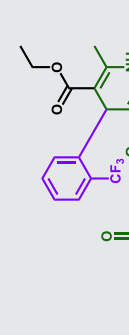
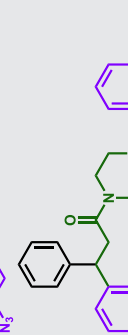
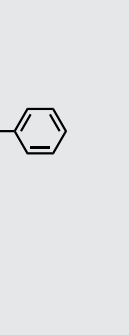
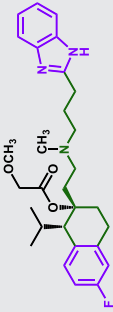
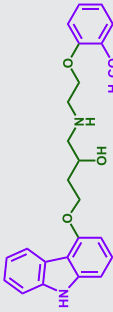
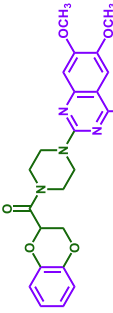
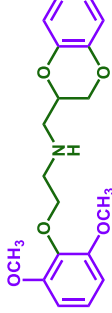
Bio-target	Sybyte	Type of action	Localization	Therapeutic effect in the cardiovascular system	Name of example	Structure of biaromatic compound	K _d /IC ₅₀	Effect	Reference
Calcium channels	Cav1.1	Blocking	Skeletal muscle, smooth muscle, ventricular myocytes (VM), dendrites of cortical neurons	Cav1.1 has a role in pathophysiology of the skeletal muscle diseases.	Desmethoxy-verapamil		K _d = 2.2 nM	The affinity and state-dependence of 4-desmethoxyverapamil (D888) to calcium channels is comparable to that of verapamil.	[75, 76]
	Cav1.2	Blocking		Reduction in AVN conduction, terminating reentry Reduction in early afterdepolarization (EAD)/-delayed afterdepolarization (DAD)-induced triggered activity.	Fantofarone		IC ₅₀ = 22 nM	Fantofarone antagonized Ca ²⁺ -induced contractions in K ⁺ -depo-larized aorta preparations with IC ₅₀ = 5.6 nM. Fantofarone has been shown to lead to a notable improvement of cardiac functioning in rats that have experienced an ischemic injury. On anesthetized dogs, fantofarone was seen to reduce oxygen consumption in the heart during times of regular HR, but not when the HR was increased.	[77, 78]
	Cav1.3	Blocking			Azidopine		IC ₅₀ = 0.65 nM	Azidopine blocks different Ca ²⁺ channels including Cav1.3.	[79]
	Cav2.1	Blocking	Purkinje neurons in the cerebellum	?	Z160		IC ₅₀ = 120 nM	Z160 is the first small molecule inhibitor of Cav2.1 to be administered to humans in clinical studies. When given orally to animals with neuropathic pain, Z160 showed a decrease in thermal hyperalgesia and tactile allodynia, similar to the effects of	[80]
	Cav2.2	Blocking	Brain and peripheral nervous system	?			IC ₅₀ = 40 nM		

TABLE 2 (Continued)

Bio-target	Sybytype	Type of action	Localization	Therapeutic effect in the cardiovascular system	Name of example	Structure of biaromatic compound	K _i /IC ₅₀	Effect	Reference
								morphine and gabapentin, but without any motor disruptions as measured by the rotarod test.	
	Cav3.1	Blocking	Neurons, cells that have pacemaker activity, thalamus	Inhibition of sinoatrial node (SAN) pacing, prolonged His-Purkinje phase 4 repolarization, absent from ventricular cells.	Mibefradil		IC ₅₀ = 64 nM IC ₅₀ = 130 nM	Mibefradil has been found to be effective in treating arrhythmia and angina during ischemia and reperfusion by numerous animal studies. It was given the green light by the FDA in 1997, and has since been used to treat high blood pressure and chest pain.	[81, 82]
	Cav3.2	Blocking							
	RyR2	Inhibition	Heart muscle	Reducing the occurrence and frequency of Suppresses store overload-induced Ca ²⁺ release (SOICR) in cardiomyocytes.	VK-II-86		IC ₅₀ = 1.15 μM	VK-II-86, when administered at a concentration 0.3 – 1 μM, effectively inhibited stress-induced ventricular tachyarrhythmias in RyR2-mutant mice, with no adverse effects on the HR, and was even more effective when combined with either metoprolol or bisoprolol.	[83]
α-Adrenoreceptors	α1A	Inhibition	α1-AR are located on postsynaptic effector cells such as those on the smooth muscles of the vascular, genitourinary, intestinal, and cardiac systems	Inhibition of vascular resistance in arterioles from α-adrenergic inhibition results in an increase in venous capacitance and lowering of blood pressure.	Doxazosin		K _i = 0.81 nM K _d = 0.31 nM K _i = 1 nM K _i = 0.81 nM	Doxazosin is an α-1 antagonist used for the treatment of hypertension and benign prostatic hypertrophy. Doxazosin decreases standing and supine blood pressure.	[84, 85]
	α1B	Inhibition							
	α1C	Inhibition							
	α1D	Inhibition							
	α2A	Inhibition	Brain, spinal cord, and dorsal root ganglia.	Selectively inhibition of the α2B-AR is discussed as the mechanism to treat	WB-4101		K _i = 3.5 nM K _i = 28 nM	WB-4101 is α-AR antagonist. WB-4101 was found to produce negative inotropic	[86–88]
	α2B	Inhibition	Thalamus						

(Continues)

TABLE 2 (Continued)

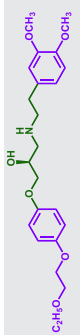
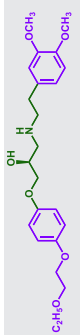
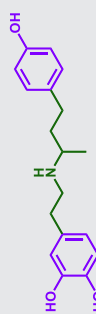
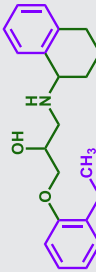
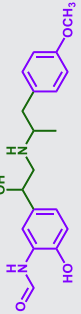
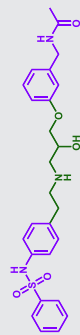
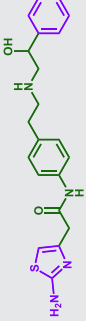
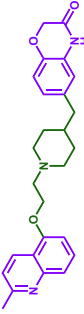
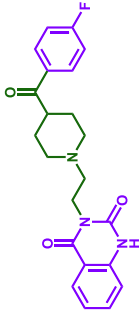
Bio-target	Sybytype	Type of action	Localization	Therapeutic effect in the cardiovascular system	Name of example	Structure of biomimetic compound	K_i/IC_{50}	Effect	Reference
α_2C	α_2C	Inhibition	Brain and dorsal root ganglia	hypertension, ischemic heart disease and heart failure (HF).			$K_i = 0.8 \text{ nM}$	action in a dose dependent manner.	[89, 90]
β_1 -Adrenoreceptors	β_1	Inhibition	Predominantly in cardiac tissues	Reduction in SAN, AVN automaticity Reduction in EAD/DAD-induced triggered activity Reduced SAN reentry Reduction in AVN conduction terminating reentry.	D140S		$K_d = 50 \text{ nM}$	D140S was a highly specific β_1 -AR antagonist ($pK_d(\beta_1) = 8.15$, $pK_d(\beta_2) < 4.5$; selectivity > 4400; in vitro rat atria and trachea experiments). The conscious rat model showed that the influence on the HR increase due to isoprenaline and the pharmacodynamic half-life of D140S was comparable to that of esmolol.	[89, 90]
		Activation		Increased escape ventricular automaticity Suppression of bradycardia-related triggered activity.	Dobutamine		$K_d = 2.5 \mu\text{M}$	Dobutamine is used to treat acute HF, which is reversible and can occur during cardiac surgery or due to septic or cardiogenic shock, as it has a positive effect on the heart's contractility.	[91, 92]
	β_2	Inhibition	Predominantly in airway smooth muscles. Also cardiac muscles, epithelial cells, vascular endothelium, skeletal muscles	?	SR-59230A		$pK_i = 9.3$	-	[93]
		Activation		?	Formoterol		$K_i = 2.6 \text{ nM}$	Formoterol used as a bronchodilator in the management of asthma and chronic obstructive pulmonary disease.	[94]
	β_3	Inhibition	Myocardium, retina, myometrium, adipose tissue, gallbladder, brain, urinary bladder, and blood vessels	Decrease endothelial nitric oxide synthase (eNOS) activity.	L 748337		$pK_i = 8.4$	Treatment with L 748337 reduces the amount of cyclic adenosine monophosphate (cAMP) generated in response to isoproterenol, with an	[93, 95]

TABLE 2 (Continued)

Bio-target	Sybype	Type of action	Localization	Therapeutic effect in the cardiovascular system	Name of example	Structure of biomimetic compound	K _i /IC ₅₀	Effect	Reference
								IC ₅₀ of 6 nM. Additionally, it decreases eNOS expression, impairs nitric oxide-mediated cell growth, and induces cell death in a melanoma cell line.	
		Activation		β3-AR agonists exert their relaxative effects on vasculature is by promoting eNOS activity and NO bioavailability.	Mirabegron		EC ₅₀ = 22.4 nM	Mirabegron reduces the tension of the detrusor muscles in the urinary bladder. Stimulation of the β3-adrenergic receptor decreases the tension of the smooth muscles of the bladder, allowing it to retain larger amounts of urine. Additionally, mirabegron decreases the frequency of nonvoiding contractions. The efficacy of mirabegron in prevention of HF is studied now.	[96, 97]

Serotonin receptors	5-HT _{1A}	Antagonist	Raphe nuclei, Hippocampus, Cholinergic heteroreceptor, in myenteric plexus	Activation of central 5-HT _{1A} receptors causes a fall in blood pressure and HR.	SB-649915		K _i = 2.51 nM	B-649915 demonstrated acute anxiolytic activity in both rodent and nonhuman primate and reduced the latency to onset of anxiolytic behavior, compared to paroxetine, in the rat social interaction paradigm.	[98, 99]
	5-HT _{1B}	Antagonist	Subiculumsubstantiagra, Vascular smooth muscle	Vasoconstriction			K _i = 10 nM		
	5-HT _{1D}	Antagonist	cranial blood vessel, vascular smooth muscle				K _i = 1.58 nM		
	5-HT _{2A}	Antagonist	Cerebral cortex, gastrointestinal tract, vascular and bronchial smooth muscle, platelets	Vasodilation	Ketanserin		K _i = 0.2 nM	Ketanserin reduces blood pressure by causing vasodilation and reducing total peripheral resistance. The reflex tachycardia seen with other vasodilators is not seen with ketanserin. This 5-	[100-102]
	5-HT _{2B}	Antagonist	Cerebellum, hypothalamus, vascular				K _i = 180 nM		

(Continues)

TABLE 2 (Continued)

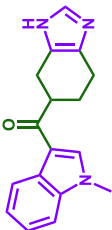
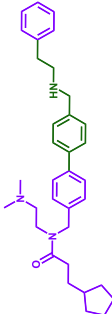
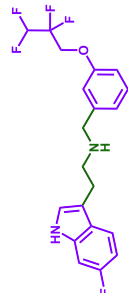
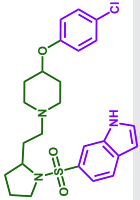
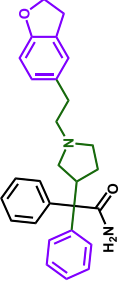
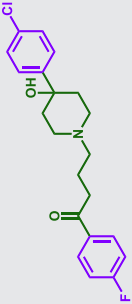
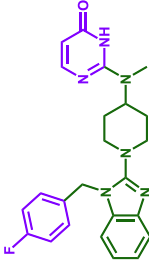

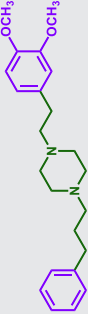
Bio-target	Sybyte	Type of action	Localization	Therapeutic effect in the cardiovascular system	Name of example	Structure of biomimetic compound	K _i /IC ₅₀	Effect	Reference
			endothelium, stomach					HT ₂ receptor inhibition may be very useful in protecting the microcirculatory bed against the detrimental effects of serotonin, which is massively released by aggregation of platelets, particularly when the vascular bed is predamaged by atherosclerosis, diabetes mellitus and old age. Ketanserin has also been reported to be more effective in the elderly.	
	5-HT _{2c}	Antagonist	Choroid plexus, hippocampus, hypothalamus				K _i = 2.7 nM		
	5-HT ₃	Antagonist	Area postrema, abdominal visceral afferent neurons	Reflex bradycardia and hypotension.	Ramosetron		K _i = 0.06 nM	Oral administration of ramosetron dose-dependently suppressed 5-HT-induced transient bradycardia (the BJ reflex), with an EC ₅₀ value of 1.2 µg/kg.	[103, 104]
	5-HT _{5A}	Antagonist	Olfactory bulb, Habenula	Reduce sympathetic drive.	SB 699551		K _i = 6.3 nM	SB-699551 5-HT _{5A} affinity is approximately 100 times greater than its affinity for other types of 5-HT receptors.	[105]
	5-HT ₆	Antagonist	Caudate putamen, hippocampus, superior cervical ganglia	?	Idalopirdine		K _i = 0.83 nM	Idalopirdine has been studied as a possible enhancer for the improvement of cognitive issues related to Alzheimer's and schizophrenia, acting as an antagonist of the 5-HT ₆ receptor.	[106]

TABLE 2 (Continued)

Bio-target	Sybtpe	Type of action	Localization	Therapeutic effect in the cardiovascular system	Name of example	Structure of biaromatic compound	K_i / IC_{50}	Effect	Reference
	5-HT ₇	Antagonist	Hypothalamus, the gastro-intestinal tract, vascular smooth muscle	Vasodilation	SB-656104		$K_i = 2 \text{ nM}$	SB-656104 attenuated the reflex bradycardia and hypotension.	[107, 108]
Serotonin transporter	SERT	Antagonist	Brain tissues, placenta, heart, blood vessels, platelets, adrenal gland and kidney	The risk of myocardial infarction and pulmonary hypertension is increased with increased expression and function of SERT.	Paroxetine	See above	$K_d = 0.08 \text{ nM}$	Paroxetine, belonging to the selective serotonin reuptake inhibitors class of antidepressants, is used to treat a variety of mental health conditions such as major depressive disorder, obsessive-compulsive disorder, panic disorder, social anxiety disorder, posttraumatic stress disorder, generalized anxiety disorder and premenstrual dysphoric disorder.	[109, 110]
Muscarinic receptors	M ₁	Antagonist	Cerebral cortex, gastric and salivary glands	Activation of M ₁ on sympathetic postganglionic cells results in catecholamine-mediated cardiac stimulation.	Darifenacin		$K_i = 5.5 \text{ nM}$	Darifenacin is used to treat an overactive bladder.	[111, 112]
	M ₂	Antagonist	Brain, heart, sympathetic ganglia, lung, ileum, uterus and other smooth muscles	The stimulation of M ₂ receptors on the intact vascular endothelium produces a profound vasodilation by stimulating the production and release of NO.			$K_i = 50 \text{ nM}$		
	M ₃	Antagonist	Brain, secretory glands, smooth muscles	M ₃ has a role in parasymphathetic control of heart function under normal physiological conditions and in the setting of a variety of pathological processes including HF, myocardial ischemia and dysrhythmias.			$K_i = 0.74 \text{ nM}$		

(Continues)

TABLE 2 (Continued)

Bio-target	Sy/Type	Type of action	Localization	Therapeutic effect in the cardiovascular system	Name of example	Structure of biaromatic compound	K _i /IC ₅₀	Effect	Reference
Dopamine receptors	D ₁	Antagonist	Brain, cardiac tissues	Cardiac dopamine D ₁ receptor triggers ventricular arrhythmia in chronic heart failure (CHF).	Haloperidol		K _i = 6.2 nM	Haloperidol is used in multiple psychiatric conditions and motor abnormalities.	[113–116]
	D ₂	Antagonist	Brain, cardiac tissues	D ₂ receptors involved in ischemic preconditioning. Dopamine preconditioning may offer significant cardioprotection in hyperlipidemic rat hearts.			K _i = 0.12 nM		
	D ₃	Antagonist	Brain	?			K _i = 2 nM		
Histamine receptors	H ₁	Antagonist	Smooth muscle, endothelial cells, adrenal medulla, heart, and CNS	H ₁ - and H ₂ -receptors are present throughout the heart and may be involved in disturbances of cardiac rhythm that occur during anaphylaxis.	Mizolastine		K _i = 2.7 nM	Mizolastine is a highly selective, long-acting second generation H ₁ -receptor antagonist that is used clinically as an anti-allergy medication.	[117, 118]
	H ₂	Antagonist			Lafutidine		K _i = 330 nM	Lafutidine is an H ₂ receptor antagonist of the second generation that works through multiple pathways and is used to address gastrointestinal issues.	[119, 120]
Sigma-receptors	σ ₁	Agonistic	Neurons and oligodendrocytes in many different tissue types	σ ₁ receptor is found to be implicated in cardioprotection, via stimulating the Akt-eNOS pathway, and reduction of Ca ²⁺ leakage into the certain calcium channels. σ ₁ receptors modulate other cardiac ion channels and modulate intracardiac neuron excitability.	SA4503, Cutamesine		K _i = 4.63 nM	Sigma-1 (σ ₁) receptor stimulation has been shown to improve cardiac hypertrophy and malfunction by increasing mitochondrial calcium mobilization and energy production with the use of SA4503.	[121, 122]

Nav1.5 channels and has been shown to be effective in treating patients with arrhythmias associated with Brugada syndrome.^[133]

4.3 | Potassium channels

Potassium channels play a critical role in cardiovascular function by regulating the resting membrane potential, APD, and contractility of cardiac myocytes. There are multiple types of potassium channels expressed in cardiac myocytes, including the voltage-gated K⁺ channels (Kv), the inward-rectifier K⁺ channels (Kir), the ATP-sensitive K⁺ channels (K_{ATP}), Ca²⁺-activated K⁺ channels, and others. Each of these channel types has a unique role in regulating cardiac function.^[134–136]

hERG channels are a type of Kv channel that conducts the rapid component of the delayed rectifier potassium current (*I_{Kr}*) and that plays a critical role in the repolarization phase of the cardiac AP. hERG channels are predominantly expressed in the ventricles of the heart, where they contribute to the rapid repolarization phase of the AP. hERG channels are unique among Kv channels in their slow deactivation kinetics, which allows them to remain open during the plateau phase of the AP and contribute to the repolarization of the VM.^[137] Mutations in the *hERG* gene have been associated with LQT and sudden cardiac death. In LQT, the delayed repolarization caused by hERG dysfunction leads to an increased risk of EADs and triggered activity, which can precipitate ventricular arrhythmias.^[138]

hERG channel blockers are historically class III antiarrhythmic agents according to the Vaughan Williams classification and class IIIa according to the modern Lei classification.^[18]

At the same time, hERG channels are currently considered the most important anti-target. This is because nonantiarrhythmic drugs and their metabolites can also interact with the hERG channel and cause QT interval prolongation, thereby increasing the risk of ventricular arrhythmia and fibrillation and sometimes leading to TdP and sudden death.^[139] The FDA now requires all new drugs to undergo hERG channel testing as part of the drug approval process to minimize the risk of drug-induced QT prolongation and TdP.^[140]

Kv1.5 channels are another important biotarget of the heart. They are predominantly expressed in the atria of the heart, where they contribute to the repolarization phase of the AP. These channels are responsible for the ultra-rapid delayed rectifier potassium current (*I_{Kur}*), which is important for the regulation of atrial excitability and contractility.^[141] Mutations in the Kv1.5 gene and dysfunction of this channel have been associated with a variety of cardiac arrhythmias, including AF and Brugada syndrome.^[132] Several drugs that target Kv1.5 channels are currently under investigation for the treatment of this condition.

Kv1.5 channels also play a role in the regulation of arterial smooth muscle tone. These channels are expressed in vascular smooth muscle cells and contribute to the repolarization of the membrane potential, which is important for regulating vascular tone and blood pressure.^[142]

Kv1.1 potassium channel α -subunits are broadly expressed in the nervous system where they act as critical regulators of neuronal excitability. Mutations in the *KCNA1* gene, which encodes Kv1.1, are associated with neurological diseases such as episodic ataxia and epilepsy. Studies in mouse models have shown that Kv1.1 is important for neural control of the heart and that *KCNA1* deletion leads to cardiac dysfunction that appears to be brain-driven. Recent studies have revealed that Kv1.1 subunits are not only present in cardiomyocytes but that they also make an important heart-intrinsic functional contribution to outward K⁺ currents and AP repolarization.^[143]

Kv1.3 channels are highly expressed in platelets and are able to regulate agonist-evoked increases in intracellular calcium ([Ca²⁺]_i) concentration, which is essential for almost all platelet functions. Modulation of Ca²⁺ influx and [Ca²⁺]_i in platelets has been emerging as a possible strategy for preventing and treating platelet-dependent thrombosis. Specific inhibition of Kv1.3 by a monoclonal antibody has been shown to suppress platelet functions and platelet-dependent thrombosis through modulating platelet [Ca²⁺]_i elevation. These results indicate that Kv1.3 could act as a promising therapeutic target for antiplatelet therapies.^[144]

Kir channels especially Kir2.1 and Kir2.3 are widely expressed in various cardiac cells, including atrial and ventricular myocytes, sinoatrial node cells, and Purkinje fibers. In cardiac myocytes, Kir channels are responsible for maintaining the resting membrane potential and modulating APD. These channels predominantly allow inward potassium current during the diastolic phase of the cardiac cycle, contributing to phase 3 repolarization. The activation of Kir channels leads to membrane hyperpolarization, which opposes depolarizing influences and helps to stabilize the resting membrane potential. This activity allows for proper electrical signal propagation and efficient contraction of the heart.^[145]

K_{ATP} channels are contributed in the control of cardiac contractility, coronary blood flow, and vascular tone. They are widely expressed in cardiac myocytes, smooth muscle cells, and endothelial cells within the cardiovascular system. K_{ATP} channels are activated by a decrease in intracellular ATP levels and play a role in cardiac ischemia. Activation of K_{ATP} channels can lead to hyperpolarization of the cell membrane and a subsequent decrease in Ca²⁺ influx, which reduces myocardial oxygen consumption and protects against ischemic injury.^[146]

In coronary smooth muscle cells, these channels respond to local metabolic factors such as hypoxia, low pH, and adenosine. Activation of K_{ATP} channels in response to these factors leads to hyperpolarization and subsequent relaxation of smooth muscle cells, resulting in coronary vasodilation.^[147]

4.4 | HCN channels

HCN channels especially the HCN4 subtype have a key role in the regulation of cardiac pacemaking, HR, and autonomic control. These ion channels are predominantly expressed in the SAN, AVN, and

certain regions of the conducting system within the heart.^[148] HCN channels are responsible for the “funny” or “pacemaker” current, also known as I_f current. These channels are activated by hyperpolarization and cyclic nucleotides, such as cAMP. In the SAN, HCN channels are primarily responsible for the initiation and regulation of the cardiac rhythm. The gradual depolarization of the SAN cells, known as pacemaker potential, is generated by a balance between inward I_f and outward potassium currents. The activation of HCN channels during the diastolic phase of the cardiac cycle allows the influx of sodium and potassium ions, contributing to the slow depolarization and the spontaneous firing of AP in the SAN.^[149] HCN channel dysfunction or mutations have been associated with cardiac arrhythmias, such as sick sinus syndrome and AF, highlighting their clinical relevance.^[150,151]

4.5 | β -Adrenoreceptors

β -ARs (primarily β_1 subtype) mediate cardiovascular function induced by activation of the sympathetic nervous system upon binding the catecholamines. These receptors are widely expressed in cardiac myocytes, smooth muscle cells, and endothelial cells within the cardiovascular system. Stimulation of β_1 -adrenergic receptors by catecholamines activates a signaling cascade that leads to increased intracellular levels of cAMP. Elevated cAMP levels subsequently activate protein kinase A (PKA), which phosphorylates various target proteins, including ion channels, calcium-handling proteins, and contractile proteins.^[152]

Activation of β_1 -adrenergic receptors enhances calcium influx through L-type calcium channels, leading to increased calcium availability for myofilament contraction and augmentation of cardiac contractility. Additionally, β_1 -adrenergic receptor stimulation promotes the release of calcium from the SR, further increasing the strength of cardiac contraction. These effects contribute to the positive inotropic and chronotropic actions of β_1 -adrenergic receptor activation. Moreover, β -ARs are present in smooth muscle cells lining blood vessels. In the vasculature, the predominant β -AR subtype is β_2 . Stimulation of β_2 -adrenergic receptors leads to relaxation of vascular smooth muscle cells through a cAMP-PKA-dependent pathway. Activation of β_2 -adrenergic receptors results in vasodilation, reducing peripheral vascular resistance and lowering blood pressure.^[153]

β -ARs inhibitors are employed to reduce HR, blood pressure, and myocardial oxygen demand in conditions such as hypertension, angina, and HF. On the other hand, beta-agonists, which stimulate β -ARs, are utilized to increase cardiac contractility in acute HF conditions.^[154]

4.6 | α -Adrenoreceptors

α -ARs are catecholamine-activated G protein-coupled receptors. These receptors, especially the α_1 -subtype, are expressed in mammalian myocardium and vasculature and play essential roles in the regulation

of cardiovascular physiology. While β_1 -ARs outnumber α_1 -ARs in the heart, the activation of cardiac α_1 -ARs plays a significant role in various essential biological processes such as hypertrophy, positive inotropy, ischemic preconditioning, and protection against cell death. Clinical trial data reveals that nonselectively blockade of α_1 -ARs leads to a twofold increase in unfavorable cardiac events, including HF and angina, suggesting that activating α_1 -ARs may also provide cardioprotective benefits in humans. Growing evidence indicates that the α_1A -AR subtype is involved in these adaptive effects, as demonstrated by the prevention and reversal of HF in animal models using α_1A -agonists. On the other hand, α_1 -ARs inhibition in vasculature results in the reducing of peripheral vascular resistance and an overall reduction of blood pressure.^[155,156]

4.7 | Serotonin receptors

The cardiovascular effects of serotonin are diverse and mediated by several receptor types, including 5-HT₁, 5-HT₂, 5-HT₃, and possibly 5-HT₄-receptors. Serotonin can elicit bradycardia or tachycardia, hypotension or hypertension, and vasodilation or vasoconstriction. The specific effects depend on the receptor subtype activated and the experimental conditions. For example, selective activation of 5-HT_{1A} receptors can decrease HR and arterial blood pressure. Initially, serotonin-induced bradycardia occurs through a transient decrease in blood pressure, known as the von Bezold-Jarisch reflex, mediated by 5-HT₃ receptors located on sensory vagal nerve endings in the heart. When this reflex is suppressed, such as during anesthesia or vagotomy, serotonin can increase HR through various mechanisms in different species (5-HT₁, 5-HT₂, and 5-HT₄-receptors in cats, rats, and pigs, respectively). In dogs and rabbits, serotonin-induced tachycardia is mainly due to catecholamine release, involving 5-HT₂-receptors on the adrenal medulla and 5-HT-receptors on postganglionic cardiac sympathetic nerve fibers. Recently, 5-HT₃-receptors have also been implicated in serotonin-induced tachycardia in conscious dogs. Thus, 5-HT-receptors are also a target for cardiovascular pathologies such as hypertension, peripheral vascular diseases, and HF.^[157]

4.8 | Muscarinic receptors

Several subtypes of muscarinic receptors are expressed in various cardiovascular tissues, including the heart and blood vessels where they mediate the effects of acetylcholine on cardiac function. In the heart, M₂-receptors play a dominant role. Activation of M₂-receptors in cardiac myocytes leads to the inhibition of adenylyl cyclase and a subsequent decrease in cAMP levels. This results in a reduction in HR, cardiac contractility, and conduction velocity. M₂-receptors also mediate the negative chronotropic effect of acetylcholine, contributing to the parasympathetic control of HR and electrical conduction.

In vascular smooth muscle cells, M-receptors are involved in the regulation of vascular tone. Activation of M₃-receptors leads to the production of inositol trisphosphate and diacylglycerol, which promote

the release of intracellular calcium ions and subsequent vasoconstriction. M_3 -receptors also play a role in endothelium-dependent vasodilation through the release of nitric oxide and prostacyclin. The activation of M_3 -receptors in endothelial cells leads to the activation of eNOS and the production of nitric oxide, which diffuses to vascular smooth muscle cells, causing relaxation and vasodilation.^[158]

Recent studies have further highlighted the clinical relevance of M-receptors in CVD. For example, the development of selective M_3 -receptor antagonists has been explored as a potential therapeutic approach for the treatment of hypertension and other cardiovascular disorders.^[159] Additionally, the role of M_2 -receptors in modulating cardiac remodeling and hypertrophy has been investigated, suggesting their involvement in the pathogenesis of HF.^[160]

4.9 | Dopamine receptors

There are four subtypes of dopamine receptors (D_1 -, D_2 -, D_4 -, and D_5 - receptors), which are expressed in various cardiovascular tissues. Dopamine appears to stimulate these receptors in the SAN, atrium, and ventricle of the human heart.

D_1 -receptors contribute to the regulation of systemic blood pressure through their actions on peripheral blood vessels. Stimulation of D_1 - and D_5 -receptors in vascular smooth muscle cells promotes vasodilation, reducing vascular resistance and lowering blood pressure. Mice with a global knock-out of the D_2 - and D_4 -receptors developed hypertension, and this led to cardiac hypertrophy.

Simulated ischemia and reperfusion led isolated neonatal rat cardiomyocytes to an increased expression of D_1 -receptors, but also a heightened expression of D_2 -receptors, which led to impaired mitochondrial function. Even nowadays, dopamine is used in the clinic to raise blood pressure, for instance, in patients with sepsis. There are data in patients that noted after intravenous infusion a direct positive inotropic effect of fenoldopam (a D_1 -receptor agonist) or propylbutyldopamine (a D_2 -receptor agonist), suggesting that the D_1 -receptors and the D_2 -receptors in the human heart can directly or indirectly increase the force of heart contraction.^[161]

4.10 | Histamine receptors

In the heart, two types of histamine receptors are present: H_1 - and H_2 -receptors. H_2 -receptors cause an increase in HR and contractility as well as coronary vasodilatation, whereas H_1 -receptors mediate chronotropic effects and coronary vasoconstriction.

Histamine and its receptors profoundly impact the pathophysiology of the heart, resulting in hypertension-induced cardiac hypertrophy and other cardiac anomalies. Histamine possesses arrhythmogenic effects and once locally released, may enhance automaticity and induce triggering activity resulting in severe tachyarrhythmias. The major arrhythmogenic effects of histamine consist in increasing sinus rate and ventricular automaticity, and in slowing atrioventricular conduction. In addition,

histamine may interfere with depolarization and repolarization through its effects on calcium and potassium currents.

Preclinical and clinical studies using histamine receptor antagonists report improvement in cardiac function. For example, the administration of the H_2 -receptor antagonist famotidine reduced the incidence of HF in humans. Similar results were observed in a clinical study where the incidence of cardiac remodeling in HF patients decreased with famotidine treatment.^[162,163]

4.11 | Sigma-1 (σ_1) receptor

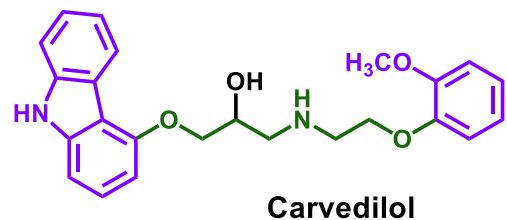
The σ_1 receptor is a ligand-operated chaperone protein that modulates signal transduction during cellular stress processes. While these receptors have been extensively studied in the CNS, they have been found to be present in multiple tissues, including the cardiovascular system. Moreover, the σ_1 -receptor protein levels are higher in heart tissue than brain tissue in rats.

σ_1 -Receptors engage in interactions with different ligands and proteins, resulting in specific cellular responses among which are increasing of $[Ca^{2+}]_i$, modulation of ion channels activity, and neurotransmitter systems. This characteristic makes them a promising target for pharmacological modulation. Additionally, ligands that bind to σ_1 -receptors activate signaling pathways that promote cardioprotective effects, alleviate damage caused by ischemic injury, and influence the activation of myofibroblasts and the development of fibrosis. In preclinical models, the ligands of σ_1 -receptors have demonstrated considerable advantages, including enhanced cardiac function, diminished ventricular remodeling and hypertrophy, as well as reduced ischemic damage.^[164,165]

5 | THE MOST WELL-STUDIED MULTITARGET DRUGS WITH LINKED BIAROMATIC STRUCTURE

5.1 | Carvedilol

Carvedilol was opened by Boehringer Mannheim GmbH in 1985 in the process of creating carbazole-containing biaromatic compounds with β -antagonistic activity. The drug showed the best combination of vasodilating and β -antagonistic activity during the initial screening tests.^[166] Later carvedilol became one of the representatives of the "β-blockers" group.



Carvedilol was approved for use in patients with HF in the United States in May 1997, as it was found to be effective in reducing all-cause mortality, hospitalizations, sudden death, and death due to progressive HF. Moreover, carvedilol had beneficial effects on the remodeling process of the heart, such as a decrease in left ventricular (LV) size and improvement in ejection fraction, as well as antioxidant and antiproliferative actions.^[167]

The carvedilol molecule contains carbazole and *o*-methoxyphenyl aromatic nuclei connected by a linear linker 9 bonds long. This linker has the 1,2-dihydroxy-3-aminopropane pharmacophore characteristic of β -blockers and an additional oxygen atom. Thus, the structure of carvedilol predetermines its multitargeting against the targets of compounds that have a biaromatic nature. It should be noted that carvedilol is used as a mixture of enantiomers that additionally affects the increase in the spectrum of its biotargets since in some cases individual enantiomers have different affinity values.^[168]

A study of the pharmacokinetic characteristics of carvedilol showed that it is absorbed rapidly, with C_{\max} reaching 1–2 h postdose. The C_{\max} values are linearly related to the dose, and in different studies of the doses from 12.5 to 50 mg carvedilol the C_{\max} values were in the range of 21–262 mg/L (i.e., from 52 to 644 nM). Carvedilol undergoes extensive first-pass liver metabolism that results in an absolute bioavailability of about 25%. The (S)-(-)-enantiomer appears to be metabolized more rapidly than the (R)-(+)-enantiomer and has an absolute bioavailability of 15% compared with the absolute bioavailability of 31% for the (R)-(+)-enantiomer. Because it is highly lipophilic, carvedilol distributes extensively throughout the body and has a volume of distribution between 1.5 and 2 L/kg. The drug is highly protein bound (95%), with the (R)-(+)-enantiomer being more tightly bound than the (S)-(-)-enantiomer. Thus, the resultant exposure of the tissues to the β -antagonistic and α -antagonistic effects of carvedilol as well as to the other mechanisms is a complex interaction depending on the proportions of drug present in the mixture, the rate of liver metabolism and the degree of protein binding. Due to its basic nature and lipophilicity, carvedilol accumulates in milk (in animals) to an extent similar to that of other β -blockers.^[169]

5.1.1 | Carvedilol calcium channels blocking

Carvedilol blocks L-type calcium current ($I_{Ca,L}$) current with $IC_{50} = 3.59 \mu\text{M}$ measured using whole cell patch clamp in rabbit VM.^[170] Liu et al. demonstrated that carvedilol has a protective effect on the abnormality of $I_{Ca,L}$ induced by oxygen-free radicals in cardiomyocytes. Carvedilol at a concentration of $0.5 \mu\text{M}$ was able to counteract the inhibitory effect of H_2O_2 on $I_{Ca,L}$, and to reverse the changes in its dynamics caused by H_2O_2 . This suggests that carvedilol could ameliorate the disruption of the $I_{Ca,L}$ due to oxygen free radicals in cardiomyocytes, thus partly explaining its efficacy in CHF.^[171]

The effects of carvedilol on $[\text{Ca}^{2+}]_i$ mobilization and $I_{Ca,L}$ in rat vascular smooth muscle cells were investigated by Nakajima et al. and compared to those of metoprolol. Carvedilol did not inhibit the Ca^{2+}

release but significantly suppressed the sustained rise due to Ca^{2+} entry concentration-dependently. Under voltage clamp conditions, carvedilol ($0.2\text{--}10 \mu\text{M}$) reversibly and concentration-dependently inhibited the $I_{Ca,L}$ without altering the current-voltage relationships of the current. Carvedilol shifted the steady-state inactivation of $I_{Ca,L}$ to more negative potentials and inhibited $I_{Ca,L}$ in a voltage-dependent way. Moreover, carvedilol didn't impede Ca^{2+} release from store sites induced by thapsigargin but did limit the sustained rise due to capacitive Ca^{2+} entry unrelated to $I_{Ca,L}$. Metoprolol, on the other hand, did not show the same effects as carvedilol did. These results suggest that carvedilol inhibits $I_{Ca,L}$, as well as the channels for agonist (vasopressin and endothelin-1)-induced Ca^{2+} entry in vascular smooth muscle cells, which may explain its vasorelaxing and antiproliferative effects.^[172]

Deng et al. investigated the impacts of carvedilol on T-type calcium current ($I_{Ca,T}$) in the murine HL-1 cell line. Results suggested that carvedilol reversibly inhibited $I_{Ca,T}$ in a concentration-dependent way, with an IC_{50} of $2.1 \mu\text{M}$. When $3 \mu\text{M}$ carvedilol was applied, the peak $I_{Ca,T}$ amplitude at -20 mV decreased. Additionally, the steady-state inactivation curve of $I_{Ca,T}$ shifted towards more negative potentials by 12.8 mV and the recovery from inactivation of $I_{Ca,T}$ was delayed. Stimuli frequency enhancement increased carvedilol-induced inhibition rate in $I_{Ca,T}$ and the amplitude of $I_{Ca,T}$ still decreased significantly even in the presence of H-89, a PKA inhibitor. Moreover, carvedilol significantly inhibited the amplitude of the calcium transient in a concentration-dependent way. These outcomes demonstrate that carvedilol suppresses $I_{Ca,T}$ in atrial cells through a mechanism that entails preferential interaction with the inactivated state of T-type Ca^{2+} channels.^[173]

The mechanism of fatal ventricular arrhythmias involves, in part, an overload of Ca^{2+} in the SR, which results in spontaneous Ca^{2+} efflux through the RyR2 Ca^{2+} -release channel. In turn, this SOICR through a defective RyR2 triggers DADs, which have been implicated in catecholaminergic polymorphic VT as well as in ventricular tachyarrhythmias and sudden death.

Carvedilol suppresses SOICR independently of its α - and β -antagonistic activity and its antioxidant properties, and it is instead principally because of its ability to stabilize Ca^{2+} handling via the RyR2. This drug inhibited SOICR in the RyR2-R4496C mutant human embryonic kidney 293 cells (HEK293) cell line with IC_{50} of $15.9 \mu\text{M}$.^[174]

There are suggestions in the literature that the unique anti-SOICR activity of carvedilol, combined with its β -antagonistic activity, probably contributes to its favorable antiarrhythmic effect. Zhou et al. showed that carvedilol suppresses SOICR by directly altering the function of single native RyR2 from SR microsomes fused into lipid bilayers and single purified recombinant RyR2. Carvedilol at $1 \mu\text{M}$ significantly reduced RyR2 mean open time and open probability and increased the event frequency. It was also demonstrated that carvedilol at clinically relevant concentrations ($0.3\text{--}1 \mu\text{M}$) suppresses SOICR in cardiomyocytes from mice harboring the SOICR-promoting, CPVT-causing RyR2 mutation, R4496C.^[83]

5.1.2 | Carvedilol sodium channels blocking

Bankston and Kass while studying molecular determinants of local anesthetic action of different β -blockers analyzed carvedilol blocking activity against peak and late current through Nav1.5 channels.

The authors showed that carvedilol Nav1.5 channel blocking was 51% at 40 μM and 8% at 4 μM . Since $I_{\text{Na,L}}$ is critical to the pathology of LQT3 syndrome due to mutation of the *SCN5A* gene as well as potentially important to other disease pathogenesis, such as ischemia-reperfusion injury and HF, the blocking of $I_{\text{Na,L}}$ by carvedilol was also examined. Carvedilol blocked 65% of mutation-induced $I_{\text{Na,L}}$ at 4 μM . Though this concentration is in excess of the likely therapeutic dose of the drug (blood plasma concentrations for carvedilol are around 50–200 nM) the findings provide additional biophysical evidence that carvedilol is able to block disease causing $I_{\text{Na,L}}$.^[175]

Deng et al. published similar data for carvedilol blocking activity against sodium channel current in isolated VM of rats. Carvedilol decreased the sodium channel current in a dose-dependent and voltage-dependent manner with $\text{IC}_{50} = 6.35 \mu\text{M}$. Carvedilol also blocked the effect of 10 μM isoproterenol which increased sodium current (I_{Na}).^[176]

5.1.3 | Carvedilol potassium channels blocking

Carvedilol has been found to have a potently blocking effect on I_{Kr} in rabbit VM, with an IC_{50} value of 0.35 μM . This drug also demonstrates a class III antiarrhythmic effect, suppressing hERG channels at therapeutic concentrations, thereby showcasing its antiarrhythmic effectiveness.^[35] Inhibition of hERG current by carvedilol was partially but significantly attenuated in Y652A and F656C mutant hERG channels.^[177]

Yang et al. used the whole-cell configuration of the patch-clamp technique to observe the effects of carvedilol on Kv1.3 channels that were heterologously expressed in HEK293 cells. The results showed that the drug had a concentration-dependent blocking effect, with an IC_{50} value of 9.7 μM . Furthermore, carvedilol slowed down the deactivation tail current of Kv1.3 currents, resulting in a tail crossover phenomenon. Additionally, the inactivation curve of the Kv1.3 channels was shifted by 20 mV in a hyperpolarizing direction, while the activation curve was not affected. Through mutagenesis experiments, G427 and H451, two related tetraethylammonium block sites, were identified as important residues for the blocking effect of carvedilol. Therefore, the authors postulated that carvedilol acts directly on Kv1.3 currents by inducing closed- and open-channel blocks.^[178]

Exposure to carvedilol in human atrial myocytes causes a considerable block of I_{Kur} at a concentration equivalent to therapeutic plasma levels, with an IC_{50} value of 0.39 μM . This drug also demonstrates a blocking effect on cloned cardiac Kv1.5 channels expressed in Chinese hamster ovary (CHO) cells, however at a slightly higher concentration (IC_{50} of 2.56 μM).^[35,179] Other β -AR blockers

(alprenolol, oxprenolol, and carteolol) had little or no effect on Kv1.5 currents. Carvedilol Kv1.5-blocking was dependent on the concentration, voltage, time, and usage but only at concentrations slightly higher than human therapeutic plasma concentrations. These properties may explain the antiarrhythmic property of carvedilol.

The delayed rectifier K^+ current (I_{K}), which is mainly conducted through Kv2.1 channels highly expressed in the hippocampal neurons, is notably suppressed when carvedilol is applied, with an IC_{50} value of 1.3 μM . When the same drug is tested on HEK293 cells with heterologously expressed Kv2.1 channels, it is found to be strongly inhibited with an IC_{50} value of 5.1 μM . Residues Y380 and K356 located in the outer vestibule of the channel are what give the drug its affinity.^[35]

Zhang et al. studied carvedilol for inhibiting the hKv4.3 channel stably expressed in HEK293 cells as well as in ventricular epicardial myocytes of rabbit hearts using a whole-cell patch technique compared to quinidine. Quinidine is an important drug to treat Brugada syndrome by inhibition of transient outward potassium current (I_{to}) as the major mechanism but it is inaccessible in many countries.

Carvedilol blocked the hKv4.3 current in a concentration-dependent manner, with an IC_{50} of 1.2 μM —this was lower than the IC_{50} of quinidine, which was 2.9 μM . Both substances had similar properties when it came to open channel blocking, such as reducing the time to peak activation and increasing inactivation of the hKv4.3, shifting the half-activation voltage of activation and inactivation negatively, and slowing down recovery from inactivation. Carvedilol had a weaker inhibition effect than quinidine on hKv4.3 peak current, however, its effect on charge area reduction was greater at all frequencies (0.2–3.3 Hz). Furthermore, carvedilol had a greater effect on AP notch than quinidine. Therefore, the authors of the study proposed that carvedilol could be an alternative medication for preventing malignant ventricular arrhythmias in patients with Brugada syndrome in countries where quinidine is not available.^[180]

Carvedilol has been proposed to block K_{ATP} channels by binding to the bundle crossing region at a domain including C166, thereby plugging the pore region.^[181] Carvedilol has been revealed to have no effect on Kir2.1 channels as they lack the C166. Ferrer et al. found that carvedilol had a significantly greater inhibitory effect on Kir2.3 than on Kir2.1, with an IC_{50} of 0.49 μM for Kir2.3 compared to an IC_{50} of more than 50 μM for Kir2.1. Their research further demonstrated that the inhibition of Kir2.3 channels by carvedilol was both concentration-dependent and voltage-independent. Furthermore, they noticed that mutation of I213L in Kir2.3 caused a more than twentyfold decrease in the inhibitory effect of carvedilol, with an IC_{50} of 11.1 μM . Finally, when exogenous phospholipid phosphatidylinositol 4,5-bisphosphate (PIP2) was present, the inhibition of Kir2.3 channels by carvedilol was reduced by 80%, suggesting that carvedilol, like other cationic amphiphilic drugs, inhibits Kir2.3 channels by disrupting the PIP2-channel interaction.^[182]

Staudacher et al. demonstrated that carvedilol inhibits two-pore domain K^+ channel (TASK-1, K2P3.1) currents in a concentration-dependent manner in both *Xenopus* oocytes ($\text{IC}_{50} = 3.8 \mu\text{M}$) and

mammalian CHO cells ($IC_{50} = 0.83 \mu\text{M}$). Furthermore, the sensitivity of native $I_{K_{2P3.1}}$ to carvedilol was observed in human pulmonary artery smooth muscle cells. The channels were inhibited in both open and closed states, in a frequency-dependent manner, leading to a 7.7 mV depolarization of the resting membrane potential. Additionally, the current-voltage relationship was shifted by -6.9 mV towards hyperpolarized potentials, with the open rectification of K2P currents being unaffected. The authors suggested that the blockade of cardiac human K2P3.1 current by carvedilol may suppress electrical automaticity, extend atrial refractoriness, and contribute to the class III antiarrhythmic action of the drug when used by patients.^[183]

In a study conducted by Cha et al., the effects of the drug carvedilol on acetylcholine-activated potassium current ($I_{K_{ACH}}$) in mouse atrial cardiomyocytes were examined. The results indicated that carvedilol inhibited $I_{K_{ACH}}$ in a dose-dependent manner when concentrations ranged from 0.1 to $5 \mu\text{M}$. The IC_{50} was $1.03 \mu\text{M}$ for the peak and $1.04 \mu\text{M}$ for the quasi-steady-state. Furthermore, the drug was seen to suppress the shortening of the APD induced by acetylcholine. This evidence suggests that carvedilol may be a useful antiarrhythmic agent specifically for AF.^[184]

5.1.4 | Carvedilol HCN-channels blocking

Cao et al. investigated the effect of carvedilol on HCN channels assuming that these targets, which play a critical role in spontaneous rhythmic activity in the heart, may be the reason for the favorable effect of this drug compared with other β -blockers in patients with CHF. Using whole-cell patch-clamp recordings the effect of carvedilol on currents from wild-type (WT) and mutant HCN1, HCN2, and HCN4 channels expressed in CHO cells was studied. Carvedilol blocked HCN4 in a concentration-dependent manner with an EC_{50} of $4.4 \mu\text{M}$. It also blocked HCN1 and HCN2 channels with EC_{50} of 7.9 and $7.6 \mu\text{M}$, respectively. The HCN-blocking effects of the drug were determined by decelerating the rate of channel activation, increasing that of deactivation, and by strongly left-shifting the voltage dependence of hyperpolarization activation.^[185]

5.1.5 | Carvedilol α -adrenoreceptors inhibition

α 1-ARs antagonistic properties are one of the main additional carvedilol activities. Its action on α 1-ARs relaxes the smooth muscle in the vasculature, leading to reduced peripheral vascular resistance and an overall reduction in blood pressure.^[169,186] According to Morgan, carvedilol has a similar α 1-AR antagonistic activity for both enantiomers (K_d 16 and 14 nM for the (S)-(-)- and (R)-(+)-enantiomers, respectively). Monopoli and Bristow showed comparable data for carvedilol α 1-affinity in human LV tissue: 2.3 and 9.4 nM, respectively.^[27]

Koshimizu et al. conducted a thorough examination of the affinity of carvedilol to different α 1-AR subtypes. Through the use of HEK293 cells expressing an individual AR subtype, they found that

α 1D-AR and α 1B-AR had a higher affinity for carvedilol than β 1-AR, which is a major target in treating HF. The affinity rank order and pK_i values of ARs for carvedilol were as follows: α 1D-AR (8.9) > α 1B-AR (8.6) > β 1-AR (8.4) > β 2-AR (8.0) > α 1A-AR (7.9) > α 2C-AR (5.9) > α 2B-AR (5.5) > α 2A-AR (5.3). Through the use of human smooth muscle and HEK293 cells, it was found that calcium signaling mediated by α 1D- and α 1B-ARs had oscillatory patterns with frequencies ranging from 0.3–3 per minute, which could be inhibited by therapeutic concentrations of carvedilol (10 nM). When α 1B-AR and α 1A-AR were co-expressed and heteromer receptors were detected, carvedilol only suppressed the oscillatory component of global cytosolic free calcium change. These results suggest that, in addition to β -ARs, carvedilol also has an effect on α 1-ARs, particularly α 1D- and α 1B-AR-mediated signaling events, such as $[Ca^{2+}]_i$ oscillations in vascular smooth muscle.^[187]

5.1.6 | Carvedilol β -adrenoreceptors inhibition

β -Antagonistic activity is the main mechanism of carvedilol action. The generally accepted and established name for the pharmaceutical group of carvedilol is “nonselective β -blocker.” Indeed, the molecule of this drug contains a 2,3-dihydroxypropylamine fragment characteristic of all β -blockers.

Yoshikawa et al. give the following binding characteristics of carvedilol against β 1- and β 2-ARs. In the presence of guanine nucleotides (Gpp(NH)p) a comparison of the binding properties of carvedilol in multiple human systems indicates that the racemic compound does possess some relative β 1 receptor selectivity. The degree of selectivity varies from 11-fold using membranes from nonfailing ventricles, containing >80% β 1 receptors ($K_d(\beta 1) = 4.5$ nM; $K_d(\beta 2) = 49$ nM) compared to lymphocyte membranes containing 100% β 2-receptors, to two-fold using recombinant human systems ($K_d(\beta 1) = 1.2$ nM; $K_d(\beta 2) = 2.3$ nM).

Sponer and Bristow published similar affinity parameters for carvedilol. In guinea pig heart and trachea tissues, carvedilol showed the following properties: $K_d(\beta 1) = 5.6$ nM; $K_d(\beta 2) = 37.1$ nM; and in human LV tissue $K_d(\beta 1) = 4.0$ nM; $K_d(\beta 2) = 29.1$ nM.^[27] In [^3H] CGP12177 binding assay Groszek et al. determined the subnanomolar inhibition constant of carvedilol against β 1-AR ($K_i = 0.81$ nM).^[188] Gaiser et al. determined $pK_d(\beta 2) = 9.71$ (i.e., K_d of 0.2 nM) for carvedilol using [^3H]dihydroalprenolol assay and membranes of HEK293 cell lines.^[189] It is believed that the β -antagonistic properties in combination with the α -antagonistic properties play a decisive role in the cardioprotective effect of carvedilol, although it is clear that a huge number of other biological targets of this drug have a certain contribution to its overall physiological effect.^[168]

5.1.7 | Carvedilol serotonin receptors binding

Gaillard et al. found that carvedilol has a high binding affinity against the 5-HT $_{1A}$ receptor with K_i of 3.16 nM.^[190] By in vitro experiments,

Murnane et al. demonstrated that carvedilol has a high nanomolar affinity for 5-HT_{2A} receptors. This drug dose-dependently displaced [³H]ketanserin from the 5-HT_{2A} receptor with a K_i of 546.5 nM.

Experimental studies conducted in mice revealed that the administration of carvedilol led to increasing the ethanol-induced loss of the righting reflex and suppresses operant responding. These effects could be prevented by pretreatment with M100907, a selective antagonist of the 5-HT_{2A} receptor. Interestingly, carvedilol did not induce the head-twitch response in mice, indicating a lack of psychedelic activity. However, carvedilol was not found to activate the canonical 5-HT_{2A} receptor signaling pathways and instead inhibited serotonin-mediated signaling. Additionally, carvedilol reduced the head-twitch response evoked by 2,5-dimethoxy-4-iodoamphetamine, suggesting its potential antagonism, allosteric modulation, or functional bias *in vivo*.^[191]

5.1.8 | Carvedilol M₂ interaction

Xu et al. offered to explain the preference of carvedilol over selective β₁-blockers in the improved prognosis of HF by its direct actions on the sympathetic nervous system. The researchers investigated the changes of the M₂-receptors and cholinesterase-positive nerves in different regions of the hearts of rats with induced HF due to adriamycin. They also looked at the effects that carvedilol had on these M₂ receptors and cholinesterase-positive nerves. It was observed that the concentration of cholinesterase-positive nerve cells was reduced in the adriamycin-induced failing heart group, while the density of M₂ receptors increased in the groups receiving 3- and 10-mg/kg doses of carvedilol, especially in the endocardial tissue of the LV free wall. The authors concluded that the upregulation of M₂ receptors could be one of the ways in which carvedilol may be effective in treating HF.^[192]

5.1.9 | Carvedilol NMDA inhibition

Lysko et al. proposed that the antioxidant capabilities of carvedilol could be the reason for its protective action against brain ischemia, however, this did not appear to be the case for glutamate-induced excitotoxicity in cultured cerebellar granule cells as this neurotoxicity was not linked to the formation of lipid peroxidative products. Instead, it was observed that carvedilol reduced the *N*-methyl-D-aspartate (NMDA)/glycine-induced increase in [Ca²⁺]_i, with an IC₅₀ of 0.8 μM. When 5 μM dihydropyridines were added before the NMDA/glycine-stimulated response, it significantly decreased to 64% of untreated, whereas prior inclusion of 5 μM carvedilol inhibited the increase in [Ca²⁺]_i by 85%. Additionally, carvedilol displaced labeled NMDA receptor antagonist [³H]MK-801 binding to rat brain cortical membranes with K_d of 29.4 μM and no selectively for the glycine or glutamate binding sites. These results indicate that carvedilol has a neuroprotective effect as both a calcium channel blocker and a noncompetitive inhibitor at the NMDA receptor.^[193]

5.1.10 | Carvedilol NADH inhibition

Oliveira et al. conducted research to investigate the effects of carvedilol on an exogenous reduced nicotinamide adenine dinucleotide (NADH) dehydrogenase in rat heart mitochondria. They discovered that carvedilol did not affect oxygen consumption associated with the oxidation of succinate and internal NADH. Furthermore, they discovered that inhibition of the external NADH dehydrogenase by carvedilol was accompanied by the inhibition of alkalization of the external medium. Additionally, they observed that whereas the addition of glutamate/malate or succinate generates a membrane potential in rat heart mitochondria, exogenous NADH does not. Moreover, they ruled out that oxygen consumption linked to NADH oxidation was due to permeabilized mitochondria, but instead was a result of oxidase activity in the inner membrane. The enzyme had a K_d for NADH of 13 μM and carvedilol is a noncompetitive inhibitor of this external NADH dehydrogenase with K_i of 15 μM. Carvedilol is noteworthy as it was the first inhibitor described for this organospecific enzyme. The authors hypothesized that the administration of carvedilol to tumor patients treated with adriamycin, an anthracycline from the family of anticancer drugs, may be beneficial in reducing cardioselective toxicity.^[194]

5.1.11 | Carvedilol additional targets

Using rat proteins, Pauwels et al. showed the affinity of carvedilol for a variety of other targets including H₁ receptor (K_i = 3034 nM), D₂ receptor (K_i = 213 nM), μ-opioid receptor (K_i = 2700 nM), veratridine site of Nav1.5 (IC₅₀ = 1260 nM), SERT (K_i = 528 nM), norepinephrine transporter (K_i = 2406 nM), and dopamine transporter (K_i = 627 nM).^[195] In Vela's review is presented the binding affinity of carvedilol against σ₁ receptor (IC₅₀ = 1.57 μM).^[196]

5.1.12 | Conclusion on carvedilol multitargeting

The multitarget profile of carvedilol is well-known and often noticed in the literature.^[35,172] However, a detailed review of the literature regarding the full spectrum of carvedilol targets has not been performed.

Figure 2 shows a diagram with the spectrum of biological targets of carvedilol. Here and below, such diagrams show the maximum values of the drug affinities against the targets in the case of differing literature data. The affinity values are conventionally presented as pK_i* although this designation may mean one of the following parameters: pK_i, pK_d, or p(IC₅₀). As noted above, we conditionally accept that all these parameters can be compared because they are similar. The dotted lines indicate the values of the maximum drug concentrations in the blood plasma of patients (C_{max}), determined in clinical studies. The red dotted line corresponds to the maximum described value of C_{max}, and the green one corresponds to the minimum. These dotted lines allow in some ways to cut off the more

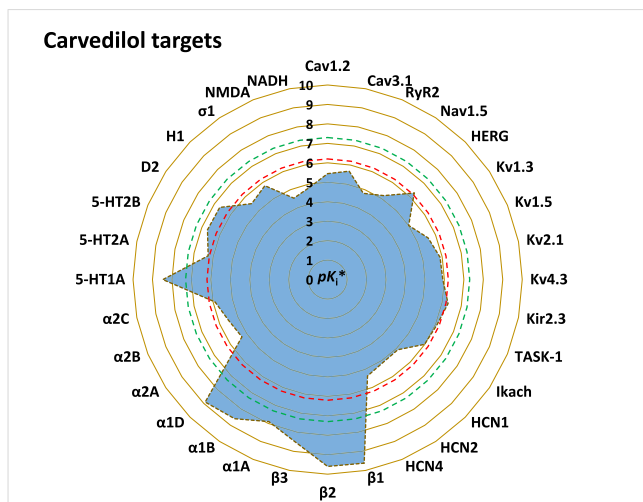


FIGURE 2 The diagram of carvedilol targets. The affinity values are presented as pK_i^* which means one of the following parameters: pK_i , pK_d or $pI(C_{50})$. For each target was taken the highest value of the affinity when there were several values in the literature. The red and green dotted lines indicate the maximal and minimal values of the peak plasma carvedilol concentrations in the clinical trials (pC_{max}), respectively.

significant pharmacological targets of the drug from the less significant ones. However, one should not forget the fact noted above that local high levels of drugs can reach in vivo significantly higher values than affinity values determined in vitro due, for example, to the high lipophilicity of the compounds.

The most pharmacologically significant targets of carvedilol which significantly exceed its plasma concentrations ($pC_{max} = 6.2-7.3$) are β_1 -, β_2 -, β_3 -ARs, and several subtypes of α_1 -ARs ($pK_i[\beta_1] = 9.6$; $pK_i[\beta_2] = 9.6$; $pK_i[\beta_3] = 8.51$; $pK_i[\alpha_1A] = 7.9$; $pK_i[\alpha_1B] = 8.6$; $pK_i[\alpha_1D] = 8.9$). These targets are believed to determine the main spectrum of the biological activity of the drug: inhibition of β -ARs provides a decrease in blood pressure, cardiac output, and a decrease in HR, while inhibition of α -ARs causes peripheral vasodilation, thereby reducing systemic vascular resistance.

It is interesting to note that carvedilol also has a high affinity for 5-HT_{1A} receptors ($pK_i = 8.5$), corresponding to adrenoceptor affinity, however, the involvement of this target in the biological effect of the drug has not been studied.

Of undoubted pharmacological significance are those biotargets of carvedilol, for which its affinity is at the level of concentrations corresponding to the plasma concentrations of the drug. Among them are a number of potassium channels: hERG ($pK_i = 6.3$); Kv1.5 ($pK_i = 5.6$); Kv2.1 ($pK_i = 5.6$); Kv4.3 ($pK_i = 5.9$); Kir2.3 ($pI_{C_{50}} = 6.3$); TASK-1 ($pK_i = 6.1$); I_{KACH} ($pK_i = 6.0$). As noted above in the works of various authors, there is a high probability that the antiarrhythmic properties of carvedilol are due to the affinity to potassium channels.

Plasma concentrations of the drug also correspond to the carvedilol affinity for 5-HT₂-receptors ($pK_i[5-HT_{2A}] = 6.3$; $pK_i[5-HT_{2B}] = 6.7$). The drug has a similar affinity for D₂-receptors

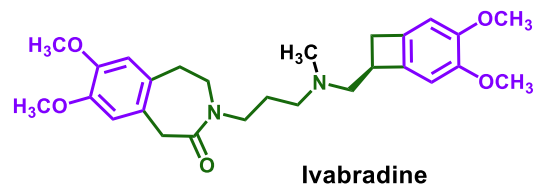
($pK_i[D_2] = 6.7$), σ_1 -receptors ($pK_i[\sigma_1] = 5.8$) and H₁-receptors ($pK_i[H_1] = 5.5$). There are no studies in the literature on the analysis of the participation of these biotargets in the cardioprotective properties of carvedilol. It can be assumed that the listed targets, including the previously mentioned 5-HT_{1A} receptor, may be involved in the presence of a positive neuropsychotropic effect of carvedilol, which favorably affects the therapy of CVD. Carvedilol is known to have antidepressant effects comparable to those observed for desvenlafaxine, which is a serotonin and norepinephrine reuptake inhibitor.^[197]

The affinity of carvedilol for calcium channels is slightly less than its clinically effective plasma concentrations ($pI_{C_{50}}(Cav1.2) = 5.4$; $pI_{C_{50}}(Cav3.1) = 5.7$). However, as noted above, it has been suggested that calcium channel blockade by carvedilol is involved in its vasorelaxant and antiproliferative effects, and also contributes to the mechanism of treatment of CHF.

Carvedilol has similar inhibition constants for the sodium channel ($pI_{C_{50}}(Nav1.5) = 5.2$), potassium channel 1.3-subtype ($pI_{C_{50}}(Kv1.3) = 5.0$), HCN channels ($pI_{C_{50}}(HCN1) = 5.1$; $pI_{C_{50}}(HCN2) = 5.1$, $pI_{C_{50}}(HCN4) = 5.4$). The literature suggests that these targets are involved in the cardioprotective properties of carvedilol, which has a favorable effect compared with other β -blockers in patients with CHF.

A few more biotargets identified for carvedilol have values that are more than an order of magnitude lower than the minimum plasma concentrations of the drug in the human blood however, even in relation to them, there are suggestions about their involvement in the positive clinical effects of this drug. Among them are the NMDA receptor ($pK_d = 4.5$), NADH dehydrogenase ($pK_i = 4.8$), and RyR2 receptor ($pI_{C_{50}} = 4.8$).

5.2 | Ivabradine



Ivabradine was discovered by Servier (France) in 1992 within a program to search for compounds with bradycardic activity in a series of zatebradine derivatives. The bradycardic effect of ivabradine was described as effective as zatebradine, but it was more specific as it induced a smaller increase in APD.^[198] The bradycardic action of ivabradine was not associated with any signs of negative inotropic action.^[199,200] Ivabradine is most often referred to in the literature as a "selective blocker of HCN channels," although, as will be seen below, this compound also has a fairly wide range of other targets.

In 2005, the European Medicines Agency (EMA) gave its approval for the use of ivabradine in the treatment of chronic stable

angina pectoris. In 2015, the US Food and Drug Administration followed suit, authorizing the drug's use in the management of stable CHF.^[201] The European Society of Cardiology guidelines in 2016 also recommended ivabradine in HF patients in sinus rhythm with an LV ejection fraction $\leq 35\%$, HR ≥ 70 , and persisting symptoms.^[202] There is a discussion in the literature about the ratio of antiarrhythmic and proarrhythmic properties of ivabradine in the context of the spectrum of its biological targets.^[36]

The structure of ivabradine contains two identical aromatic 3,4-dimethoxyphenyl pharmacophores, each of which is conjugated with saturated cycles: cyclobutane and azepinone. Together with these saturated cycles, the length of the linker that binds aromatic pharmacophores is 10 bonds. There is also a tertiary methyl-substituted nitrogen atom in the central part of the linker. The ivabradine molecule has an optically active center, the drug is a pure (S)-enantiomer.

After oral administrations, ivabradine is absorbed quickly, with a time of peak plasma concentration (T_{max}) of around 0.5–2 h, which is very similar across doses and dosing regimens. The absolute bioavailability of ivabradine is on average 40%, which reflects a sizeable first-pass effect. Ivabradine shows a mean protein binding of 70%. Ivabradine has been studied over a wide dose range in healthy subjects in single (0.5–40 mg) and multiple (8–32 mg twice a day) ascending oral dose studies. Ivabradine's area under the pharmacokinetic curve (AUC) and C_{max} were dose-linear up to 24 mg. After single and repeated doses of 5–20 mg C_{max} values were in the range of 8.7–64.1 $\mu\text{g/L}$ (i.e., from 19 to 136 nM).

Studies have shown that around 4.2% to 7.0% of the ivabradine dose was not changed and excreted in the urine, and there was no pattern detected. The calculated renal clearance range was between 84 and 136 mL/min, which implies that glomerular filtration was the main way of eliminating the drug through the kidneys.^[203–205]

5.2.1 | Ivabradine calcium channels blocking

Bois et al. found that ivabradine inhibits $I_{Ca,L}$ by about 20% at 10 μM and had no detectable effect on $I_{Ca,T}$ at the same concentration.^[206] Nevertheless, "FDA Pharmacological Review for Ivabradine" presented its significantly smaller affinity against L-type Ca^{2+} channels. The K_i value of ivabradine for the phenyl-alkyl-amine binding site of the L-type Ca^{2+} channels was 0.9 μM ($[\text{}^3\text{H}]\text{D888}$ assay), while there was no affinity for the dihydropyridine site of the same channels ($K_i > 100 \mu\text{M}$ in $[\text{}^3\text{H}]\text{PN200-110}$ assay). These data are in good agreement with the verapamil-like structure of ivabradine.^[207]

5.2.2 | Ivabradine potassium channels blocking

Though ivabradine has generally been considered to exhibit a good overall safety profile without significant effect on HR corrected QT interval, the meta-analysis of 11 clinical trials has concluded that ivabradine treatment is associated with a 15% increase in relative risk

of AF, and it was added to the list of "drugs with a conditional risk" of TdP in the "CredibleMeds" database of QT interval-prolonging drugs.^[208] Melagari et al. hypothesized that these properties can be related to ivabradine's hERG affinity. Indeed they found that ivabradine inhibits hERG channels with similar potency to that reported for native HCN channels ($\text{IC}_{50}(\text{hERG}) = 2.07\text{--}3.31 \mu\text{M}$). The drug prolonged ventricular repolarization and produced a steepening of the curve showing the restitution of the monophasic APD at 90% repolarisation in guinea pig Langendorff-perfused hearts.^[209]

Independently Lees-Miller et al. showed the same results: ivabradine prolonged AP at neonatal mouse VM and blocked the hERG current over a range of concentrations overlapping with those required to block HCN4 ($\text{IC}_{50}(\text{hERG}) = 6.8 \mu\text{M}$). The drug produced a tonic, rather than a use-dependent block. The mutation Y652A significantly suppressed the pharmacologic block of hERG by ivabradine. Disruption of C-type inactivation also suppressed the block of hERG by ivabradine.^[37] Later similar affinity values were shown by Haechl et al. for human hERG channels in tsA-201 cells ($\text{IC}_{50}(\text{hERG}) = 11 \mu\text{M}$).^[210]

Ivabradine is proposed as a potential antiarrhythmic medication due to its dual inhibitory influence on I_f and I_{Kr} currents, which leads to a rise in both the ERP and the post-repolarization refractoriness. Recently, experiments with a Langendorff-perfused rabbit heart setup revealed that ivabradine was able to decrease ventricular arrhythmias caused by digitalis and arrhythmic characteristics associated with short QT.^[211] Koncz et al. showed that ivabradine increased APD in human papillary muscles by 11% at 10 μM concentration, presumably due to I_{Kr} blockade.^[212]

Delpón et al. found that ivabradine exhibited a concentration-, voltage- and time-dependent block of hKv1.5 channels with K_d of 29.0 μM .^[213] Ivabradine also had no significant effect of Kv7.1 up to 100 μM .^[210]

5.2.3 | Ivabradine sodium channels blocking

There are several studies in the literature that show a moderate affinity of ivabradine for sodium channels. Haechl et al. showed that ivabradine inhibits human Nav1.5 channels with IC_{50} of 30 μM . The effects of ivabradine were not altered by any potential systematic current rundown. However, when 100 μM of the drug was washed out, the results showed that the process was slow and had some degree of irreversibility.^[210] In FDA Pharmacological Review for Ivabradine, its low affinity for the Nav1.5 channels ($K_i = 4.0 \mu\text{M}$) which was measured in the $[\text{}^3\text{H}]\text{batrachotoxin}$ assay is described.^[207]

In a study conducted by Hackl et al., the effects of ivabradine on Nav1 channels were examined. Native cardiomyocytes were isolated from mouse ventricles and the His-Purkinje system, and human Nav1.5 was studied in a heterologous expression system. Results showed that ivabradine inhibited Nav1 channels in a voltage- and frequency-dependent manner without changing the voltage-dependence of activation and fast inactivation, or the recovery from fast inactivation. Furthermore, the cardiac (Nav1.5), neuronal

(Nav1.2), and skeletal muscle (Nav1.4) channels isoforms, as well as sodium currents in native cardiomyocytes from the ventricles and the His-Purkinje system, were all inhibited by ivabradine within the same concentration range. Consequently, the authors suggested that ivabradine's inhibition of Nav1 channels in native cardiomyocytes and across different channel isoforms may be responsible for its antiarrhythmic potential.^[38]

5.2.4 | Ivabradine HCN channels blocking

The biological action of ivabradine is primarily attributed to its ability to block HCN channels. This drug binds to these channels and inhibits the cardiac pacemaker current (I_f)—a mixed sodium-potassium inward current that controls the spontaneous diastolic depolarization in the sinoatrial (SA) node, thereby slowing the HR. Ivabradine does not affect blood pressure, intracardiac conduction, or myocardial contractility as its effects are more specific to the SA node. In addition, ivabradine inhibits the retinal current (I_h), which is similar to the cardiac I_f and plays a role in temporal resolution of the visual system by reducing retinal responses to bright light stimuli. If I_h is partially inhibited under certain conditions such as rapid changes in light intensity, it can lead to luminous phenomena (phosphenes) experienced by patients.^[214]

Ivabradine is an effective blocker of all HCN receptor subtypes (HEK293 cells): $IC_{50}(\text{HCN1}) = 2.05 \mu\text{M}$; $IC_{50}(\text{HCN2}) = 2.29 \mu\text{M}$; $IC_{50}(\text{HCN3}) = 2.51 \mu\text{M}$; $IC_{50}(\text{HCN4}) = 2.15 \mu\text{M}$.^[44] Thollon et al. provided similar data: $IC_{50}(\text{HCN4}) = 0.54 \mu\text{M}$ (CHO cells).^[215] It was demonstrated that ivabradine block of HCN4 can occur only from the intracellular side when the channels are opened by hyperpolarization with enhanced binding upon frequent changes in the direction of ion flow. On the other hand, HCN1 channels can be blocked even when they are in a closed state.^[216] Comparison of the block efficiency of mutant versus WT HCN4 channels, measured by patch-clamp, revealed that residues Y506, F509, and I510 are involved in ivabradine binding.^[217]

5.2.5 | Ivabradine additional targets

In the FDA Pharmacological Review for ivabradine, its receptor binding profile is presented (Table 3). The receptor binding study was performed on 18 receptors and binding sites.^[207] Based on the results of these studies, the authors conclude that ivabradine showed “lack of affinity for AR ($\alpha 1$, $\alpha 2$, and β), serotonin (5-HT_{1A}, 5-HT_{1B}, 5-HT₂, and 5-HT₃), central benzodiazepine, dopamine (D₁ and D₂), adenosine (A₁), histamine (H₁), GABA_A, μ -opioid, muscarinic cholinergic receptors.” However, based on a number of the above findings, we believe that some of these targets may have pharmacological significance since the affinity values for them differ from $K_i(\text{HCN})$ by no more than an order of magnitude. Among them 5-HT₁-receptors ($K_i[5\text{-HT}_{1A}] = 29 \mu\text{M}$; $K_i[5\text{-HT}_{1B}] = 12 \mu\text{M}$), $\alpha 1$ -ARs ($K_i = 58 \mu\text{M}$), D₂-receptors ($K_i = 40 \mu\text{M}$),

TABLE 3 Ivabradine receptor binding profile according to Food and Drug Administration (FDA) Pharmacological Review.^[207]

Receptor	Ligand	K_i (μM)
5-HT _{1A}	[³ H]80-HDPAT	29
5-HT _{1B}	[¹²⁵ I]Cyanopindolol	12
5-HT ₂	[³ H]Ketanserin	>100
5-HT ₃	[³ H]BRL-34694	72
$\alpha 1$ -AR	[³ H]Prazosin	58
$\alpha 2$ -AR	[³ H]RX821002	>100
β -AR	[³ H]Dihydroalprenolol	>100
D ₁	[³ H]SCH23390	>100
D ₂	[³ H]Raclopride	40
M	[³ H]QNB	13
GABA _A	[³ H]SR95531	>100
GABA _A	[³ H]Ro15-1788	>100
H ₁	[³ H]Mepyramine	21
A ₁	[³ H]R(-)Pia	>100
μ	[³ H]DAGO	56

M₁-receptors ($K_i = 13 \mu\text{M}$), H₁-receptors ($K_i[H_{11}] = 21 \mu\text{M}$) and μ -opioid receptors ($K_i = 56 \mu\text{M}$).

Despite the absence of ivabradine binding to the GABA_A receptor when analyzing its affinity profile, Cavalcante et al. suggested the presence of this component in the drug's spectrum of action. This hypothesis was supported by the presence of anticonvulsant, antioxidant, and neuroprotective properties in ivabradine against classical seizure models, as well as its high affinity to GABA_A receptor predicted by molecular docking studies.^[218]

5.2.6 | Conclusion on ivabradine multitargeting

The so-called “selective and specific blocker of HCN channels” ivabradine actually turns out to be not so selective and specific as a number of other targets have been described that may be of physiological significance (Figure 3).

It is very interesting to note that for all biological targets of ivabradine, the values of binding constants are more than an order of magnitude higher than its maximum plasma concentration at the highest dose studied ($pC_{\text{max}} = 6.9$), and more than two orders of magnitude higher than its low-dose C_{max} values ($pC_{\text{max}} = 7.7$). At the same time, in a number of works on the analysis of additional targets of ivabradine, this fact is presented as evidence of the absence of any significance in the effects of the drug, while the same circumstance in relation to the main HCN target is not discussed in any way. In those works that clearly note the fact of a discrepancy between the C_{max} values and affinity constants for carvedilol biotargets, including HCN channels, it is suggested that the drug can significantly accumulate in

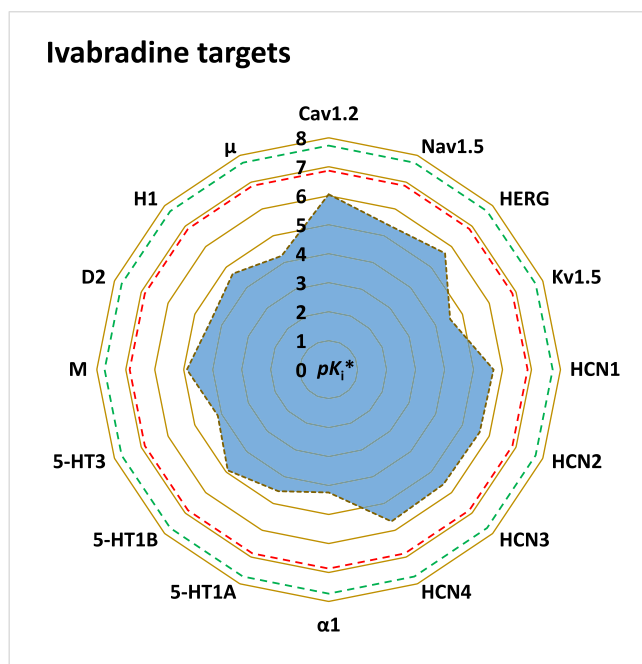
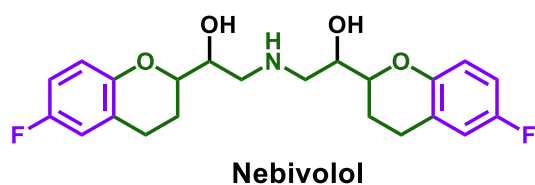


FIGURE 3 The diagram of ivabradine targets. The designations are similar to those in Figure 2.

lipid membranes due to its lipophilicity, which significantly increases its local concentrations near the targets.^[38]

Among all the identified molecular targets of ivabradine, the differences in their affinities are less than two orders of magnitude, which indicates a possible pharmacological significance for all of them. Nevertheless, an analysis of the literature allows us to conclude that, in addition to HCN blockade ($pI_{C_{50}} = 5.6-5.7$), the cardioprotective properties of ivabradine are significantly affected by its binding to the hERG channel ($pI_{C_{50}} = 5.7$) and the Nav1.5 channel ($pK_i = 5.4$). It cannot be ruled out that other ion channels also have their own contributions: Cav1.2 ($pK_i = 6.1$) and Kv1.5 ($pK_d = 4.5$). A set of nonchannel targets of ivabradine has also been described, including 5-HT₁-receptors, α_1 -ARs, D₂-receptors, M-receptors, H-receptors, and μ -opioid receptors (pK_i in the range of 4.2–4.9), however, their possible influence on the effects of the drug not explored.

5.3 | Nebivolol



Nebivolol was discovered in 1987 by Janssen Pharmaceutica during the searching of selective β_1 -blockers in a group of symmetrical 2,2'-azanediy bis[1-(chroman-2-yl) ethan-1-ol]s.^[219] In primary research, nebivolol possessed a high β_1 -affinity and β_1/β_2 -selectivity and it was selected for development.

In 1997, nebivolol came into medical use in Europe for treatment of hypertension. Lately, it was introduced in the US market after FDA approval in 2007. Nebivolol is a type of β -AR antagonist that does not have any impact on the functioning of the left ventricle. When taken over a prolonged period of time, it helps decrease peripheral resistance and widen the coronary arteries. There is no known evidence of it leading to any adverse changes in lipid metabolism or increasing the sensitivity to glucose. This medication is mainly employed as a treatment for hypertension, yet it may also be useful in managing angina, congestive HF, and arrhythmias, although it is yet to be sanctioned for these specific applications.^[220]

The biomimetic structure of nebivolol with a 9-bond linker and four optical centers predetermines its possible additional drug targets, which have been identified in various studies. Nebivolol is a combination of two isomers, ($\alpha R, \alpha' R, 2R, 2'S$)- α, α' -[iminobis(methylene)]bis[6-fluoro-3,4-dihydro-2H-1-benzopyran-2-methanol] ((S,R,R,R)-nebivolol) and ($\alpha S, \alpha' S, 2R, 2'S$)- α, α' -[iminobis(methylene)]bis[6-fluoro-3,4-dihydro-2H-1-benzopyran-2-methanol] ((R,S,S,S)-nebivolol), with each existing in equal amounts. Studies conducted on animals and humans have revealed that the antihypertensive and hemodynamic actions of this combination are more effective than those of the two isomers used separately. The β_1 -antagonistic properties of nebivolol are attributed to the (S,R,R,R)-isomer, while a decrease in the exercise-induced tachycardia is observed when the racemic mixture is used. The (R,S,S,S)-enantiomer of nebivolol is responsible for the nitric oxide-releasing effect. Moreover, the racemate and its enantiomers have been found to possess noteworthy antioxidant properties that are beneficial for the metabolism of cellular nitric oxide.^[221]

Nebivolol has a T_{max} of 1.5–4 h. Bioavailability can range from 12% to 96% for extensive to poor CYP2D6 metabolizers. For a 5–20 mg dose, nebivolol has a C_{max} of 1.78–8.02 ng/mL (i.e., 4.4–19.8 nM). Nebivolol is 98% bound to plasma proteins, mostly to serum albumin and it is metabolized mainly by glucuronidation and CYP2D6-mediated hydroxylation. Metabolites of nebivolol make a certain contribution to the action of the drug.^[222–224]

5.3.1 | Nebivolol β -adrenoreceptors inhibition

Nebivolol is well-known as the “selective β_1 -blocker” and it is proved to be the most β_1 -selective of the other β -blockers tested. In the studies of Janssen Pharmaceuticals, nebivolol possessed a high affinity for β_1 -AR ($K_d = 5.8$ nM; guinea pig right atrium) and selectivity relative to β_2 receptor ($K_d = 1.7$ μ M; guinea pig trachea).^[219]

The more detailed analysis of the affinity profile of nebivolol and its isomers was carried out using rabbit or rat lung tissues and [³H]

CGP-12177 or [³H]dihydroalprenolol radioligands respectively. Nebivolol revealed high affinity and selectivity for β -AR sites in the rabbit lung membrane preparation ($K_i = 0.9$ nM and β_2/β_1 ratio = 50). The drug dissociated slowly from these receptor sites. The activity resided in the (*S,R,R,R*)-enantiomer; the (*R,S,S,S*)-enantiomer revealed 175 times lower β_1 -AR binding affinity. The same results were obtained in the rat lung tissue. Nebivolol itself had $K_i[\beta_1] = 0.91$ nM and $K_i[\beta_2] = 44$ nM. The (*S,R,R,R*)-enantiomer had the comparable parameters ($K_i[\beta_1] = 0.54$ nM and $K_i[\beta_2] = 19$ nM) though the (*R,S,S,S*)-enantiomer was less potent with $K_i[\beta_1] = 138$ nM and $K_i[\beta_2] = 367$ nM.^[195] In human myocardium preparations, nebivolol's affinity (K_i) for the β_1 -adrenoceptor was found to be 5.8 nM which was ~300-fold higher than for β_2 -ARs ($K_i = 1700$ nM).^[225]

Inhibition of β_1 -AR by nebivolol leads to decreased resting HR, exercise HR, myocardial contractility, systolic blood pressure, and diastolic blood pressure which determines its effective antihypertension profile.^[226]

Although it is believed that affinity for the β_2 -receptor does not significantly contribute to the cardioprotective properties of nebivolol, there are reports that metabolized nebivolol by inducing a β_2 -AR-mediated rise in endothelial $[Ca^{2+}]_i$; increased endothelial cell NO production and therefore involved in NO-mediated arterial dilation in humans.^[227]

Nebivolol has been observed to not only possess β -antagonistic activity but also induce vasodilation in human and canine vascular systems when in concentrations higher than 50 μ M. This vasodilation is dependent on the endothelium and is inhibited by nitric oxide synthase (NOS) and soluble guanylate cyclase inhibitors. This indicates that its action is based on the modulation of nitric oxide production. In 2001, Gosgnach et al. found that nebivolol has a β_3 -AR agonist activity on cultured human endothelial cells which could explain its nitric oxide-dependent vasodilating properties.^[228]

Though nebivolol has a much lower affinity for β_3 - than for β_1 - or β_2 -ARs ($pK_i[\beta_3] = 5.6$ vs. $pK_i[\beta_1] = 9.17$ and $pK_i[\beta_2] = 7.96$)^[229] the direct binding of nebivolol to the β_3 -receptor remains one of the most attractive concepts that explains its specific endothelial vasodilation.^[230-233]

The effects of nebivolol on the vascular system, which are attributed to the eNOS enzyme, were observed in humans. It was found that nebivolol had direct endothelium-dependent vasodilation effects and increased the reactivity to stimuli such as hyperemia in both the arterial and venous circulation.^[226,231]

5.3.2 | Nebivolol α -adrenoreceptors inhibition

In [³H]WB410 radioligand binding assay in rat forebrain nebivolol's $pIC_{50}(\alpha_1\text{-AR})$ was measured as 5.5, and its $pIC_{50}(\alpha_2\text{-AR})$ in [³H] clonidine radioligand binding assay in rat cortex was >5.0.^[195] Rozec et al. found that nebivolol significantly shifted the concentration-response curve to phenylephrine, an α_1 -AR agonist in a concentration-dependent manner ($pK_d = 6.5$). In rat aorta, nebivolol-induced relaxation resulted from both inhibition of α_1 -ARs and

activation of β_3 -ARs.^[234] There are no other data on the α -antagonistic activity of nebivolol in the literature.

5.3.3 | Nebivolol RyRs inhibition

Tan et al. assessed the effect of nebivolol on RyR2-mediated SOICR in HEK293 cells, using single-cell Ca^{2+} imaging. They found that this drug effectively suppressed SOICR at concentrations of 3–30 μ M. The effects of *N*-nitro-L-arginine methyl ester (NOS inhibitor) and histamine or prostaglandin E2 (NOS activator) on nebivolol's SOICR inhibition were tested, but neither had any effect. This suggests that nebivolol's SOICR inhibition is independent of NOS stimulation. Furthermore, nebivolol was found to reduce the opening of single RyR2, as well as suppress spontaneous Ca^{2+} waves, in both intact hearts and mice exhibiting catecholaminergic polymorphic VT that had a RyR2 mutation (R4496C). Additionally, (*R,S,S,S*)-nebivolol that lacks an β -antagonistic effect was found to suppress SOICR and CPVT without reducing the HR. This evidence suggests that nebivolol has a RyR2-targeted action that can suppress SOICR and the VT associated with it. The authors believe that the found properties can position nebivolol as a promising agent for Ca^{2+} -triggered arrhythmias.^[235]

5.3.4 | Nebivolol 5-HT receptors inhibition

(*S,R,R,R*)-Nebivolol demonstrated similar affinity to the β_1 - and human 5-HT_{1A} receptors (with K_i values of 1.7 and 2.8 nM, respectively), while (*R,S,S,S*)-nebivolol displayed a far lower binding potency to the β_1 -adrenoceptor (with a K_i of 90 nM) but still had a strong affinity to the 5-HT_{1A} receptor (K_i of 15 nM).

The literature suggests that the 5-HT_{1A} receptor affinity of nebivolol can cause its vasodilating properties. The effects of nebivolol on the vascular bed of rats' kidneys and aorta were counteracted by NAN 190, a selective inhibitor of 5-HT_{1A} receptors. This finding suggests that the 5-HT_{1A} receptor may play a role in the vasodilating and NO-releasing effects of nebivolol, which could be due to the compound's strong binding affinity for these receptors as demonstrated in binding tests.^[236]

Nebivolol also has an affinity against 5-HT₂ receptors. In [³H] ketanserin radioligand binding assay in rat frontal cortex tissues, K_i value for nebivolol was found to be 700 nM.^[195]

5.3.5 | Nebivolol additional targets

Several sources present the results of studying the binding profile of nebivolol to various targets. Among them, the main ones are the research of Pauwels et al. and Mirams et al.^[195,237] (Table 4). These studies have data on the interaction of nebivolol with some potassium channels. The IC_{50} value in relation to hERG measured using manual patch clamp assay for the nebivolol was 0.3 μ M.^[237,238]

TABLE 4 Binding profile of neбиволол according. [195,237]

Target	pIC ₅₀	Assay	pIC ₅₀	Assay	pIC ₅₀	Assay
H ₁	5.25	[³ H] pyrilamin radioligand binding assay in guinea-pig cerebellum	-	-	-	-
D ₂	5.00	[¹²⁵ I] 2'-iodospiperone radioligand binding assay in rat striatum	-	-	-	-
Cav1.2	5.75	Radioligand binding assays using rat brain membrane preparations, dihydropyridine site	4.8	Inhibition of I _{Ca,L} in HEK293 cells measured using IonWorks Barracuda automated patch clamp platform (IWB)	-	-
Nav1.5	5.60	Radioligand binding assays using rat brain synaptosomes, veratridine site	5.2	Inhibition of I _{Na} in CHO K1 cells transfected with human Nav1.5 measured using IonWorks Quattro automated patch clamp platform (IWQ)	5.1	Inhibition of I _{Na} in HEK293 cells transfected with human Nav1.5 measured using IWQ
HERG	-	-	5.2	Inhibition of I _{Kr} in CHO cells stable expressing hERG measured using IWB	5.2	Inhibition of I _{Kr} in CHO K1 cells stably expressing hERG measured using IWQ
Kv7.1	-	-	4.8	Inhibition of I _{Ks} in CHO cells expressing human Kv7.1/human minK measured using IWQ	4.4	Inhibition of I _{Ks} in CHO cells transfected with Kv7.1/minK measured using IWQ
Kv4.3	-	-	4.3	Inhibition of I _{to} current in CHO K1 cells expressing human Kv4.3 measured using IWQ	-	-
Reference	[195]		[237]			

Mirams et al. measured the inhibition of I_{to} current in CHO K1 cells expressing human Kv4.3 and inhibition of slow delayed inward rectifying potassium current (I_{Ks}) in the same cells expressing human Kv7.1/human minK (minimal potassium channel subunit encoded by *KCNE1* gene) for nebivolol using IonWorks Quattro (IWQ) automated patch clamp platform. The pIC_{50} values were found to be 4.3 for Kv4.3 and 4.8 for Kv7.1.^[238]

There is practically no information in the literature on the involvement of potassium channels in the cardioprotective properties of nebivolol. Altunkaynak-Camca found that K_{ATP} channels involved in the nebivolol-induced vasorelaxation in the endothelium-intact aorta precontracted with potassium chloride. However, the analysis of direct blocking activity in relation to this channel was not carried out.^[239]

Nebivolol inhibited fast I_{Na} in HEK293 cells and in CHO K1 cells transfected with human Nav1.5 measured using IWQ with pIC_{50} 5.1 and 5.2, respectively.^[237] In the rat brain synaptosomes nebivolol inhibited veratridine site of Nav1.5 channel with $pIC_{50} = 5.6$.^[195]

According to Mirams et al., nebivolol blocks I_{CaL} in HEK293 cells with IC_{50} of 15.8 μ M measured using IonWorks Barracuda (IWB) automated patch clamp platform.^[237]

In radioligand binding assays using rat brain membrane preparation nebivolol showed affinity to the dihydropyridine site of Cav1.2 with $pIC_{50} = 5.75$. Pauwels et al. also found that nebivolol has a moderate affinity to H_1 and D_2 receptors with pIC_{50} values of 5.21 and 5.00, respectively.^[195]

5.3.6 | Conclusion on nebivolol multitargeting

Nebivolol is not positioned in the literature as a multitarget drug. On the contrary, it is considered the most selective β_1 -blocker. Nevertheless, the analysis of the drug binding profile according to various literary sources indicates the presence of a fairly large range of targets for this drug (Figure 4), which may be of pharmacological significance. Unfortunately, for most of the additional targets of nebivolol, there are no data on their involvement in biological effects, which requires further study.

Nebivolol has the highest affinity for the β_1 -AR ($pK_i = 9.2$), which is considered the key target of the drug. This value is almost an order of magnitude lower than the plasma concentration value for the lowest studied dose of nebivolol (5 mg, $pC_{max} = 8.4$). The drug has a similar high affinity for the 5-HT_{1A} receptor ($pK_i = 8.6$), which may contribute to its vasodilating properties. It is believed that both β_2 - ($pK_i = 8.0$) and β_3 -ARs ($pK_i = 5.7$), as well as α_1 -AR ($pK_i = 6.5$) also can contribute to the vasodilating activity of nebivolol by increasing endothelial cell NO production.

The affinities of nebivolol for all other targets are more than an order of magnitude higher than the plasma concentration value for the highest studied dose of the drug (20 mg, $pC_{max} = 7.7$), but they may also be involved in its biological effects. Thus, it is believed that the antiarrhythmic effect of nebivolol may be caused by its inhibition

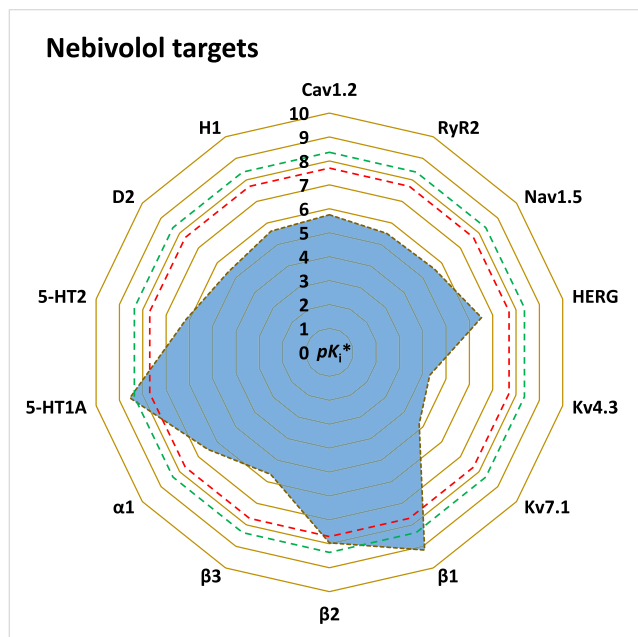
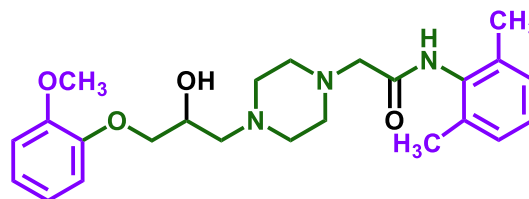


FIGURE 4 The diagram of nebivolol targets. The designations are similar to those in Figure 2.

of the RyR2 receptor, which suppresses SOICR ($pK_i \sim 5.5$ calculated from active doses).

The inhibitory activity of nebivolol to potassium (pK_i [hERG] = 6.5; pK_i [Kv4.3] = 4.3; pK_i [Kv7.1] = 4.8), sodium (pK_i [Nav1.5] = 5.6), calcium channels (pK_i [Cav1.2] = 5.8), dopamine (pK_i [D₂] = 5.4), histamine (pK_i [H₁] = 5.6) and serotonin (pK_i [5-HT₂] = 6.2) receptors was determined. However, the biological significance of these interactions has not been investigated.

5.4 | Ranolazine



Ranolazine

Ranolazine was designed by Syntex Inc. in 1986 as a lead in the group of cardioselective aryloxy- and arylthio-hydroxypropylene-piperazinyl acetanilides with calcium entry blockade properties.^[240] Clinical studies showed its efficacy as an anti-ischemic agent.^[241] Ranolazine was approved by FDA for the treatment of chronic angina in 2006 and by EMA in 2008 for the same indication. Later ranolazine has become one of the most used cardioprotective agents in the

world.^[242] Off-label uses of ranolazine include the treatment of some arrhythmias, such as VT.^[243]

The ranolazine molecule also has a biaromatic structure with a 12-bond linker. One aromatic ring contains an *o*-methoxy group, and the second contains two methyl groups. The linker contains a piperazine ring, an amide group, and a 1,2-diol system. Ranolazine is a racemate due to the optical center at the hydroxyl group.

In clinical practice, very significant doses of ranolazine are used: from 500 to 2000 mg twice a day. The time to reach peak serum concentration is quite variable but has been observed to be in the range of 2–6 h. Approximately 62% of the administered dose of ranolazine is bound to plasma proteins. C_{max} values for various doses range from 1450 to 5710 ng/mL, which is from 3.4 to 13.4 μ M. Ranolazine is rapidly heavily metabolized in the liver and gastrointestinal tract through the activity of the CYP3A4 enzyme. The presence of a large number of metabolites (more than 40) makes an additional contribution to the multitargeting of the drug.^[244,245]

5.4.1 | Ranolazine sodium channels blocking

A series of studies indicate that ranolazine has inhibitory properties to a large number of sodium channel subtypes. Inhibition of $I_{Na,L}$ by ranolazine in heart muscle is considered as one of its main mechanisms of action.

Inhibition of canine VM Nav1.5 by ranolazine assessed as reduction in sea anemone toxin (ATX-2) induced $I_{Na,L}$ by manual single-patch clamp assay occurred with $IC_{50} = 5.9 \mu$ M.^[246] Ranolazine also inhibited the human Nav1.5 channels expressed in HEK293 cells with $IC_{50} = 6.7 \mu$ M. This value was determined by blocking of tefluthrin-induced $I_{Na,L}$ using -20 mV voltage steps at a holding potential of -120 mV by whole cell patch clamp Qpatch method.^[247]

Ranolazine inhibits not only $I_{Na,L}$ but also peak I_{Na} in a voltage and frequency-dependent manner. Furthermore, sodium channel inhibition by ranolazine is tissue-specific, with different potencies in the atria and ventricles. The drug has a different potency to inhibit peak and late I_{Na} . While ranolazine inhibits $I_{Na,L}$ with IC_{50} values of 5.85 and 6.5 μ M in VM from normal and failing hearts, respectively, its inhibition of peak I_{Na} almost an order of magnitude lower, with IC_{50} values of 294 and 244 μ M in myocytes from normal and failing hearts, respectively. Ranolazine displays a greater capacity to obstruct peak I_{Na} in atrial myocytes than in VM. The cause of this atrial-targeted peak I_{Na} blocking by ranolazine includes a more negative half-inactivation voltage, a more depolarized resting membrane and a more gradual phase 3 of AP in atrial as compared to VM.^[248,249]

In pituitary GH3 cells, the IC_{50} values required for the blocking effects of ranolazine on transient and late components of I_{Na} were 7.4 and 1.5 μ M, respectively.^[250] It is believed that the Nav1.5 blocking activity of ranolazine determines to a large extent not only its antianginal properties but also antiarrhythmic action.

Kahlig et al. discovered that ranolazine selectively blocks the persistent current which is evoked by Nav1.1 mutations related to

epilepsy. At a concentration of 30 μ M ranolazine, there was no effect on the current density, activation, or steady-state fast inactivation of the WT Nav1.1 channels, but it did result in a mild slowing of recovery from the inactivation. The persistent current was blocked by ranolazine with 16 times more selectivity than the tonic block of peak current and 3.6 times more selectivity than the use-dependent block of peak current. The same selectivity was seen for ranolazine blocking the persistent current with Nav1.1 channel mutations associated with three different clinical syndromes—generalized epilepsy with febrile seizures plus (R1648H and T875M), severe myoclonic epilepsy of infancy (R1648C and F1661S) and familial hemiplegic migraine type 3 (L263V and Q1489K). Applying concentration levels found in the brain (1.3 μ M) to cells expressing the R1648H channels was enough to suppress the channel activation during slow voltage ramps, which is in line with the inhibition of the persistent current.^[251]

Peters et al. suggested that ranolazine may have an anti-convulsant effect through affinity for sodium channels exposed in the brain. They characterized how ranolazine affects the brain Nav1.2 channels. In patch-clamp experiments, it was observed that the administration of ranolazine caused a faster onset and slower recovery of both fast and slow inactivation. Additionally, use-dependent inactivation was seen to be maximized, while sodium currents on the macroscopic and ramp levels were decreased when ranolazine was applied at pH 7.4. However, at pH 6.0, the speeding up of fast inactivation recovery was inhibited and use-dependent block was reduced by ranolazine. The time constants of both slow inactivation onset and recovery were considerably increased when 100 μ M of ranolazine was applied at pH 6.0 in comparison to pH 7.4.^[252]

In HEK 293T cells, ranolazine blocked Nav1.4 with $IC_{50} = 2.4 \mu$ M. Use-dependent block of Nav1.4 channel isoform by ranolazine during repetitive pulses ($+50$ mV/10 ms at 5 Hz) was strong at 100 μ M, up to 77% peak current reduction. On- and off-rates of ranolazine were 8.2 μ M(-1) s(-1) for Nav1.4 open channel.^[253]

El-Bizri et al. studied the ranolazine block of human Nav1.4 sodium channels. It was found that ranolazine interacts with the open state and stabilizes the inactivated state of Nav1.4 channels, causes voltage- and use-dependent block of I_{Na} and suppresses persistent I_{Na} ($IC_{50}(\text{Nav1.4}) = 3.8 \mu$ M). The authors suggested that ranolazine might be useful to reduce the sustained AP firing seen in paramyotonia congenital (PMC).^[254]

LoRusso et al. conducted an open-label, single-center trial of ranolazine to evaluate efficacy and tolerability in patients with PMC. The results showed that both subjective symptoms and clinical myotonia were significantly improved. Myotonia duration was reduced, but this change was not statistically significant in all muscles tested.^[255]

Using the patch-clamp technique, Rajamani et al. investigated the effects of ranolazine on the human Nav1.7 (hNav1.7 + β 1 subunits) and rat Nav1.8 (rNav1.8) channels expressed in HEK293 and ND7-23 cells, respectively. At a holding potential of -120 or -100 mV, ranolazine reduced the I_{Na} of hNav1.7 and rNav1.8 with IC_{50} values

of 10.3 and 21.5 μM , respectively. When 5-s depolarizing prepulses to -70 mV (for hNav1.7) and -40 mV (for rNav1.8) were applied, the potency of I_{Na} block by ranolazine increased to 3.2 and 4.3 μM , respectively. Additionally, ranolazine caused a hyperpolarizing shift of the steady-state fast, intermediate and slow inactivation of hNav1.7, and slow and intermediate inactivation of rNav1.8, implying an interaction between ranolazine and the inactivated states of both channels. With a concentration of 30 μM , ranolazine demonstrated a use-dependent block (10-ms pulses at 1, 2, and 5 Hz) of hNav1.7 and rNav1.8 I_{Na} and accelerated the onset of, as well as slowed the recovery from inactivation, of both channels. A longer depolarizing pulse duration between 3 and 200 ms did not modify the effects of 100 μM ranolazine. So ranolazine was shown to block the open state and interact with the inactivated states of Nav1.7 and Nav1.8 channels, potentially leading to an increased effect of the drug at higher firing frequencies, such as in injured neurons.^[256] According to Wang et al. ranolazine is able to block Nav1.7 in HEK 293 T cells with IC_{50} 1.7 μM .^[253]

Since Nav1.7 and Nav1.8 channels are implicated in neuropathic pain, Gould III et al. suggested that ranolazine can be used to treat this pathology. Indeed, administration of ranolazine in a dose-dependent manner effectively suppressed the mechanical and cold allodynia that was caused by a spared nerve injury, without causing any detrimental effects such as ataxia or other behavioral side effects in rats.^[257]

Estacion et al. demonstrated that ranolazine is capable of producing comparable inhibition of peak and ramp currents of WT Nav1.7 and mutant Nav1.7 ion channels associated with inherited erythromelalgia and paroxysmal extreme pain disorder. In addition, at a concentration commonly used in clinical settings, ranolazine was found to be effective in blocking rapid firing of DRG neurons harboring WT Nav1.7 channels, yet had no effect on cells expressing the mutant variant of the channel.^[258]

5.4.2 | Ranolazine potassium channels blocking

In the isolated canine VM, ranolazine exerts a concentration-dependent inhibition of I_{Kr} with IC_{50} of 11.5 μM .^[246] In conventional voltage clamp using HEK 293 cells stably expressing WT hERG channels, ranolazine inhibited I_{Kr} with an IC_{50} of 8.03 μM ; peak I_{Kr} during ventricular AP clamp was inhibited ~62% at 10 μM .^[259]

Ranolazine inhibition of hERG channels expressed in CHO cells using voltage step to -50 mV for 300 ms from -80 mV holding potential by automated patch clamp assay with IC_{50} of 13.4 μM .^[247]

Ranolazine has been found to produce a blocking effect on hERG channels that leads to an extended period of repolarization and an increased QTc. However, this effect is countered by the drug's ability to inhibit $I_{\text{Na,L}}$, which prevents ventricular arrhythmias and TdP. Studies have demonstrated that in patients with LQT3 syndrome, which is caused by an increase in $I_{\text{Na,L}}$, ranolazine has proven to suppress arrhythmias by reducing QTc in a dose-dependent manner. It has been observed that at a plasma concentration of approximately

4 μM , QTc can be shortened by 22–40 ms, and by 24 ms for every 2 μM increase in plasma concentration. This effect has been seen in patients with both LQT1 (LQT with mutation of *KCNQ1* gene that encodes for the I_{Ks} current) and LQT2 (LQT with mutation of *KCNH2* gene that encodes for the I_{Kr} current) as well.

As a result, ranolazine has both a clinically relevant effect on I_{Na} and I_{Kr} , which appears to give it a more beneficial impact on the regularity of cardiac repolarization than that of solely I_{Kr} blockers. In fact, it has been demonstrated that ranolazine has a more desirable effect on the atrial ERP than that of single I_{Kr} blockers, like dofetilide.^[260]

The effects of ranolazine on Kv4.3 channels were examined in the whole-cell patch-clamp experiment by Kim et al. Ranolazine was found to inhibit the peak amplitude of Kv4.3 in a reversible, concentration-dependent manner with an IC_{50} of 128.31 μM . Its effect on activation kinetics did not differ at concentrations of up to 100 μM . The Kv4.3 inhibition by ranolazine increased steeply between -20 and $+20$ mV. However, in the full activation voltage range, no voltage-dependent inhibition was found. The drug also shifted the voltage dependence of the steady-state inactivation of Kv4.3 in the hyperpolarizing direction in a concentration-dependent manner. Ranolazine blocked an inactivated state of Kv4.3 with K_i of 0.32 μM . Little use-dependent inhibition was observed at 1 and 2 Hz. In addition, ranolazine had no effect on the time course of recovery from the inactivation of Kv4.3. It is possible that the cardioprotective effects of the drug are linked to its ability to inhibit Kv4.3 in the inactivated state, especially in pathologic conditions such as cardiac ischemia, where membrane potentials of myocytes are depolarized and the fraction of Kv4.3 channels in the inactivated state is abnormally high.^[261]

Ratel et al. discovered that ranolazine acts as a suppression agent for TASK-1 potassium channels, reducing TASK-1 currents with an IC_{50} of 30.6 μM when tested on mammalian cells and 198.4 μM when tested on *Xenopus laevis* oocytes. They determined that the inhibition of TASK-1 by ranolazine is not reliant on frequency, but is impacted by voltage, displaying a higher level of inhibition at more depolarized membrane potentials. The authors postulated that the interruption of TASK-1 could contribute to the antiarrhythmic effects of ranolazine that were observed.^[262]

Chen et al. investigated the blocking of Kir by ranolazine in pituitary GH3 cells hyperpolarizing from -10 to -120 mV. They compared the peak amplitudes of Kir in the presence of ranolazine to those obtained after the application of E-4031 (10 μM). It was observed that ranolazine (0.1–30 μM) suppressed the amplitudes of E-4031-sensitive currents in a concentration-dependent manner. The IC_{50} value of ranolazine on Kir was determined to be 0.92 μM .^[250]

5.4.3 | Ranolazine calcium channels blocking

Antzelevitch et al. found that in dogs' ventricular tissues ranolazine inhibited late $I_{\text{Ca,L}}$ with an IC_{50} of 50 μM , and the significant inhibition (25%–30%) occurred within the therapeutic range (2–6 μM). The

drug weakly inhibited I_{Na-Ca} (inward sodium-calcium exchange current), peak $I_{Ca,L}$, with 91 and 296 μM , respectively.^[246] So ranolazine is a weak direct vasodilator and has a minimal direct effect on atrioventricular nodal conduction.^[260]

Sicouri studied the impact of ranolazine in a Timothy syndrome experimental model by utilizing Cav1.2 agonist BayK8644 to imitate the gain of $I_{Ca,L}$. Clinically relevant concentrations of ranolazine (10 μM) suppressed APD and QT prolongation actions of BayK8644. The drug also prevented the development of ventricular extrasystoles and tachycardia (monomorphic, bidirectional, or TdP) induced by BayK8644.^[263]

5.4.4 | Ranolazine RyRs inhibition

Parikh's research has shown that ranolazine also inhibits RyR2, possibly contributing to its antiarrhythmic effect, namely in suppression of EADs and TdP. Direct effects of ranolazine on cardiac RyR2 were investigated in single channels and changes in Ca^{2+} -dependent high-affinity ryanodine binding. Ranolazine (10 μM) suppressed APD prolongation, EAD, and TdP induced by E4031. Simulations with the Mahajan model closely reproduced experimental data except for EAD suppression by the drug. Ranolazine reduced the open state probability of RyR2 ($\text{IC}_{50} = 10 \mu\text{M}$) in bilayers and shifted EC_{50} of Ca^{2+} -dependent ryanodine-binding from 0.42 to 0.64 μM at 30 μM concentration.^[264]

5.4.5 | Ranolazine α -adrenoreceptors inhibition

Virsolvy et al. proposed that dynamic coronary stenosis could be alleviated by ranolazine through its action on the α_1 -adrenergic mediated vasoconstriction. Clinical trials have suggested a correlation between the anti-anginal effects of ranolazine and improved regional coronary blood flow. However, ranolazine has not been observed to cause hemodynamic side effects like orthostatic hypotension or tachycardia, unlike other α_1 -AR antagonists used to treat hypertension. Though there have been reports of orthostatic hypotension in healthy volunteers with high doses of ranolazine (2000 mg), no such effect was seen at therapeutic doses (500–1000 mg). The IC_{50} value for α_1 -AR was 8.4 μM , which is within the range of therapeutic concentrations. At this concentration, ranolazine exhibited partial vasorelaxation without any vasodilatory effect. At higher concentrations, however, complete vasorelaxation was observed. This could account for the lack of hemodynamic effects and match up with clinical evidence.^[265]

Zhao et al. analyzed the adrenergic binding profile using a radioligand binding assay in rat tissues. They found that ranolazine bound to α -ARs with micromolar affinity, the K_i values for ranolazine ranged from a low of 8.2 μM for binding to α_{1A} receptors in membranes from rat salivary gland to a high of 19.5 μM for binding to α_{1B} in membranes from rat liver.

Ranolazine administered intravenously in bolus form caused a temporary and dose-dependent decrease in LV systolic pressure, mean

arterial pressure (MAP), and mean coronary vascular resistance, as well as an increase in LV positive dP/dt, HR, and CBF in dogs. Although 4–5 μM and 11–13 μM concentrations of ranolazine did not alter the changes in blood pressure and HR caused by stimulation of both α - and β -ARs, these effects were significantly reduced by the higher concentration of the drug. When the transmission of autonomic ganglia was blocked with hexamethonium, both 4–5 μM and 11–13 μM concentrations of ranolazine significantly reduced the changes in MAP and HR caused by stimulation of α - and β -ARs. In the hexamethonium-treated dog, ranolazine decreased MAP but had no effect on HR, implying that the drug was responsible for vasodilation but not a direct effect on HR. The authors concluded that ranolazine had a weak anti-adrenergic effect, which became more prominent when autonomic reflex regulation of cardiovascular function was disabled.^[266]

The Pharmacology Review of FDA Approval Documents for ranolazine (Drug Products: Ranexa) presented a similar α -adrenergic binding profile. At the concentration of 10 μM , ranolazine inhibits the various subtypes of α -ARs with the following values: 57% for α_{1A} ; 50% for α_{1B} ; 59% for α_{2A} ; 36% for α_{2B} . Thus, ranolazine also has an affinity for the α_2 subtype of ARs, however, the involvement of this target in the effects of the drug has not yet been studied.^[267]

5.4.6 | Ranolazine β -adrenoreceptors inhibition

β -ARs antagonistic properties of ranolazine were studied by Zhao et al. Radioligand binding assay demonstrated that in rat ventricle tissue $K_i(\beta_1) = 8.6 \mu\text{M}$ and in guinea pig lung $K_i(\beta_2) = 14.8 \mu\text{M}$. It has already been noted above that the joint α - and β -ARs antagonistic properties are involved in the vascular effects of ranolazine.^[266]

FDA Approval Documents for ranolazine presented the binding characteristics of the drug for three β -ARs isoforms. At the concentration of 10 μM , ranolazine inhibited β_1 -AR for 43%, β_2 -AR for 65%, and β_3 -AR for 31%.^[267]

According to radioligand binding studies performed by Létienne et al. in rat hearts and guinea-pig lungs for β_1 - and β_2 -ARs affinity, respectively, an even greater affinity for these targets was shown (pK_i 5.8 and 6.3, respectively). The authors also studied the functional β -ARs antagonist activity of ranolazine in the rat cardiovascular system. The drug had a weak effect when blocking isoprenaline-induced positive inotropic responses, requiring concentrations of 0.32–10 μM . In rats with bivagotomy and atropinization, intravenous injections of ranolazine in doses higher than 10 mg/kg caused pronounced bradycardia, which appears to be unrelated to inhibition of β_1 - and β_2 -ARs. Cumulative incremental doses of isoprenaline administered to pithed rats induced concomitant depressor and chronotropic responses. Ranolazine dose-dependently and competitively antagonized isoprenaline-induced decreases in diastolic arterial pressure and increases in HR. These data indicate that ranolazine behaves as a weak β_1 - and β_2 -ARs antagonist in the rat cardiovascular system.^[268]

Flenner et al. found that ranolazine improved tolerance to high workload in cardiomyocytes of mice with hypertrophic cardiomyopathy by antagonizing β -adrenergic stimulation and slightly desensitizing

myofilaments to Ca^{2+} and not by blocking late Na^{+} -current. Although this effect did not translate into therapeutic efficacy *in vivo*.^[269]

5.4.7 | Mitochondrial fatty acid oxidation inhibition by ranolazine

At medically appropriate amounts, ranolazine demonstrates the characteristics of a slight inhibitor of fatty acid oxidation. Treatment with ranolazine leads to an increase in pyruvate dehydrogenase activity and glucose oxidation. This drug has been recognized to boost the interconnection between glycolysis and glucose oxidation, and it restrains the electron transport chain in weakened or unlinked mitochondria, avoiding ATP wastage due to pointless cycling. Because of these properties, it is thought that the inhibition of fatty acid oxidation and the following augmented glycolysis-glucose oxidation connection is the cause of the helpful impacts of ranolazine in HF.^[270,271]

5.4.8 | Ranolazine additional targets

In the Pharmacology Review of FDA Approval Documents for ranolazine (Drug Products: Ranexa) the data on the affinity of ranolazine for a series of biological targets are available. At the concentration of 10 μM ranolazine inhibits dopamine D_5 receptors by 22%; M_3 -receptors by 21%; neuropeptide Y_2 by 31%; 5-HT_{1A} receptors by 65%; 5-HT₂ receptor by 23%; σ_1 receptor by 25%.^[267]

Ranolazine in high doses has been found to prevent the uptake of noradrenaline and serotonin in the pig brain. Tolunay theorizes that the side effects of hallucinations, anxiety, insomnia, tremors, headaches, dizziness, nausea, palpitations, and prolonged effects can be attributed to the drug's ability to act as a serotonin agonist.^[272]

5.4.9 | Conclusion on ranolazine multitargeting

Ranolazine has multiple molecular targets and is not highly specific. Figure 5 shows a diagram of the spectrum of biological targets of ranolazine. The analysis of this diagram indicates that the affinity of the drug for most of the proven biological targets is quite similar, the spread does not exceed two orders of magnitude, and for the majority, they are within the same order. At the same time, the binding characteristics of these targets are mainly within the plasma concentrations of the drug ($\text{pC}_{\text{max}} = 4.9\text{--}5.5$). It is interesting to note that the K_i value for the $\text{I}_{\text{Na,L}}$, which is considered the main target of ranolazine, is less than for some other targets. While the maximum value of pK_i for Nav1.5 is 5.23, the affinity of ranolazine for Kv4.3 and Kir is 6.49 and 6.04, respectively, and the affinity for β_1 - and β_2 -ARs is 5.8 and 6.3, respectively.

Various studies indicate that β -ARs antagonistic properties are involved in the vascular effects of ranolazine. At the same time, the affinity of ranolazine for various potassium channels, including hERG ($\text{pK}_i = 5.1$) and TASK-1 (4.51), determines, at least to some extent, its antiarrhythmic effect.

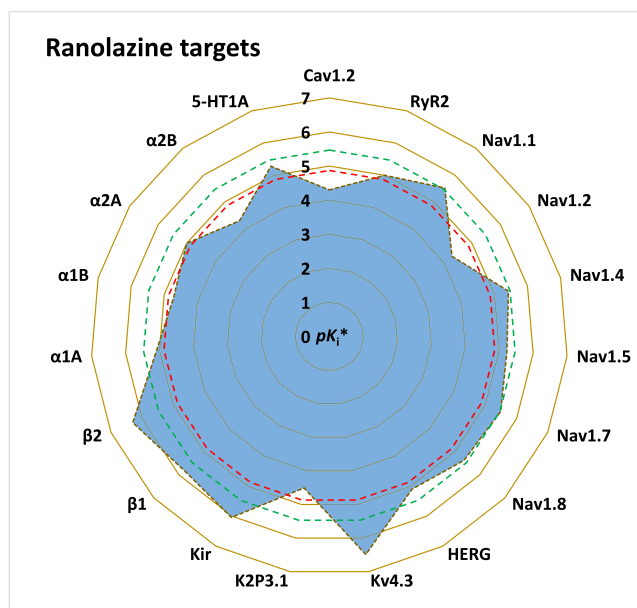


FIGURE 5 The diagram of ranolazine targets. The designations are similar to those in Figure 2.

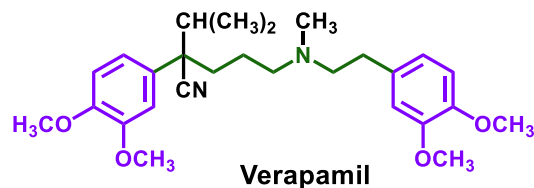
The interaction of ranolazine with a series of different sodium channels has been widely studied, among which, in addition to Nav1.5, there were Nav1.1 (active doses 1–3 μmol), Nav1.2 (active doses 10–100 μmol), Nav1.4 ($\text{pK}_i = 5.42$), Nav1.7 ($\text{pK}_i = 5.49$), and Nav1.8 ($\text{pK}_i = 5.37$). It is believed that the ability of ranolazine to bind to these channels, which are present to a greater extent in the central and peripheral neurons, as well as in the skeletal muscle, determines its ability to prevent neuropathic pain, myotonia, and even epilepsy.

At a therapeutically significant concentration, ranolazine inhibits RyR2 receptors ($\text{pK}_i = 5.0$). There is evidence that the antiarrhythmic effect of the drug is also due to this target.

It was shown that ranolazine has an affinity for α -ARs ($\text{pK}_i[\alpha_1\text{A}] = 5.09$; $\text{pK}_i[\alpha_1\text{B}] = 4.71$; $\text{pK}_i[\alpha_2\text{A}] = 5.0$; $\text{pK}_i[\alpha_2\text{B}] \sim 4.3$), which may be involved in its vasoconstriction and anti-anginal properties.

Finally, there is information about the ability of ranolazine to block the Cav1.2 channel ($\text{pK}_i = 4.3$) and 5-HT-receptors, primarily 5-HT_{1A} ($\text{pK}_i = 5.28$) and some others. However, their role in the activity of the drug has not yet been studied.

5.5 | Verapamil



Verapamil was the first cardioprotective drug of a biaromatic nature, it was discovered in the 1960s by Knoll. Primary studies have shown that verapamil is a calcium channel blocker. Over more than half a century of successful history of clinical use and detailed study of the drug, a wide range of other drug targets have been identified, many of which are undoubtedly pharmaceutically significant.^[273]

Verapamil is used for the treatment of ischemic heart disease including variant angina, unstable angina, chronic stable angina, supraventricular tachyarrhythmias, and hypertension.^[274] Among the non-FDA-approved indications for verapamil are as follows: acute coronary syndrome, hypertrophic cardiomyopathy, and idiopathic VT.^[275]

Verapamil's molecule contains two 3,4-dimethoxyphenyl groups linked by an *N*-containing linker 8 bonds long with cyano-, isopropyl-, and *N*-methyl groups. The molecule has one optical center, due to which the drug is a mixture of (*R*)- and (*S*)-enantiomers. Dimethoxyphenyl pharmacophores, which are characteristic of a large number of different compounds with cardioprotective activity, are one of the reasons for the multitargeting of the drug.

In medical practice, verapamil is mostly used in doses of 40–240 mg. Only 10%–20% out of the 90% of the dose absorbed from the digestive tract penetrates the circulatory system in an unchanged form. About 90% of verapamil binding with plasma proteins. The drug is metabolized to about 10 metabolites with norverapamil as the most important of them. Its pharmacological activity attains about 20% of the activity of verapamil.

Verapamil has a short plasma half-life of approximately 2–7 h and when taking repeated doses—4.5–12 h. After single and repeated doses of 40–240 mg verapamil the C_{\max} values were in the range of 28.3–272 ng/mL (i.e., from 62 to 598 nM).^[276–279]

5.5.1 | Verapamil calcium channels blocking

Verapamil was the first representative of the calcium channel blockers family discovered at Knoll AG during the synthesis of papaverine derivatives in the late 1950s—early 1960s. Wiśniowska et al. collected literature data on the affinity of verapamil obtained in various whole-cell patch clamp experiments with different cellular models, temperatures, the concentration of Ca^{2+} cations in experimental bath solutions, pulse width, holding potential and depolarization/measurement voltage (Table 5). The IC_{50} values vary from 0.1 to 50 μM .^[288]

Radioligand binding assays which were performed by Fermini et al. for verapamil by using [³H]-nitrendipine (dihydropyridine site), [³H]-verapamil (phenylalkylamine site) and [³H]-diltiazem (benzothiazepine site) as the respective radioligands for the various L-type calcium channel binding sites (rat cerebral cortex membranes) demonstrated the selectivity of verapamil for the phenylalkylamine over the benzothiazepine sites and especially over dihydropyridine site ($\text{pK}_i = 8.00$ vs. $\text{pK}_i = 6.39$ and $\text{pK}_i < 5.00$ [36%], respectively).^[289]

It is believed that the primary way in which verapamil works to treat angina and hypertension is by inhibiting L-type calcium channels. This inhibition of calcium influx reduces the contraction of the smooth muscle in the peripheral circulation, leading to the relaxation and dilation of blood vessels. This, in turn, decreases systemic vascular resistance and lowers blood pressure. Additionally, the decrease in vascular resistance decreases the amount of force the heart needs to use, reducing the energy consumption and oxygen requirements of the heart muscle and, as a result, relieving angina.^[290]

Verapamil acts to slow down the HR of patients with arrhythmia by restricting the influx of calcium and lengthening the refractory period of the AVN. This consequently decreases conduction and slows HR.

TABLE 5 Cav1.2-affinity of verapamil obtained in various experiments.

IC_{50} (μM)	Cellular model	Temperature ($^{\circ}\text{C}$)	Ca^{2+} bath solution (mM)	Pulse width (s)	Holding potential (mV)	Depolarization/measurement voltage (mV)	Reference
23.5	CHO cells	Room	0	0.025	−100	0	[280]
0.1	Guinea pig VM	Room	1.8	0.4	−40	0	[281]
0.164	Guinea pig VM	Room	2	0.2	−50	10	[282]
0.6	Guinea pig VM	36–37	1.8	0.3	−40	10	[283]
0.79	Guinea pig VM	20–25	0	0.2	−70	10	[284]
0.94	Guinea pig VM	20–22	1.8	0.25	−40	10	[285]
24	HEK293 cells	Room	10	0.5	−80	10	[286]
47	HEK293 cells	20–25	0	0.1	−60	20	[284]
0.15	Kitten heart ventricle membranes	37	-	-	-	-	[287]

Verapamil inhibits [³H]D-888 binding to Cav1.1 channels with K_i of 58 nM.^[291] Tarabova et al. studied the influence of verapamil on calcium currents (I_{Ca}) in mouse inner hair cells (IHCs) that are carried by the Cav1.3 subtype of L-type calcium channels. They play an important role in the synaptic transmission of sound-evoked mechanical stimuli. Whole-cell I_{Ca} was measured using the patch-clamp technique in mouse IHCs aged postnatal Day 3–7 with 5 mM calcium as a charge carrier. Verapamil blocked I_{Ca} in IHCs in a concentration-dependent and voltage-independent manner with IC_{50} of 199 μ M. The drug (300 μ M) enhanced current inactivation from –20 to +20 mV.^[292]

In addition to blocking L-type channels, verapamil has been reported to block T-type calcium channels.^[293] This type of cross-reactivity is likely to be beneficial in the effective control of blood pressure. Verapamil has been shown to block T-channels, with IC_{50} values of 30 μ M in vascular smooth muscle^[294] and 70 μ M in spermatogenic cells.^[295]

Freeze et al. conducted experiments in which they stably expressed human Cav3.1 T-type channels in HEK293 cells, to determine the effects of verapamil on the macroscopic and gating currents. The drug blocked $I_{Ca,T}$ -current at a micromolar concentration (21.4 μ M) at polarized potentials similar to those reported for Cav1.2 channels. However, unlike for $I_{Ca,L}$ -current verapamil did not affect the current time course. The drug also had a use-dependent effect and significantly slowed the recovery from inactivation. Moreover, the inhibition of current was dependent on potential, with an IC_{50} of 4.9 μ M at –70 mV, and this dependence was only seen at negative potentials. Furthermore, the gating currents were not affected by verapamil. The authors theorize that verapamil inhibits the channel pore through an open/inactivated conformation of the channel.^[126]

In Perez-Reyes' research the authors identified compounds that block the Cav3.2 T-type channel with high affinity. Using a validated Ca^{2+} influx assay into a cell line (HEK 293) expressing recombinant Cav3.2 channels it was shown that verapamil blocks Cav3.2 T-type channel with $IC_{50} = 32.7 \mu$ M.^[296]

In robust high-throughput human Cav-channel assays using IWB verapamil had $IC_{50s}(Cav3.2) = 14.3; 21.2, \text{ and } 12.7$ at prepulse –50 mV; prepulse –90 mV and 0.1 Hz, respectively.^[297]

The putative inhibitory effects of verapamil on neuronal Ca^{2+} channels were studied by Dabrov et al. by investigating its effects on either K^+ - or veratridine-evoked [³H]-dopamine release in rat striatal slices. Involvement of Cav2.2, Cav2.3, and Cav2.3 channels was identified by sensitivity of [³H]-dopamine release to ω -conotoxin GVIA (ω -CTx-GVIA), ω -agatoxin IVA (ω -Aga-IVA), and ω -conotoxin MVIIC (ω -CTx-MVIIC), respectively. The authors found that verapamil can block Cav2.1 ($IC_{50} \sim 30 \mu$ M) and at higher concentrations possibly Cav2.2 and Cav2.3 channels linked to [³H]-dopamine release.^[298] There are suggestions that the blockade of Cav2 channels is involved in its mechanism of action in the treatment of cluster headaches.^[299]

Ishibashi et al. investigated the effects of verapamil, on Cav2.1 channels in freshly isolated rat Purkinje neurons. The drug blocked

Cav2.1 current in a concentration-dependent manner without any change in the current-voltage relation ($IC_{50} = 62 \mu$ M).^[300] Kurushev et al. using robust high-throughput human Cav channel IWB assays found that verapamil has $IC_{50s}(Cav2.1) = 5.0; 22.1; \text{ and } 12.4$ at prepulse –50 mV; prepulse –90 mV and 0.1 Hz, respectively; and $IC_{50s}(Cav2.2) = 13.1; 46.0; \text{ and } 17.8$ at prepulse –50 mV; prepulse –90 mV and 0.1 Hz, respectively.^[297]

5.5.2 | Verapamil sodium channel blocking

Mirams et al. measured the inhibition of I_{Na} by verapamil using whole-cell patch clamp experiments in HEK293 cells stably transfected with human Nav1.5 cDNA. The IC_{50} value was found to be 41.5 μ M. The authors suggest that Nav1.5 blocking by verapamil together with Cav1.2 blocking involved in preventing clinical torsadogenic risk associated with its hERG-blocking potential.^[281] Kramer et al. present a similar verapamil's Nav1.5 blocking activity ($IC_{50} = 32.5 \mu$ M).^[301] In the highly invasive breast cancer cell line MDA-MB-231 verapamil blocked I_{Na} with $IC_{50} = 37.6 \mu$ M).^[302]

In the HEK293 cell line stably expressing human Nav1.5 α - and β 1-subunits verapamil blocked peak Na^+ current with IC_{50} of 17.9 and 10.8 μ M in the presence of ATX-2 and veratridine as agonists, respectively.^[303]

5.5.3 | Verapamil potassium channels blocking

In a study conducted by Zhang et al., the effects of verapamil on hERG channels in HEK293 cells were analyzed. It was found that verapamil caused a high-affinity block of hERG current with an IC_{50} of 143.0 nM. The block of channels was both use- and frequency-dependent, and verapamil could be unbound from hERG channels at voltages comparable to the normal cardiac cell resting potential or through drug washout. Additionally, the block of hERG current by verapamil was reduced with a decrease in pHo, which reduces the proportion of the drug in the membrane-permeable neutral form. Further, verapamil was found to antagonize the block of hERG channels by dofetilide, implying that they may share a common binding site. The C-type inactivation-deficient mutations, S620T and S631A, were observed to reduce verapamil block, which is in line with C-type inactivation being involved with high-affinity drug block, although the S620T mutation decreased verapamil block 20-fold more than the S631A mutation.^[304]

In a series of various independent studies, rather similar affinity values of verapamil for the hERG channel from 141 to 530 nM have been published (Table 6).

So, verapamil has been demonstrated to have a high affinity for the hERG channel, which is shared with other class III antiarrhythmic drugs, potentially contributing to its antiarrhythmic activity. Studies have revealed that in heart cells, small amounts of verapamil can extend the cardiac APD, however, a high dosage shortens it. Certain types of VT are particularly sensitive to verapamil and it has been

TABLE 6 Human ether-a-go-go-related gene (hERG) channel affinity of verapamil.

Assay	IC ₅₀ (nM)	Reference
Inhibition of hERG channels expressed in Chinese hamster ovary (CHO) cells at holding potential of -90 mV by patch clamp method	530	[305]
Inhibition of hERG channels in MCF7 cells	145	[306]
Inhibition of human Kv11.1 (hERG) channels in open state	145	[307]
K ⁺ channel blocking activity in HEK293 cells expressing hERG	143	[308]
Inhibition of K ⁺ -channel activity in CHO cells expressing hERG	143	[309]
Inhibition of hERG channels expressed in mammalian cells	141	[310]
Inhibition of hERG channels expressed in CHO cells by whole cell patch clamp technique	141	[311]

found to prolong the atrial ERP in human subjects, as well as prevent a shortening of the atrial ERP which is caused by atrial tachycardia and fibrillation (known as “electrical remodeling”).^[304]

Waldegger et al. studied the effect of verapamil on cardiac AP repolarizing potassium channels. The potassium channels Kv1.1, Kv1.5, Kir2.1, and the IsK subunit of the I_{Ks}-channel complex were expressed in *Xenopus* oocytes, and two-electrode voltage-clamp experiments were performed. Verapamil induced a concentration-dependent block of Kv1.1-, Kv1.5-, and I_{Ks}-induced currents with IC₅₀ values of 14.0, 5.1, and 161.0 μM, respectively.^[312]

Ding et al. found that verapamil preferentially blocked the human Kv1.5 channel in its open state with IC₅₀ of 2.4 μM. The blocking effect of verapamil was significantly attenuated in T479A, T480A, I502A, V505A, I508A, L510A, V512A, and V516A mutants, compared with WT hKv1.5 channel. The authors suggest that the blocking effect of verapamil on hKv1.5 channel appears to contribute at least partly to prolongation of atrial ERP and resultant antiarrhythmic action on AF in humans^[313]

Madeja conducted a study to observe the impacts of verapamil on both native and cloned hippocampal Kv channels. He used the whole-cell patch-clamp technique to measure the native channels in acutely isolated CA1 neurons from guinea pigs, while the two-electrode voltage-clamp technique was used to measure the cloned channels that were expressed in oocytes of *X. laevis*. The IC₅₀ value of verapamil was determined to be 3 μM, indicating a variety of potassium channels that had distinct sensitivities to verapamil. The effects of verapamil were observed in micromolar concentrations on hippocampal potassium channels Kv1.1, Kv1.2, Kv1.3, Kv2.1, Kv3.1, and Kv3.2. As the depolarization time increased, the effects of verapamil increased in a voltage-dependent manner and reached 90% of the maximum within 40 s. Even after wash-out times of 6 min, the effects of verapamil did not return to the initial control values. The IC₅₀ values for each of the potassium channels varied significantly: IC₅₀(Kv1.1) was 35 μM, IC₅₀(Kv1.2) was 98 μM, IC₅₀(Kv1.3) was 12 μM, IC₅₀(Kv2.1) was 226 μM, IC₅₀(Kv3.1) was 6 μM and IC₅₀(Kv3.2) was 11 μM.^[314]

Verapamil inhibits Kv1.3 expressed in mouse L929 cells exposed to depolarizing step pulses from -80 to +40 mV with IC₅₀ of 8 μM, that was measured by whole cell patch clamp method.^[315] Grissmer analyzed the action of verapamil on currents through WT and mutant hKv1.3 and mKv1.3 channels in the open state using the whole-cell patch clamp technique. They found that position 420 in hKv1.3 channels maximally interferes with verapamil reaching its binding site to block the channel. Positions 417 and 418 in hKv1.3 channels partially hinder verapamil reaching its binding site to block the channel whereas position 419 may not interfere with verapamil at all. K_d values for WT Kv1.3 was 2.8–18 μM.^[316–318]

Xu et al. used the two-electrode voltage clamp technique to observe the effect of verapamil on Kv1.4 C-type inactivation. The drug blocked fKv1.4ΔN (N-terminal deleted Kv1.4 channel from ferret heart) in voltage- and frequent-dependent manners with IC₅₀ of 263.26 μM.^[319] The same results were obtained for verapamil by Chen et al. (IC₅₀[fKv1.4ΔN] = 260.71 μM).^[320]

Verapamil blocks Kv1.7 with IC₅₀ of 280 μM according to Wiśniowska et al.^[288] In *X. laevis* oocytes the drug was shown to inhibit Kv1.8 with K_i of 53 μM.^[59]

Ninomiya et al. investigated the ability of verapamil to block ATP-sensitive K⁺ (K_{ATP}) channels that consist of Kir6.2 subunits and sulfonylurea receptors. In whole-cell patch experiments, verapamil inhibited cardiac type K_{ATP} channels previously activated by 100-μM pinacidil in reversibly manner. In inside-out patch experiments, verapamil inhibited the C-terminal truncated form of Kir6.2 in a concentration-dependent manner; IC₅₀ was obtained at 11.5 μM when Kir6.2 was expressed without sulfonylurea receptors. Verapamil also inhibited K_{ATP} with a similar potency with IC₅₀ of 8.9 μM.^[321]

5.5.4 | Verapamil α-adrenoreceptors inhibition

Motulsky et al. studied verapamil binding to α-AR s using radioligand assay. The drug competed for [³H] prazosin binding to α1-ARs and for [³H]yohimbine binding to α2-ARs in several tissues (rat kidney,

heart, and cultured muscle cells, and human platelets) with K_d of 0.6–6 μM .^[322]

Staneva-Stoytcheva et al. showed that long-term treatment with verapamil induces changes in rat brain α -adrenoceptors, namely significant reduction of the binding sites (B_{max}) for α -adrenoceptor radioligand [³H]WB4101 in crude synaptosomal membrane fraction from cerebral cortex after verapamil treatment.^[323]

The kind of interaction of verapamil with both α_2 -AR agonist and antagonist binding on human platelets was investigated by Galinier et al. The drug interacted in vitro with platelet α_2 -adrenoceptors on [³H]yohimbine or [³H]UK-14304 binding. Verapamil behaved as a weak antagonist competitor for α_2 -adrenoceptors.^[324]

According DrugMatrix in vitro pharmacology data^[325] verapamil inhibits $\alpha_1\text{A}$ -AR in radioligand binding assay with prazosin as radioligand with K_i of 847 nM and $\alpha_1\text{B}$ -AR in the same assay with K_i of 940 nM. In radioligand binding assay with MK-912 as radioligand verapamil inhibited $\alpha_2\text{A}$ -AR with K_i of 217 nM.

Shibata et al. studied effects of verapamil on human cardiovascular α_1 -adrenoceptors. Pharmacological profiles verapamil actions on the α_1 -AR subtypes were characterized with CHO cells stably expressing cloned human α_1 -AR subtypes. Radioligand binding studies with [¹²⁵I]HEAT showed that verapamil had high affinities for all α_1 -AR subtypes ($K_i[\alpha_1\text{A}] = 1 \mu\text{M}$; $K_i[\alpha_1\text{B}] = 1.9 \mu\text{M}$; $K_i[\alpha_1\text{D}] = 3.8 \mu\text{M}$). The authors concluded that clinically observed hypotension after verapamil use can be explained by its inhibitory effects on human α_1 -ARs.^[326]

5.5.5 | Verapamil β -adrenoreceptors inhibition

Feldman et al. performed a study to understand the impact of calcium-channel blockers on β -ARs, by utilizing radioligand binding assays to survey the relationship of verapamil with both human lymphocyte β_2 -AR and rat myocardial β_1 -AR. Furthermore, they assessed the functional consequences of these interactions by measuring adenylate cyclase activity. The radioligand binding studies showed a K_i of verapamil for the lymphocyte β_2 -receptor of 32 μM . Studies of adenylate cyclase activity revealed that verapamil worked as a competitive β -receptor antagonist. Moreover, norverapamil, the active metabolite of verapamil, had the greatest affinity for the β -receptor of any of the calcium-channel blockers studied ($K_i = 4.2 \mu\text{M}$). After 1 week of verapamil administration in six regular people, isoproterenol-prompted adenylate cyclase activity in lymphocytes was increased from 60% to 83% over basal activity. This was connected with an increase in lymphocyte β -receptor affinity for agonist as symbolized by the decrease in the IC_{50} for isoproterenol restraint of [¹²⁵I]iodocyanopindolol binding. Additionally, plasma norepinephrine levels were reduced with 1 week of verapamil treatment. These results suggest that verapamil influences lymphocyte β -receptors in vitro and with long-term administration modulates lymphocyte β -receptor function either directly or indirectly through a decrease in plasma catecholamine levels.^[327]

Xu et al. found that verapamil increased β -AR density and inhibited norepinephrine-induced β -AR downregulation of cardiomyocytes.^[328] Staneva-Stoytcheva et al. studied the influence of long-term treatment with verapamil, on β -adrenoceptors in rat cerebral cortex. They found that 13-day treatment of rats with verapamil significantly reduced (by about 30%) the number (B_{max}) of β -adrenoceptors.^[329]

The hypothesis that verapamil's pharmacological antihypertensive effects may partially be attributed to β -inhibition was tested by Drici et al. In a double-blind randomized study, 40 patients with mild to moderate hypertension received either verapamil 240 mg (once a day) or captopril 20 mg (twice a day) over a period of 30 days, after a placebo run-in period. The lymphocytic membrane β_2 -AR density (B_{max}) was examined before and after 15 days of treatment. After a month of treatment, most patients displayed a considerable decrease in their diastolic blood pressure. Meanwhile, verapamil induced an upregulation of β_2 -ARs from 39.5 fmol/mg protein to 58.5 fmol/mg protein ($p < 0.05$). As opposed to the verapamil group, there was no noteworthy change in the captopril group's B_{max} . Neither group experienced any significant change in the two dissociation constants. This increase in β_2 -AR density, a common occurrence among β_2 -blockers, provides evidence for the hypothesis that verapamil does indeed possess β -antagonistic potency.^[330]

5.5.6 | Verapamil 5HT-receptors inhibition

Verapamil interfered with [³H]ketanserin and [³H]spiropendol binding in membranes of rat cerebral cortex with $p\text{IC}_{50} = 6.29$ and 5.90, respectively. In human blood platelets verapamil in therapeutic concentrations inhibited the shape change reaction induced by 5-hydroxytryptamine ($p\text{IC}_{50} = 5.48$).^[331] According to Taylor and Defeudis inhibition of [³H]spiperone binding to rats cortical 5-HT₂ receptors by verapamil was with IC_{50} of 290 nM.^[332]

Adachi and Shoji used a radioligand binding technique to assess the affinity of verapamil to 5-HT-receptors in rat brain membranes. They found that verapamil competed for [³H]ketanserin binding sites at low concentrations, with a K_i value of 0.41 μM . However, much higher concentrations were needed to inhibit [³H]serotonin binding sites, indicating a stronger affinity of verapamil for 5-HT₂ than 5-HT₁ receptors. Furthermore, the inhibitory action of verapamil on the [³H]ketanserin binding was stereoselective; the (-)-isomer was about 10 times more potent than the (+)-isomer. The interaction between verapamil and [³H]ketanserin was competitive and reversible.^[333]

The specific interaction of verapamil with 5-HT_{2A} receptors was also confirmed by Goppelt-Struebe by a whole cell binding assay using [³H]ketanserin as specific ligand ($p\text{IC}_{50} \sim 5.3$).^[334] Okkoro found that verapamil inhibited 5-HT-induced contractions of rat aorta with mean IC_{50} value of 540 nM.^[335]

The research conducted by Glusa et al. examined the influence of verapamil on 5-HT-induced platelet aggregation. Tests were conducted using samples of both human whole blood and platelet-rich plasma (PRP). It was determined that verapamil was able to inhibit

TABLE 7 5-HT inhibition activity of verapamil according DrugMatrix.^[325]

Radioligand binding assay	Radioligand	K_i (nM)
Rat 5-HT _{1A} receptor	[³ H]8-OH-DPAT	1726
Human 5-HT _{2A} receptor	[³ H]Ketanserin	126
Human 5-HT _{2B} receptor	[³ H]Lysergic acid diethylamide	105
Human 5-HT _{2C} receptor	[³ H]Mesulergine	155
Human SERT	[³ H]Paroxetine	127

5-HT-induced platelet aggregation at much lower concentrations (with an IC₅₀ of approximately 1 μM) than what was required for the inhibition of aggregation induced by other agents. The antiaggregatory effects of verapamil were comparable, but not exactly the same, across both whole blood and PRP.^[336]

It is interesting to note that the long-term treatment with verapamil decreases the activity of 5-HT₁ receptors in rat cerebral cortex and hippocampus.^[337] DrugMatrix in vitro pharmacology project^[325] presented the following data about verapamil inhibition activity to 5-HT receptors and SERT (Table 7).

5.5.7 | Verapamil additional targets

Tamura et al. examined effects of verapamil on the HCN4 channel current in HEK293 cells. Verapamil weakly inhibited the HCN4 channel current, especially at hyperpolarizing voltages below -100 mV. The calculated IC₅₀ value of verapamil for inhibiting the HCN4 channel current at -70 mV was 44.9 μM. The authors suggested these HCN4-channel effect of verapamil is a useful information for treatment of various arrhythmias while minimizing adverse effects.^[338]

Karliner et al. analyzed the affinity of verapamil to M₁-receptors by studying its effect on the binding of [³H]quinclidinyl benzilate (QNB) to membranes prepared from rat heart. Verapamil competed for the binding of this radioligand with K_i of 7 μM. The drug (30 μM) competitively inhibited [³H]QNB binding in both atria and ventricles and increased the apparent K_d of [³H]QNB fivefold (from 0.07 nM to 0.32 nM) without decreasing B_{max} .^[339]

Similar results have been obtained by Katayama et al. They studied the effects of verapamil on muscarinic acetylcholine antagonist binding in the synaptosomal fraction of the rat cerebral cortex using either [³H]QNB or [³H]pirenzipine as the radioactive ligand. The IC₅₀ values of verapamil was 12.8 μM.^[340]

Verapamil displaces D₁ antagonist [³H]SCH-23390 specific binding (K_i of 9 μM) and D₂ antagonist [³H]spiroperidol specific binding (K_i of 2.4 μM) from striatal synaptosomal membranes. At 10 μM verapamil (for 5 min) increases endogenous dopamine release by 70% independently on the presence of external Ca²⁺.^[341] According DrugMatrix in vitro pharmacology data^[325] verapamil inhibits dopamine D₃ receptor in radioligand binding

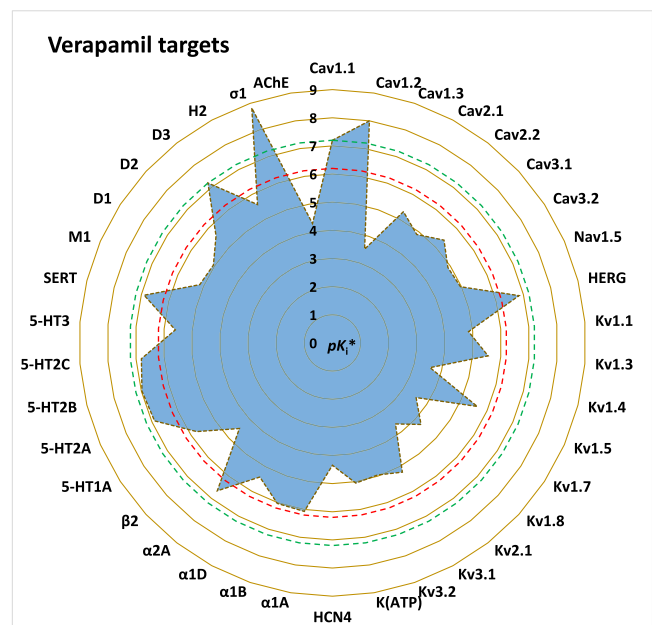
assay with [³H]spiperone as radioligand with K_i of 63 nM; human H₂-receptor in [¹²⁵I]aminopotentidine radioligand binding assay with K_i of 2547 nM.

Staneva-Stoytcheva et al. examined the binding of [³H]flunitrazepam to benzodiazepine receptors in the cerebral cortex and hippocampus (membrane synaptosomal fraction) after 13 days of male Wistar rats being orally treated with verapamil (50 mg/kg). It was found that there was a sizable decrease of the [³H]flunitrazepam B_{max} due to the verapamil, with the decrease being notably more extreme in the hippocampus. However, there was no evidence from in vitro experiments that verapamil had a direct effect on the brain benzodiazepine receptors.^[342] According to Almansa et al. verapamil is a high affinity σ1-ligand with K_i = 1.5 nM.^[343]

5.5.8 | Conclusion on verapamil multitargeting

Verapamil has a very significant number of biological targets, although information about their involvement in the pharmacological effects of the drug for most of them is not available (Figure 6). It is believed that the main biotargets of verapamil are the calcium Cav1.2 channel and the potassium hERG channel. The drug has similar affinity values for these channels (pK_i [Cav1.2] = 4.3–8.0; pK_i [hERG] = 6.0–6.8) that are similar to the pC_{max} value for the lowest studied dose of verapamil (40 mg). In addition, the physiological role of Cav1.2 and hERG channels in the action of verapamil has been studied in detail.

It is interesting to note that despite the fact that verapamil is one of the strongest hERG blockers, it carrying no proarrhythmia risk. The literature notes that the absence of this risk is precisely due to the combined effect of verapamil on hERG and the calcium channel. This

**FIGURE 6** The diagram of verapamil targets. The designations are similar to those in Figure 2.

is likely because blocking inward currents can prevent EADs, which trigger TdP. The strong calcium block opposes effects of hERG block on early and late repolarization.^[288,344,345]

Despite the leading role of Ca_v1.2 and hERG channels in the cardioprotective properties of verapamil, there is a biotarget for which the drug has a significantly higher activity—the σ 1-receptor ($pK_i = 8.82$). Unfortunately, there is no information on the involvement of the σ 1-receptor in the biological effects of the drug, although this chaperone protein is known to be significantly involved in cardioprotection.

Among the most significant biotargets of verapamil, whose K_i values are within the plasma concentrations of therapeutic dosages of the drug ($pC_{max} = 6.2-7.2$), are the following: Cav1.1 channel ($pK_i = 7.2$), α 2A-AR ($pK_i = 6.7$), 5-HT₂-receptors ($pK_i = 6.8-7.0$), SERT ($pK_i = 6.9$) and D₃-receptor ($pK_i = 7.2$). Probably due to its affinity for 5-HT-receptors, verapamil inhibited 5-HT-induced platelet aggregation at much lower concentrations than were required for inhibition of aggregation induced by other aggregating agents.

At slightly higher concentrations compared to pC_{max} interval, verapamil inhibits α 1-AR subtypes ($pK_i[\alpha 1A] = 6.07$; $pK_i[\alpha 1B] = 6.03$; $pK_i[\alpha 1D] = 5.42$). It is assumed that clinically observed hypotension after verapamil use can be explained by its inhibitory effects on human α 1ARs.

In addition to Cav1.2 and Cav1.1, for which verapamil exhibits the highest affinity, in the range of calcium channels, the drug also has an affinity for a number of their other subtypes ($pK_i[Cav1.3] = 3.52$; $pK_i[Cav2.1] = 5.3$; $pK_i[Cav2.2] = 4.9$; $pK_i[Cav3.1] = 5.4$; $pK_i[Cav3.2] = 4.9$). Although the values of the inhibition constants for the listed channels are already lower than the plasma concentrations of the drug, it is assumed that they may be involved in its physiological effects.

Also, at sufficiently high concentrations ($pK_i = 3.7-5.6$), verapamil blocks a whole range of different potassium channels, including Kv1.1, Kv1.3, Kv1.4, Kv1.5, Kv1.7, Kv1.8, Kv2.1, Kv3.1, Kv3.2, and K_{ATP}. The blocking effect of verapamil on Kv1.5 channel ($pK_i = 5.6$) appears to contribute at least partly to prolongation of atrial ERP and resultant antiarrhythmic action on AF in humans.

Verapamil blocks Nav1.5 channel with $pK_i = 4.97$, which is about an order of magnitude lower than the minimum pC_{max} . It is suggested that Nav1.5 blocking by verapamil together with Cav1.2 blocking involved in preventing clinical torsadogenic risk associated with its hERG-blocking potential.

It has been established that verapamil is able to bind to the HCN4 channel ($pI_{C50} = 4.4$). Thus, the affinity of verapamil for this biotarget is only an order of magnitude higher than that for ivabradine ($pI_{C50} = 5.6$). Taking into account the fact that the value of pC_{max} for the maximum dosages of these drugs also differ by almost an order of magnitude (6.9 for ivabradine vs. 6.2 for verapamil), it can be assumed that HCN4 channels are also involved in the antiarrhythmic effects of verapamil.

Finally, verapamil targets also include M₁-receptor ($pK_i[M_1] = 5.2$), D₁- and D₂-receptors ($pK_i[D_1] = 5.1$; $pK_i[D_2] = 5.6$), H₂-receptor

($pK_i[H_2] = 5.6$), 5-HT_{1A}- and 5-HT₃-receptors ($pK_i[5-HT_{1A}] = 5.5$; $pK_i[5-HT_3] = 5.6$) and acetylcholinesterase ($pK_i[AChE] = 4.3$).

6 | CONCLUSION

Linked biaromatic pharmacophore can be considered as a basic one for cardioprotective agents with different mechanisms of action. Moreover, many compounds corresponding to this pharmacophore have affinities for a big range of biological targets characteristic of other types of drugs, such as neuropsychotropic agents. As a result, most biaromatic cardioprotectors have a multitarget mechanism of action that is fully consistent with the modern conception that effective and safe cardioprotectors should be multitargeted. This review collects data on the biological targets of the five most well-known and studied cardioprotective agents—carvedilol, ivabradine, nebivolol, ranolazine and verapamil. These examples clearly show the multitargeting of drugs with biaromatic structure. Also, the review is another confirmation of the hypothesis that all the drugs have a complex mechanism of action, and there are no mono-targeted drugs.

ACKNOWLEDGMENTS

This project was funded by the Ministry of Science and Higher Education of the Russian Federation within the State task of the Zakuov Research Institute of Pharmacology for 2022–2024 No. FGFG-2022-0005 “Creation of New Chemical Structures—Potential Ligands of Pharmacological Targets for the Treatment of Neuropsychiatric and Cardiovascular Diseases”

CONFLICTS OF INTEREST STATEMENT

The author declares no conflict of interest.

ORCID

Grigory V. Mokrov  <http://orcid.org/0000-0003-2617-0334>

REFERENCES

- [1] J. L. Medina-Franco, M. A. Giulianotti, G. S. Welmaker, R. A. Houghten, *Drug Discov. Today* **2013**, *18*, 495.
- [2] J. Zhou, X. Jiang, S. He, H. Jiang, F. Feng, W. Liu, W. Qu, H. Sun, *J. Med. Chem.* **2019**, *62*, 8881.
- [3] A. L. Hopkins, *Nat. Chem. Biol.* **2008**, *4*, 682.
- [4] M. J. Oset-Gasque, J. Marco-Contelles, *ACS Chem. Neurosci.* **2018**, *9*, 401.
- [5] A. Zięba, P. Stępnicki, D. Matosiuk, A. A. Kaczor, *Expert Opin. Drug Discov.* **2022**, *17*, 673.
- [6] R. R. Ramsay, M. R. Popovic-Nikolic, K. Nikolic, E. Uliassi, M. L. Bolognesi, *Clin. Transl. Med.* **2018**, *7*, 3.
- [7] A. Shaito, D. T. B. Thuan, H. T. Phu, T. H. D. Nguyen, H. Hasan, S. Halabi, S. Abdelhady, G. K. Nasrallah, A. H. Eid, G. Pintus, *Front. Pharmacol.* **2020**, *11*, 422.
- [8] World Health Organization: Cardiovascular Diseases (CVDs), **2021**. Accessed May 2023. [https://www.who.int/en/news-room/fact-sheets/detail/cardiovascular-diseases-\(cvds\)](https://www.who.int/en/news-room/fact-sheets/detail/cardiovascular-diseases-(cvds))
- [9] N. S. Hendren, M. H. Drazner, B. Bozkurt, L. T. Cooper, *Circulation* **2020**, *141*, 1903.

- [10] S. M. Davidson, P. Ferdinandy, I. Andreadou, H. E. Bøtker, G. Heusch, B. Ibáñez, M. Ovize, R. Schulz, D. M. Yellon, D. J. Hausenloy, D. Garcia-Dorado, *J. Am. Coll. Cardiol.* **2019**, *73*, 89.
- [11] M. Barman, *J. Atr. Fibrillation* **2015**, *8*, 1091.
- [12] S. Polak, M. K. Pugsley, N. Stockbridge, C. Garnett, B. Wiśniowska, *AAPS. J.* **2015**, *17*, 1025.
- [13] L. Song, Z. Zhang, L. Hu, P. Zhang, Z. Cao, Z. Liu, P. Zhang, J. Ma, *Front. Physiol.* **2020**, *11*, 978.
- [14] D. J. Hausenloy, D. Garcia-Dorado, H. E. Bøtker, S. M. Davidson, J. Downey, F. B. Engel, R. Jennings, S. Lecour, J. Leor, R. Madonna, M. Ovize, C. Perrino, F. Prunier, R. Schulz, J. P. G. Sluijter, L. W. Van Laake, J. Vinten-Johansen, D. M. Yellon, K. Ytrehus, G. Heusch, P. Ferdinandy, *Cardiovasc. Res.* **2017**, *113*, 564.
- [15] S. Der Sarkissian, H. Aceros, P. M. Williams, C. Scalabrini, M. Borie, N. Noiseux, *Br. J. Pharmacol.* **2020**, *177*, 3378.
- [16] M. G. Katselou, A. N. Matralis, A. P. Kourounakis, *Curr. Med. Chem.* **2014**, *21*, 2743.
- [17] T. Crespo-García, A. Cámara-Checa, M. Dago, M. Rubio-Alarcón, J. Rapún, J. Tamargo, E. Delpón, R. Caballero, *Biochem. Pharmacol.* **2022**, *204*, 115206.
- [18] M. Lei, L. Wu, D. A. Terrar, C. L. H. Huang, *Circulation* **2018**, *138*, 1879.
- [19] I. Cavero, J. M. Guillon, V. Ballet, M. Clements, J. F. Gerbeau, H. Holzgreffe, *J. Pharmacol. Toxicol. Methods* **2016**, *81*, 21.
- [20] Z. Li, C. Garnett, D. G. Strauss, *CPT Pharmacomet. Syst. Pharmacol.* **2019**, *8*, 371.
- [21] J. Bernardi, K. A. Aromolaran, A. S. Aromolaran, *Int. J. Mol. Sci.* **2020**, *22*, 1.
- [22] N. M. Batelaan, A. Seldenrijk, O. A. van den Heuvel, A. J. L. M. van Balkom, A. Kaiser, L. Reneman, H. L. Tan, *Front. Psychiatry* **2022**, *12*, 813518.
- [23] P. Severino, M. V. Mariani, A. Maraone, A. Piro, A. Ceccacci, L. Tarsitani, V. Maestrini, M. Mancone, C. Lavallo, M. Pasquini, F. Fedele, *Cardiol Res. Pract.* **2019**, *2019*, 1208505.
- [24] I. L. Piña, K. E. Di Palo, H. O. Ventura, *J. Am. Coll. Cardiol.* **2018**, *71*, 2346.
- [25] Home | IUPHAR/BPS Guide to PHARMACOLOGY. **2023**. Accessed May 2023. <https://www.guidetopharmacology.org/>
- [26] L. Sun, J. Lu, X. J. Yu, D. L. Li, X. L. Xu, B. Wang, K. Y. Ren, J. K. Liu, W. J. Zang, *J. Pharmacol. Sci.* **2011**, *115*, 205.
- [27] T. Yoshikawa, J. D. Port, K. Asano, P. Chidiak, M. Bouvier, D. Dutcher, R. L. Roden, W. Minobe, K. D. Tremmel, M. R. Bristow, *Eur. Heart J.* **1996**, *17*(Suppl B), 8.
- [28] K. E. Knockenhauer, R. A. Copeland, *Br. J. Pharmacol.* **2023**, *180*, in press. <https://doi.org/10.1111/BPH.16104>
- [29] M. Bernetti, M. Masetti, W. Rocchia, A. Cavalli, *Annu. Rev. Phys. Chem.* **2019**, *70*, 143.
- [30] D. R. J. Owen, R. N. Gunn, E. A. Rabiner, I. Bennacef, M. Fujita, W. C. Kreisl, R. B. Innis, V. W. Pike, R. Reynolds, P. M. Matthews, C. A. Parker, *J. Nucl. Med.* **2011**, *52*, 24.
- [31] M. S. Salahudeen, P. S. Nishtala, *Saudi Pharmaceut. J.* **2017**, *25*, 165.
- [32] J. Vaidyanathan, K. Yoshida, V. Arya, L. Zhang, *J. Clin. Pharmacol.* **2016**, *56*(Suppl 7), S59.
- [33] B. T. Burlingham, T. S. Widlanski, *J. Chem. Educ.* **2003**, *80*, 214.
- [34] J. L. Sebaugh, *Pharm. Stat.* **2011**, *10*, 128.
- [35] X. T. Li, *Biomed. Pharmacother.* **2022**, *150*, 113057.
- [36] M. Oknińska, A. Paterek, Z. Zambrowska, U. Mackiewicz, M. Mączewski, *J. Clin. Med.* **2021**, *10*, 4732.
- [37] J. P. Lees-Miller, J. Guo, Y. Wang, L. L. Perissinotti, S. Y. Noskov, H. J. Duff, *J. Mol. Cell Cardiol.* **2015**, *85*, 71.
- [38] B. Hackl, P. Lukacs, J. Ebner, K. Pesti, N. Haechl, M. C. Földi, E. Lilliu, K. Schicker, H. Kubista, A. Stary-Weinzinger, K. Hillber, A. Mike, H. Todt, X. Koenig, *Front. Pharmacol.* **2022**, *13*, 798.
- [39] H. Wang, N. Mulgaonkar, L. M. Pérez, S. Fernando, *ACS Omega* **2022**, *7*, 12707.
- [40] N. Handler. in *Drug Selectivity: An Evolving Concept in Medicinal Chemistry* (Eds: N. Handler, H. Buschmann), Wiley-VCH Verlag GmbH & Co. KGaA **2018**, ch. 10.
- [41] G. V. Mokrov, *Arch. Pharm. (Weinheim)* **2022**, *355*, 2100428.
- [42] A. Granetzny, U. Schwanke, C. Schmitz, G. Arnold, D. Schäfer, H. Schulte, E. Gams, J. Schipke, *Thorac. Cardiovasc. Surg.* **1998**, *46*, 63.
- [43] P. P. Van Bogaert, F. Pittoors, *Eur. J. Pharmacol.* **2003**, *478*, 161.
- [44] J. Stieber, K. Wieland, G. Stöckl, A. Ludwig, F. Hofmann, *Mol. Pharmacol.* **2006**, *69*, 1328.
- [45] K. McCormack, S. Santos, M. L. Chapman, D. S. Krafte, B. E. Marron, C. W. West, M. J. Krambis, B. M. Antonio, S. G. Zellmer, D. Printzenhoff, K. M. Padilla, Z. Lin, P. K. Wagoner, N. A. Swain, P. A. Stupple, M. De Groot, R. P. Butt, N. A. Castle, *Proc. Natl. Acad. Sci. U.S.A.* **2013**, *110*, E2724.
- [46] S. Mishra, V. Reznikov, V. A. Maltsev, N. A. Undrovinas, H. N. Sabbah, A. Undrovinas, *J. Physiol.* **2015**, *593*, 1409.
- [47] K. Silver, D. Soderlund, *Neurotoxicology* **2005**, *26*, 397.
- [48] J. A. Zablocki, E. Elzein, X. Li, D. O. Koltun, E. Q. Parkhill, T. Kobayashi, R. Martinez, B. Corkey, H. Jiang, T. Perry, R. Kalla, G. T. Notte, O. Saunders, M. Graupe, Y. Lu, C. Venkataramani, J. Guerrero, J. Perry, M. Osier, R. Strickley, G. Liu, W.-Q. Wang, L. Hu, X.-J. Li, N. El-Bizri, R. Hirakawa, K. Kahlig, C. Xie, C. H. Li, A. K. Dhalla, S. Rajamani, N. Mollova, D. Soohoo, E.-I. Lepist, B. Murray, G. Rhodes, L. Belardinelli, M. C. Desai, *J. Med. Chem.* **2016**, *59*, 9005.
- [49] J. Müller-Ehmsen, K. Brixius, R. H. G. Schwinger, *J. Cardiovasc. Pharmacol.* **1998**, *31*, 684.
- [50] K. H. Yuill, M. K. Convery, P. C. Dooley, S. A. Doggrell, J. C. Hancox, *Br. J. Pharmacol.* **2000**, *130*, 1753.
- [51] N. A. Swain, D. Batchelor, S. Beaudoin, B. M. Bechle, P. A. Bradley, A. D. Brown, B. Brown, K. J. Butcher, R. P. Butt, M. L. Chapman, S. Denton, D. Ellis, S. R. G. Galan, S. M. Gaulier, B. S. Greener, M. J. De Groot, M. S. Glossop, I. K. Gurrell, J. Hannam, M. S. Johnson, Z. Lin, C. J. Markworth, B. E. Marron, D. S. Millan, S. Nakagawa, A. Pike, D. Printzenhoff, D. J. Rawson, S. J. Ransley, S. M. Reister, K. Sasaki, R. I. Storer, P. A. Stupple, C. W. West, *J. Med. Chem.* **2017**, *60*, 7029.
- [52] T. Yang, T. C. Atack, D. M. Stroud, W. Zhang, L. Hall, D. M. Roden, *Circ. Res.* **2012**, *111*, 322.
- [53] M. J. C. Scanio, L. Shi, I. Drizin, R. J. Gregg, R. N. Atkinson, J. B. Thomas, M. S. Johnson, M. L. Chapman, D. Liu, M. J. Krambis, *Bioorg. Med. Chem.* **2010**, *18*, 7816.
- [54] A. Schmitz, A. Sankaranarayanan, P. Azam, K. Schmidt-Lassen, D. Homerick, W. Hänsel, H. Wulff, *Mol. Pharmacol.* **2005**, *68*, 1254.
- [55] Š. Gubič, L. A. Hendrickx, Ž. Toplak, M. Sterle, S. Peigneur, T. Tomašič, L. A. Pardo, J. Tytgat, A. Zega, L. P. Mašič, *Med. Res. Rev.* **2021**, *41*, 2423.
- [56] N. Zidar, A. Žula, T. Tomašič, M. Rogers, R. W. Kirby, J. Tytgat, S. Peigneur, D. Kikelj, J. Ilaš, L. P. Mašič, *Eur. J. Med. Chem.* **2017**, *139*, 232.
- [57] E. Wettwer, G. Amos, J. Gath, H. R. Zerkowski, J. C. Reidemeister, U. Ravens, *Cardiovasc. Res.* **1993**, *27*, 1662.
- [58] S. Wu, A. Fluxe, J. M. Janusz, J. B. Sheffer, G. Browning, B. Blass, K. Coburn, R. Hedges, M. Murawsky, B. Fang, G. M. Fadayel, M. Hare, L. Djandjighian, *Bioorg. Med. Chem. Lett.* **2006**, *16*, 5859.
- [59] R. Lang, G. Lee, W. Liu, S. Tian, H. Rafi, M. Orias, A. S. Segal, G. V. Desir, *Am. J. Physiol. Renal Physiol.* **2000**, *278*, F1013.
- [60] J. Herrington, K. Solly, K. S. Ratliff, N. Li, Y. P. Zhou, A. Howard, L. Kiss, M. L. Garcia, O. B. McManus, Q. Deng, R. Desai, Y. Xiong, G. J. Kaczorowski, *Mol. Pharmacol.* **2011**, *80*, 959.

- [61] Z. A. McCrossan, T. K. Roepke, A. Lewis, G. Panaghie, G. W. Abbott, *J. Membr. Biol.* **2009**, 228, 1.
- [62] H. M. Lee, O. H. Chai, S. J. Hahn, B. H. Choi, *Korean J. Physiol. Pharmacol.* **2018**, 22, 71.
- [63] H. S. Kim, H. Li, H. W. Kim, S. E. Shin, W. K. Jung, K. S. Ha, E. T. Han, S. H. Hong, A. L. Firth, I. W. Choi, W. S. Park, *Clin. Exp. Pharmacol. Physiol.* **2017**, 44, 480.
- [64] P. R. Kowey, R. V. Mudumbi, J. W. Aquilina, P. M. DiBattiste, *Drugs R&D* **2011**, 11, 1.
- [65] G. L. Stump, G. R. Smith, A. J. Tebben, H. Jahansou, J. J. Salata, H. G. Selnick, D. A. Claremon, J. J. Lynch, *J. Cardiovasc. Pharmacol.* **2003**, 42, 105.
- [66] G. Gessner, M. Zacharias, S. Bechstedt, R. Schönherr, S. H. Heinemann, *Mol. Pharmacol.* **2004**, 65, 1120.
- [67] P. E. Cross, J. E. Arrowsmith, G. N. Thomas, M. Gwilt, R. A. Burges, A. J. Higgins, *J. Med. Chem.* **1990**, 33, 1151.
- [68] D. L. Wolbrette, S. Hussain, I. Maraj, G. V. Naccarelli, *J. Cardiovasc. Pharmacol. Ther.* **2018**, 24, 3.
- [69] H. R. Wang, M. Wu, H. Yu, S. Long, A. Stevens, D. W. Engers, H. Sackin, J. S. Daniels, E. S. Dawson, C. R. Hopkins, C. W. Lindsley, M. Li, O. B. McManus, *ACS Chem. Biol.* **2011**, 6, 845.
- [70] M. Delgado-Ramírez, F. J. Rodríguez-Leal, A. A. Rodríguez-Menchaca, E. G. Moreno-Galindo, J. A. Sanchez-Chapula, T. Ferrer, *Acta Pharm.* **2021**, 71, 317.
- [71] H. Gögelein, J. Hartung, H. Englert, B. Schölkens, *J. Pharmacol. Exp. Ther.* **1998**, 286, 1453.
- [72] P. Pasdois, B. Beauvoit, A. D. T. Costa, B. Vinassa, L. Tariosse, S. Bonoron-Adèle, K. D. Garlid, P. D. Santos, *J. Mol. Cell Cardiol.* **2007**, 42, 631.
- [73] S. Peukert, J. Brendel, B. Pirard, A. Brüggemann, P. Below, H.-W. Kleemann, H. Hemmerle, W. Schmidt, *J. Med. Chem.* **2003**, 46, 486.
- [74] M. A. Skarsfeldt, T. A. Jepps, S. H. Bomholtz, L. Abildgaard, U. S. Sørensen, E. Gregers, J. H. Svendsen, J. G. Diness, M. Grunnet, N. Schmitt, S. P. Olesen, B. H. Bentzen, *Pflügers Arch. Eur. J. Physiol.* **2016**, 468, 643.
- [75] A. Goll, D. R. Ferry, J. Striessnig, M. Schober, H. Glossmann, *FEBS Lett.* **1984**, 176, 371.
- [76] B. E. Flucher, *Pflügers Arch. Eur. J. Physiol.* **2020**, 472, 739.
- [77] K. Yasui, P. Palade, *Br. J. Pharmacol.* **1995**, 114, 468.
- [78] J. Gubin, H. de Vogelaer, H. Inion, C. Houben, J. Lucchetti, J. Mahaux, G. Rosseels, M. Peiren, M. Clinet, *J. Med. Chem.* **2002**, 36, 1425.
- [79] M. J. Sinnegger-Brauns, I. G. Huber, A. Koschak, C. Wild, G. J. Obermair, U. Einzinger, J. C. Hoda, S. B. Sartori, J. Striessnig, *Mol. Pharmacol.* **2009**, 75, 407.
- [80] M. Lee, T. Snutch, *J. Pain* **2013**, 14, S71.
- [81] O. Bezençon, B. Heidmann, R. Siegrist, S. Stamm, S. Richard, D. Pozzi, O. Corminboeuf, C. Roch, M. Kessler, E. A. Ertel, I. Reymond, T. Pfeifer, R. De Kanter, M. Toeroek-Schafroth, L. G. Moccia, J. Mawet, R. Moon, M. Rey, B. Capeleto, E. Fournier, *J. Med. Chem.* **2017**, 60, 9769.
- [82] N. Szentandrassy, D. Nagy, B. Hegyi, J. Magyar, T. Banyasz, P. P. Nanasi, *Curr. Pharm. Des.* **2015**, 21, 977.
- [83] Q. Zhou, J. Xiao, D. Jiang, R. Wang, K. Vembaiyan, A. Wang, C. D. Smith, C. Xie, W. Chen, J. Zhang, X. Tian, P. P. Jones, X. Zhong, A. Guo, H. Chen, L. Zhang, W. Zhu, D. Yang, X. Li, J. Chen, A. M. Gillis, H. J. Duff, H. Cheng, A. M. Feldman, L.-S. Song, M. Fill, T. G. Back, S. R. W. Chen, *Nat. Med.* **2011**, 17, 1003.
- [84] D. Giardinà, D. Martarelli, G. Sagratini, P. Angeli, D. Ballinari, U. Gulini, C. Melchiorre, E. Poggesi, P. Pompei, *J. Med. Chem.* **2009**, 52, 4951.
- [85] B. A. Kenny, A. M. Naylor, A. J. Carter, A. M. Read, P. M. Greengrass, M. G. Wyllie, *Urology* **1994**, 44, 52.
- [86] J. P. Hieble, W. Bondinell, R. R. Ruffolo, *J. Med. Chem.* **1995**, 38, 3415.
- [87] I. Gavras, A. J. Manolis, H. Gavras, *J. Hypertens.* **2001**, 19, 2115.
- [88] I. Kocić, *Gen. Pharmacol. Vasc. Syst.* **1994**, 25, 1191.
- [89] L. A. Rezmann-Vitti, T. L. Nero, G. P. Jackman, C. A. Machida, B. J. Duke, W. J. Louis, S. N. S. Louis, *J. Med. Chem.* **2006**, 49, 3467.
- [90] G. P. Jackman, D. Iakovidis, T. L. Nero, N. S. Anavekar, L. A. Rezmann-Vitti, S. N. S. Louis, M. Mori, O. H. Drummer, W. J. Louis, *Eur. J. Med. Chem.* **2002**, 37, 731.
- [91] S. Tariq, W. Aronow, *Int. J. Mol. Sci.* **2015**, 16, 29060.
- [92] R. S. Williams, T. Bishop, *J. Clin. Invest.* **1981**, 67, 1703.
- [93] M. R. Candelore, L. Deng, L. Tota, X. M. Guan, A. Amend, Y. Liu, R. Newbold, M. A. Cascieri, A. E. Weber, *J. Pharmacol. Exp. Ther.* **1999**, 290, 649.
- [94] D. Beattie, M. Bradley, A. Brearley, S. J. Charlton, B. M. Cuenoud, R. A. Fairhurst, P. Gedeck, M. Gosling, D. Janus, D. Jones, C. Lewis, C. McCarthy, H. Oakman, R. Stringer, R. J. Taylor, A. Tuffnell, *Bioorg. Med. Chem. Lett.* **2010**, 20, 5302.
- [95] M. Dal Monte, I. Fornaciari, G. P. Nicchia, M. Svelto, G. Casini, P. Bagnoli, *Naunyn-Schmiedeberg's Arch. Pharmacol.* **2014**, 387, 533.
- [96] T. Takasu, M. Ukai, S. Sato, T. Matsui, I. Nagase, T. Maruyama, M. Sasamata, K. Miyata, H. Uchida, O. Yamaguchi, *J. Pharmacol. Exp. Ther.* **2007**, 321, 642.
- [97] G. Schena, M. J. Caplan, *Cells* **2019**, 8, 357.
- [98] H. T. Serafinowska, F. E. Blaney, P. J. Lovell, G. G. Merlo, C. M. Scott, P. W. Smith, K. R. Starr, J. M. Watson, *Bioorg. Med. Chem. Lett.* **2008**, 18, 5581.
- [99] A. Ramage, C. Villalon, *Trends Pharmacol. Sci.* **2008**, 29, 472.
- [100] S. P. Runyon, P. D. Mosier, B. L. Roth, R. A. Glennon, R. B. Westkaemper, *J. Med. Chem.* **2008**, 51, 6808.
- [101] A. B. Pithadia, S. M. Jain, *J. Clin. Med. Res.* **2009**, 1, 72.
- [102] A. R. Germain, L. C. Carmody, P. P. Nag, B. Morgan, L. Verplank, C. Fernandez, E. Donckele, Y. Feng, J. R. Perez, S. Dandapani, M. Palmer, E. S. Lander, P. B. Gupta, S. L. Schreiber, B. Munoz, *Bioorg. Med. Chem. Lett.* **2013**, 23, 1834.
- [103] D. D. Manning, C. L. Cioffi, A. Usyatinsky, K. Fitzpatrick, L. Masih, C. Guo, Z. Zhang, S. H. Choo, M. I. Sikkander, K. N. Ryan, J. Naginskaya, C. Hassler, S. Dobritsa, J. D. Wierschke, W. G. Earley, A. S. Butler, C. A. Brady, N. M. Barnes, M. L. Cohen, P. R. Guzzo, *Bioorg. Med. Chem. Lett.* **2011**, 21, 58.
- [104] T. Hirata, Y. Keto, T. Funatsu, S. Akuzawa, M. Sasamata, *J. Pharmacol. Sci.* **2007**, 104, 263.
- [105] D. F. Corbett, T. D. Heightman, S. F. Moss, S. M. Bromidge, S. A. Coggon, M. J. Longley, A. M. Roa, J. A. Williams, D. R. Thomas, *Bioorg. Med. Chem. Lett.* **2005**, 15, 4014.
- [106] D. Vanda, M. Soral, V. Canale, S. Chaumont-Dubel, G. Satała, T. Kos, P. Funk, V. Fülöpová, B. Lemrová, P. Koczurkiewicz, E. Pékala, A. J. Bojarski, P. Popik, P. Marin, P. Zajdel, *Eur. J. Med. Chem.* **2018**, 144, 716.
- [107] Á. A. Kelemen, G. Satała, A. J. Bojarski, G. M. Keserű, *Bioorg. Med. Chem. Lett.* **2018**, 28, 2418.
- [108] D. O. Kellett, A. G. Ramage, D. Jordan, *J. Physiol.* **2005**, 563, 319.
- [109] J. A. Coleman, E. M. Green, E. Gouaux, *Nature* **2016**, 532, 334.
- [110] W. Ni, S. W. Watts, *Clin. Exp. Pharmacol. Physiol.* **2006**, 33, 575.
- [111] J. P. Starck, P. Talaga, L. Quérré, P. Collart, B. Christophe, P. L. Brutto, S. Jadot, D. Chimmanamada, M. Zanda, A. Wagner, C. Mioskowski, R. Massingham, M. Guyaux, *Bioorg. Med. Chem. Lett.* **2006**, 16, 373.
- [112] O. Fischer, J. Hofmann, H. Rampp, J. Kaindl, G. Pratsch, A. Bartuschat, R. V. Taudte, M. F. Fromm, H. Hübner, P. Gmeiner, M. R. Heinrich, *J. Med. Chem.* **2020**, 63, 4349.
- [113] L. Carro, E. Raviña, E. Domínguez, J. Brea, M. I. Loza, C. F. Masaguer, *Bioorg. Med. Chem. Lett.* **2009**, 19, 6059.

- [114] M. Leopoldo, F. Berardi, N. A. Colabufo, P. De Giorgio, E. Lacivita, R. Perrone, V. Tortorella, *J. Med. Chem.* **2002**, *45*, 5727.
- [115] J. Xiao, R. B. Free, E. Barnaeva, J. L. Conroy, T. Doyle, B. Miller, M. Bryant-Genevier, M. K. Taylor, X. Hu, A. E. Dulcey, N. Southall, M. Ferrer, S. Titus, W. Zheng, D. R. Sibley, J. J. Marugan, *J. Med. Chem.* **2014**, *57*, 3450.
- [116] T. Yamaguchi, T. S. Sumida, S. Nomura, M. Satoh, T. Higo, M. Ito, T. Ko, K. Fujita, M. E. Sweet, A. Sanbe, K. Yoshimi, I. Manabe, T. Sasaoka, M. R. G. Taylor, H. Toko, E. Takimoto, A. T. Naito, I. Komuro, *Nat. Commun.* **2020**, *11*, 1.
- [117] T. Coon, W. J. Moree, B. Li, J. Yu, S. Zamani-Kord, S. Malany, M. A. Santos, L. M. Hernandez, R. E. Petroski, A. Sun, J. Wen, S. Sullivan, J. Haelewyn, M. Hedrick, S. J. Hoare, M. J. Bradbury, P. D. Crowe, G. Beaton, *Bioorg. Med. Chem. Lett.* **2009**, *19*, 4380.
- [118] J. Benavides, H. Schoemaker, C. Dana, Y. Claustre, M. Delahaye, M. Prouteau, P. Manoury, J. Allen, B. Scatton, S. Z. Langer, *Arzneimittelforschung.* **1995**, *45*, 551.
- [119] M. Shibata, T. Yamaura, N. Inaba, S. Onodera, Y. Chida, H. Ohnishi, *Eur. J. Pharmacol.* **1993**, *235*, 245.
- [120] S. Masahiro, Y. Tetsuaki, S. Akihiro, N. Masashi, C. Yuriko, O. Haruo, *Jpn. J. Pharmacol.* **1990**, *54*, 277.
- [121] K. Hirano, H. Tagashira, K. Fukunaga, *Yakugaku Zasshi* **2014**, *134*, 707.
- [122] J. R. Lever, J. L. Gustafson, R. Xu, R. L. Allmon, S. Z. Lever, *Synapse* **2006**, *59*, 350.
- [123] K. Shah, S. Seeley, C. Schulz, J. Fisher, S. Gururaja Rao, *Cells* **2022**, *11*, 943.
- [124] T. Godfraind, *Front. Pharmacol.* **2017**, *8*, 286.
- [125] J. A. Hennessey, N. J. Boczek, Y. H. Jiang, J. D. Miller, W. Patrick, R. Pfeiffer, B. S. Sutphin, D. J. Tester, H. Barajas-Martinez, M. J. Ackerman, C. Antzelevitch, R. Kanter, G. S. Pitt, *PLoS One* **2014**, *9*, e106982.
- [126] B. S. Freeze, M. M. McNulty, D. A. Hanck, *Mol. Pharmacol.* **2006**, *70*, 718.
- [127] D. M. Bers, *Nature* **2002**, *415*, 198.
- [128] N. Tiso, *Hum. Mol. Genet.* **2001**, *10*, 189.
- [129] C. Van Der Werf, P. J. Kannankeril, F. Sacher, A. D. Krahn, S. Viskin, A. Leenhardt, W. Shimizu, N. Sumitomo, F. A. Fish, Z. A. Bhuiyan, A. R. Willems, M. J. Van Der Veen, H. Watanabe, J. Laborderie, M. Haïssaguerre, B. C. Knollmann, A. A. M. Wilde, *J. Am. Coll. Cardiol.* **2011**, *57*, 2244.
- [130] A. Beyder, J. L. Rae, C. Bernard, P. R. Strega, F. Sachs, G. Farrugia, *J. Physiol.* **2010**, *588*, 4969.
- [131] A. Hugues, *Cardiovasc. Res.* **2007**, *76*, 381.
- [132] S. G. Priori, C. Napolitano, *Ann. N. Y. Acad. Sci.* **2004**, *1015*, 96.
- [133] X. Wu, Y. Li, L. Hong, *Front. Physiol.* **2022**, *13*, 904664.
- [134] E. Grandi, M. C. Sanguinetti, D. C. Bartos, D. M. Bers, Y. Chen-Izu, N. Chiamvimonvat, H. M. Colecraft, B. P. Delisle, J. Heijman, M. F. Navedo, S. Noskov, C. Proenza, J. I. Vandenberg, V. Yarov-Yarovoy, *J. Physiol.* **2017**, *595*, 2209.
- [135] U. Ravens, K. E. Odening, *Pharmacol. Ther.* **2017**, *176*, 13.
- [136] U. Ravens, *Can. J. Physiol. Pharmacol.* **2017**, *95*, 1313.
- [137] J. I. Vandenberg, M. D. Perry, M. J. Perrin, S. A. Mann, Y. Ke, A. P. Hill, *Physiol. Rev.* **2012**, *92*, 1393.
- [138] D. M. Roden, *J. Intern. Med.* **2006**, *259*, 59.
- [139] D. J. Leishman, M. M. Abernathy, E. B. Wang, *J. Pharmacol. Toxicol. Methods* **2020**, *105*, 106900.
- [140] J. P. Valentin, T. Hammond, *J. Pharmacol. Toxicol. Methods* **2008**, *58*, 77.
- [141] S. Nattel, L. Yue, Z. Wang, *Cell Physiol. Biochem.* **1999**, *9*, 217.
- [142] M. A. Vos, *J. Cardiovasc. Electrophysiol.* **2004**, *15*, 1451.
- [143] E. Glasscock, *Channels* **2019**, *13*, 299.
- [144] C. Fan, X. Yang, W. W. Wang, J. Wang, W. Li, M. Guo, S. Huang, Z. Wang, K. Liu, *Arterioscler. Thromb. Vasc. Biol.* **2020**, *40*, 2360.
- [145] G. Bhawe, D. Lonergan, B. A. Chauder, J. S. Denton, *Future Med. Chem.* **2010**, *2*, 757.
- [146] G. J. Gross, J. A. Auchampach, *Circ. Res.* **1992**, *70*, 223.
- [147] J. M. Quayle, M. T. Nelson, N. B. Standen, *Physiol. Rev.* **1997**, *77*, 1165.
- [148] O. Postea, M. Biel, *Nat. Rev. Drug Discov.* **2011**, *10*, 903.
- [149] H. Peter Larsson, *J. Gen. Physiol.* **2010**, *136*, 237.
- [150] F. Roubille, J. C. Tardif, *Circulation* **2013**, *127*, 1986.
- [151] M. Novella Romanelli, L. Sartiani, A. Masi, G. Mannaioni, D. Manetti, A. Mugelli, E. Cerbai, *Curr. Top. Med. Chem.* **2016**, *16*, 1764.
- [152] F. Y. Fisker, D. Grimm, M. Wehland, *Basic Clin. Pharmacol. Toxicol.* **2015**, *117*, 5.
- [153] J. Motiejunaite, L. Amar, E. Vidal-Petiot, *Ann. Endocrinol. (Paris)* **2021**, *82*, 193.
- [154] J. G. Baker, S. M. Gardiner, J. Woolard, C. Fromont, G. P. Jadhav, S. N. Mistry, K. S. J. Thompson, B. Kellam, S. J. Hill, P. M. Fischer, *FASEB. J.* **2017**, *31*, 3150.
- [155] J. Zhang, P. C. Simpson, B. C. Jensen, *Am. J. Physiol. Heart Circ. Physiol.* **2021**, *320*, H725.
- [156] J. Akinaga, J. A. García-Sáinz, A. S Pupo, *Br. J. Pharmacol.* **2019**, *176*, 2343.
- [157] P. R. Saxena, C. M. Villaló, *J. Cardiovasc. Pharmacol.* **1990**, *15*, S17.
- [158] H. C. Saternos, D. A. Almarghalani, H. M. Gibson, M. A. Meqdad, R. B. Antypas, A. Lingireddy, W. A. Aboualawi, *Physiol. Genomics* **2018**, *50*, 1.
- [159] R. Alves-Lopes, K. B. Neves, R. M. Touyz, *Can. J. Cardiol.* **2019**, *35*, 555.
- [160] M. K. Levay, K. A. Krobert, A. Vogt, A. Ahmad, A. Jungmann, C. Neuber, S. Pasch, A. Hansen, O. J. Müller, S. Lutz, T. Wieland, *Basic. Res. Cardiol.* **2022**, *117*, 8.
- [161] J. Neumann, B. Hofmann, S. Dhein, U. Gergs, *Int. J. Mol. Sci.* **2023**, *24*, 5042.
- [162] J. Neumann, U. Kirchhefer, S. Dhein, B. Hofmann, U. Gergs, *Front. Pharmacol.* **2021**, *12*, 732842.
- [163] S. Saheera, A. G. Potnuri, A. Guha, S. S. Palaniyandi, R. A. Thandavarayan, *Drug Discov. Today* **2022**, *27*, 234.
- [164] F. J. Munguia-Galaviz, A. G. Miranda-Diaz, M. A. Cardenas-Sosa, R. Echavarría, *Int. J. Mol. Sci.* **2023**, *24*, 1997.
- [165] R. Lewis, J. Li, P. J. McCormick, C. L-H Huang, K. Jeevaratnam, *Int. J. Cardiol. Heart Vasc.* **2020**, *26*, 100449.
- [166] F. Wiedemann, W. Kampe, M. Thiel, G. Sponer, E. Roesch, K. Dietmann, *US Patent 4503067*, **1985**.
- [167] W. M. Book, *Congest. Heart Failure* **2002**, *8*, 173.
- [168] G. V. Naccarelli, M. A. Lukas, *Clin. Cardiol.* **2005**, *28*, 165.
- [169] T. Morgan, *Clin. Pharmacokinet.* **1994**, *26*, 335.
- [170] J. Cheng, R. Niwa, K. Kamiya, J. Toyama, I. Kodama, *Eur. J. Pharmacol.* **1999**, *376*, 189.
- [171] N. Liu, R. Yu, Y. Ruan, Q. Zhou, J. Pu, Y. Li, *J. Huazhong. Univ. Sci. Technol. Med. Sci.* **2004**, *24*, 433.
- [172] T. Nakajima, J. Ma, H. Iida, K. Iwasawa, T. Jo, M. Omata, R. Nagai, *Jpn. Heart J.* **2003**, *44*, 963.
- [173] C. Deng, F. Rao, S. Wu, S. Kuang, X. Liu, Z. Zhou, Z. Shan, Q. Lin, W. Qian, M. Yang, Q. Geng, Y. Zhang, X. Yu, S. Lin, *Eur. J. Pharmacol.* **2009**, *621*, 19.
- [174] C. D. Smith, A. Wang, K. Vembaiyan, J. Zhang, C. Xie, Q. Zhou, G. Wu, S. R. W. Chen, T. G. Back, *J. Med. Chem.* **2013**, *56*, 8626.
- [175] J. R. Bankston, R. S. Kass, *J. Mol. Cell Cardiol.* **2010**, *48*, 246.
- [176] C.-Y. Deng, S.-G. Lin, M. Yang, W.-M. Qian, Y. Zhang, S.-L. Wu, *Chinese Pharmacol. Bull.* **2005**, *21*, 568.
- [177] K. Kawakami, T. Nagatomo, H. Abe, K. Kikuchi, H. Takemasa, B. D. Anson, B. P. Delisle, C. T. January, Y. Nakashima, *Br. J. Pharmacol.* **2006**, *147*, 642.
- [178] J. F. Yang, N. Cheng, S. Ren, X. M. Liu, X. T. Li, *Eur. J. Pharmacol.* **2018**, *834*, 206.

- [179] I. Jeong, B. H. Choi, S. H. Yoon, S. J. Hahn, *Biochem. Pharmacol.* **2012**, *83*, 497.
- [180] R. Zhang, L. J. Jie, W. Y. Wu, Z. Q. Wang, H. Y. Sun, G. S. Xiao, Y. Wang, Y. G. Li, G. R. Li, *Eur. J. Pharmacol.* **2019**, *853*, 74.
- [181] J. Kikuta, M. Ishii, K. Kishimoto, Y. Kurachi, *Eur. J. Pharmacol.* **2006**, *529*, 47.
- [182] T. Ferrer, D. Ponce-Balbuena, A. López-Izquierdo, I. A. Aréchiga-Figueroa, T. P. de Boer, M. A. G. van der Heyden, J. A. Sánchez-Chapula, *Eur. J. Pharmacol.* **2011**, *668*, 72.
- [183] K. Staudacher, I. Staudacher, E. Ficker, C. Seyler, J. Gierten, J. Kisselbach, A. K. Rahm, K. Trappe, P. Schweizer, R. Becker, H. Katus, D. Thomas, *Br. J. Pharmacol.* **2011**, *163*, 1099.
- [184] T. Cha, E. K. Choi, G.-I. Yu, B. J. Kim, D. H. Park, *Circulation* **2016**, *134*, 18272.
- [185] Y. Cao, S. Chen, Y. Liang, T. Wu, J. Pang, S. Liu, P. Zhou, *Br. J. Pharmacol.* **2018**, *175*, 3963.
- [186] C. Giannattasio, B. M. Cattaneo, G. Seravalle, S. Carugo, A. A. Mangoni, G. Grassi, A. Zanchetti, G. Mancina, *J. Cardiovasc. Pharmacol.* **1992**, *19*(Suppl 1), S18.
- [187] T. Koshimizu, *Cardiovasc. Res.* **2004**, *63*, 662.
- [188] G. Groszek, M. Bednarski, M. Dybała, B. Filipek, *Eur. J. Med. Chem.* **2009**, *44*, 809.
- [189] B. I. Gaiser, M. Danielsen, E. Marcher-Rørsted, K. Røpke Jørgensen, T. M. Wróbel, M. Frykman, H. Johansson, H. Bräuner-Osborne, D. E. Gloriam, J. M. Mathiesen, D. Sejer Pedersen, *J. Med. Chem.* **2019**, *62*, 7806.
- [190] P. Gaillard, P. A. Carrupt, B. Testa, P. Schambel, *J. Med. Chem.* **1996**, *39*, 126.
- [191] K. S. Murnane, O. F. Guner, J. P. Bowen, K. M. Rambacher, N. H. Moniri, T. J. Murphy, C. M. Daphney, A. Oppong-Damoah, K. C. Rice, *Pharmacol. Biochem. Behav.* **2019**, *181*, 37.
- [192] X. L. Xu, W. J. Zang, J. Lu, X. Q. Kang, M. Li, X. J. Yu, *Auton. Neurosci.* **2006**, *130*, 6.
- [193] P. G. Lysko, K. A. Lysko, C. L. Webb, G. Feuerstein, *Neurosci. Lett.* **1992**, *148*, 34.
- [194] P. J. Oliveira, D. J. Santos, A. J. M. Moreno, *Arch. Biochem. Biophys.* **2000**, *374*, 279.
- [195] P. J. Pauwels, W. Gommeren, G. Van Lommen, P. A. J. Janssen, J. E. Leysen, *Mol. Pharmacol.* **1988**, *34*, 843.
- [196] J. M. Vela, *Front. Pharmacol.* **2020**, *11*, 1716.
- [197] C. N. S. de Sousa, I. S. Medeiros, G. S. Vasconcelos, G. A. de Aquino, F. M. S. Cysne Filho, J. C. de Almeida Cysne, D. S. Macêdo, S. M. M. Vasconcelos, *Psychopharmacology* **2022**, *239*, 297.
- [198] C. Thollon, C. Cambarrat, J. Vian, J.-F. Prost, J. L. Peglion, J. P. Vilaine, *Br. J. Pharmacol.* **1994**, *112*, 37.
- [199] L. Simon, B. Ghaleh, L. Puybasset, J. F. Giudicelli, A. Berdeaux, *J. Pharmacol. Exp. Ther.* **1995**, *275*, 659.
- [200] S. M. Gardiner, P. A. Kemp, J. E. March, T. Bennett, *Br. J. Pharmacol.* **1995**, *115*, 579.
- [201] M. A. Psołka, J. R. Teerlink, *Circulation* **2016**, *133*, 2066.
- [202] P. Ponikowski, A. A. Voors, S. D. Anker, H. Bueno, J. G. F. Cleland, A. J. S. Coats, V. Falk, J. R. González-Juanatey, V.-P. Harjola, E. A. Jankowska, M. Jessup, C. Linde, P. Nihoyannopoulos, J. T. Parissis, B. Pieske, J. P. Riley, G. M. C. Rosano, L. M. Ruilope, F. Ruschitzka, F. H. Rutten, P. van der Meer, *Eur. J. Heart Fail.* **2016**, *18*, 891.
- [203] J. Jiang, L. Tian, Y. Huang, Y. Li, L. Xu, *Clin. Ther.* **2013**, *35*, 1933.
- [204] Accessdata.fda.gov. **2015**. Accessed May 2023. https://www.accessdata.fda.gov/drugsatfda_docs/nda/2015/206143Orig1s00OClinPharmR.pdf
- [205] Ema.europa.eu. **2005**. Accessed May 2023. https://www.ema.europa.eu/en/documents/scientific-discussion/procoralan-epar-scientific-discussion_en.pdf
- [206] P. Bois, J. Bescond, B. Renaudon, J. Lenfant, *Br. J. Pharmacol.* **1996**, *118*, 1051.
- [207] Accessdata.fda.gov. **2014**. https://www.accessdata.fda.gov/drugsatfda_docs/nda/2015/206143Orig1s00PharmR.pdf
- [208] R. I. R. Martin, O. Pogoryelova, M. S. Koref, J. P. Bourke, M. D. Teare, B. D. Keavney, *Heart* **2014**, *100*, 1506.
- [209] D. Melgari, K. E. Brack, C. Zhang, Y. Zhang, A. El Harchi, J. S. Mitcheson, C. E. Dempsey, G. André Ng, J. C. Hancox, *J. Am. Heart Assoc.* **2015**, *4*, e001813.
- [210] N. Haechl, J. Ebner, K. Hilber, H. Todt, X. Koenig, *Cell Physiol. Biochem.* **2019**, *53*, 36.
- [211] H. Bueno-Levy, D. Weisbrod, D. Yadin, S. Haron-Khun, A. Peretz, E. Hochhauser, M. Arad, B. Attali, *Front. Pharmacol.* **2020**, *10*, 1566.
- [212] I. Koncz, T. Szél, M. Bitay, E. Cerbai, K. Jaeger, F. Fülöp, N. Jost, L. Virág, P. Orvos, L. Tálosi, A. Kristóf, I. Baczkó, J. G. Papp, A. Varró, *Eur. J. Pharmacol.* **2011**, *668*, 419.
- [213] E. Delpón, C. Valenzuela, O. Pérez, L. Franqueza, P. Gay, D. J. Snyders, J. Tamargo, *Br. J. Pharmacol.* **1996**, *117*, 1293.
- [214] S. Tse, N. Mazzola, P & T: A *Peer Rev. J. Formul. Manag.* **2015**, *40*, 810.
- [215] C. Thollon, S. Bedut, N. Villeneuve, F. Cogé, L. Piffard, J.-P. Guillaumin, C. Brunel-Jacquemin, P. Chomarat, J.-A. Boutin, J.-L. Peglion, J.-P. Vilaine, *Br. J. Pharmacol.* **2007**, *150*, 37.
- [216] J. Tanguay, K. M. Callahan, N. D'Avanzo, *Sci. Rep.* **2019**, *9*, 465.
- [217] A. Bucchi, M. Baruscotti, M. Nardini, A. Barbuti, S. Micheloni, M. Bolognesi, D. DiFrancesco, *PLoS One* **2013**, *8*, e53132.
- [218] T. M. B. Cavalcante, J. M. A. De Melo, L. B. Lopes, M. C. Bessa, J. G. Santos, L. C. Vasconcelos, A. E. Vieira Neto, L. T. N. Borges, M. M. F. Fonteles, A. J. M. Chaves Filho, D. Macêdo, A. R. Campos, C. C. T. Aguiar, S. M. M. Vasconcelos, *Biomed. Pharmacother.* **2019**, *109*, 2499.
- [219] G. R. E. Van Lommen, M. F. L. De Bruyn, M. F. J. Schroven, *US Patent 4654362A*, **1984**.
- [220] K. Bylund, in *xPharm: The Comprehensive Pharmacology Reference* (Eds: S. J. Enna, D. B. Bylund), Elsevier **2007**, ch. "Nebivolol".
- [221] E. J. Toblli, F. Digennaro, F. J. Giani, P. F. Dominici, *Vasc. Health Risk. Manag.* **2012**, *8*, 151.
- [222] C. Briciu, M. Neag, D. Muntean, C. Bocsan, A. Buzoianu, O. Antonescu, A. M. Gheldiu, M. Achim, A. Popa, L. Vlase, *Clujul Med.* **2015**, *88*, 208.
- [223] C. Briciu, M. Neag, D. Muntean, L. Vlase, C. Bocsan, A. Buzoianu, A. M. Gheldiu, M. Achim, A. Popa, *J. Clin. Pharm. Ther.* **2014**, *39*, 535.
- [224] C. L. Chen, D. Desai-Krieger, S. Ortiz, M. Kerolous, H. M. Wright, P. Ghahramani, *Am. J. Ther.* **2015**, *22*, e130.
- [225] M. R. Bristow, *Circulation* **2000**, *101*, 558.
- [226] J. Fongemie, E. Felix-Getzlik, *Drugs* **2015**, *75*, 1349.
- [227] M. A. W. Broeders, P. A. Doevendans, B. C. A. M. Bekkers, R. Bronsaer, E. Van Gorsel, J. W. M. Heemskerck, M. G. A. Egbrink, E. Van Breda, R. S. Reneman, R. Van Der Zee, *Circulation* **2000**, *102*, 677.
- [228] W. Gosgnach, C. Boixel, N. Névo, T. Poiraud, J. B. Michel, *J. Cardiovasc. Pharmacol.* **2001**, *38*, 191.
- [229] E. P. Frazier, M. B. Michel-Reher, P. Van Loenen, C. Sand, T. Schneider, S. L. M. Peters, M. C. Michel, *Eur. J. Pharmacol.* **2011**, *654*, 86.
- [230] A. Maffei, G. Lembo, *Therap. Adv. Cardiovasc. Dis.* **2009**, *3*, 317.
- [231] T. Gori, T. Münzel, *J. Am. Coll. Cardiol.* **2009**, *54*, 1491.
- [232] T. O. Bueno-Pereira, P. R. Nunes, M. B. Matheus, A. L. Vieira da Rocha, V. C. Sandrim, *Cells* **2022**, *11*, 883.
- [233] H. Cohen Arazi, M. Gonzalez, *Vasc. Dis. Ther.* **2017**, *2*, 2. <https://doi.org/10.15761/vdt.1000138>
- [234] B. Rozec, T. T. Quang, J. Noireaud, C. Gauthier, *Br. J. Pharmacol.* **2006**, *147*, 699.

- [235] Z. Tan, Z. Xiao, J. Wei, J. Zhang, Q. Zhou, C. D. Smith, A. Nani, G. Wu, L. S. Song, T. G. Back, M. Fill, S. R. W. Chen, *Biochem. J.* **2016**, 473, 4159.
- [236] L. J. Ignarro, *Cardiovasc. Ther.* **2008**, 26, 115.
- [237] G. R. Mirams, M. R. Davies, S. J. Brough, M. H. Bridgland-Taylor, Y. Cui, D. J. Gavaghan, N. Abi-Gerges, *J. Pharmacol. Toxicol. Methods* **2014**, 70, 246.
- [238] G. Gintant, *Pharmacol. Ther.* **2011**, 129, 109.
- [239] H. O. Altunkaynak-Camca, *Middle Black Sea J. Health Sci.* **2020**, 6, 201.
- [240] A. F. Kluge, R. D. Clark, A. M. Strosberg, J.-C. G. Pascal, R. Whiting, *US Patent 4567264*, **1986**.
- [241] G. Cocco, M. F. Rousseau, T. Bouvy, P. Cheron, G. Williams, J. M. Detry, H. Pouleur, G. Cocco, M. F. Rousseau, T. Bouvy, P. Cheron, G. Williams, J. M. Detry, H. Pouleur, *J. Cardiovasc. Pharmacol.* **1992**, 20, 131.
- [242] M. Reed, C. C. Kerndt, S. Gopal, D. Nicolas, *StatPearls [Internet]*, StatPearls Publishing, **2021**.
- [243] G. Bazoukis, G. Tse, K. P. Letsas, C. Thomopoulos, K. K. Naka, P. Korantzopoulos, X. Bazoukis, P. Michelongona, S. S. Papadatos, K. Vlachos, T. Liu, M. Efremidis, A. Baranchuk, S. Stavrakis, C. Tsioufis, *J. Arrhythm.* **2018**, 34, 124.
- [244] E. Rayner-Hartley, T. Sedlak, *J. Am. Heart Assoc.* **2015**, 5, e003196.
- [245] A. Mezincescu, V. J. Karthikeyan, S. K. Nadar, *Sultan Qaboos Univ. Med. J.* **2018**, 18, 13.
- [246] C. Antzelevitch, L. Belardinelli, A. C. Zygmunt, A. Burashnikov, M. Di Diego, J. M. Fish, J. M. Cordeiro, G. Thomas, *Circulation* **2004**, 110, 904.
- [247] B. K. Corkey, E. Elzein, R. H. Jiang, R. V. Kalla, D. Koltun, X. Li, R. Martinez, E. Q. Parkhill, T. Perry, J. Zablocki, C. Venkataramani, M. Graupe, J. Guerrero, *Fused Heterocyc. Comp. Ion Channel Modulat.* **2013**.
- [248] T. Gupta, S. Khera, D. Kolte, W. S. Aronow, S. Iwai, *Int. J. Cardiol.* **2015**, 187, 66.
- [249] A. C. Zygmunt, V. V. Nesterenko, S. Rajamani, D. Hu, H. Barajas-Martinez, L. Belardinelli, C. Antzelevitch, *Am. J. Physiol. Heart Circ. Physiol.* **2011**, 301, H1606.
- [250] B. S. Chen, Y. C. Lo, H. Peng, T. I. Hsu, S. N. Wu, *J. Pharmacol. Sci.* **2009**, 110, 295.
- [251] K. M. Kahlig, I. Lepist, K. Leung, S. Rajamani, A. L. George, *Br. J. Pharmacol.* **2010**, 161, 1414.
- [252] C. Peters, S. Sokolov, S. Rajamani, P. Ruben, *Br. J. Pharmacol.* **2013**, 169, 704.
- [253] G. K. Wang, J. Calderon, S. Y. Wang, *Mol. Pharmacol.* **2008**, 73, 940.
- [254] N. El-Bizri, K. M. Kahlig, J. C. Shyrock, A. L. George, Jr., L. Belardinelli, S. Rajamani, *Channels* **2011**, 5, 161.
- [255] S. Lorusso, D. Kline, A. Bartlett, M. Freimer, J. Agriesti, A. A. Hawash, M. M. Rich, J. T. Kissel, W. David Arnold, *Muscle Nerve* **2019**, 59, 240.
- [256] S. Rajamani, J. C. Shyrock, L. Belardinelli, *Channels* **2008**, 2, 449.
- [257] H. J. Gould, C. Garrett, R. R. Donahue, D. Paul, I. Diamond, B. K. Taylor, *Behav. Pharmacol.* **2009**, 20, 755.
- [258] M. Estacion, S. G. Waxman, S. D. Dib-Hajj, *Mol. Pain* **2010**, 6, 1744-8069-6-35.
- [259] C. Du, Y. Zhang, A. El Harchi, C. E. Dempsey, J. C. Hancox, *J. Mol. Cell Cardiol.* **2014**, 74, 220.
- [260] M. Saad, A. Mahmoud, I. Y. Elgendy, C. Richard Conti, *Clin. Cardiol.* **2016**, 39, 170.
- [261] H. J. Kim, H. S. Ahn, J. S. Choi, B. H. Choi, S. J. Hahn, *J. Pharmacol. Exp. Ther.* **2011**, 339, 952.
- [262] A. Ratte, F. Wiedmann, M. Kraft, H. A. Katus, C. Schmidt, *Front. Pharmacol.* **2019**, 10, 1367.
- [263] S. Sicouri, K. W. Timothy, A. C. Zygmunt, A. Glass, R. J. Goodrow, L. Belardinelli, C. Antzelevitch, *Heart Rhythm* **2007**, 4, 638.
- [264] A. Parikh, R. Mantravadi, D. Kozhevnikov, M. A. Roche, Y. Ye, L. J. Owen, J. L. Puglisi, J. J. Abramson, G. Salama, *Heart Rhythm* **2012**, 9, 953.
- [265] A. Virsolvy, C. Farah, N. Pertuit, L. Kong, A. Lacampagne, C. Reboul, F. Aimond, S. Richard, *Sci. Rep.* **2015**, 5, 17969.
- [266] G. Zhao, E. Walsh, J. C. Shryock, E. Messina, Y. Wu, D. Zeng, X. Xu, M. Ochoa, S. P. Baker, T. H. Hintze, L. Belardinelli, *J. Cardiovasc. Pharmacol.* **2011**, 57, 639.
- [267] Accessdata.fda.gov. **2006**. Accessed May 2023. https://www.accessdata.fda.gov/drugsatfda_docs/nda/2006/021526_s000_Ranexa_Pharmr.pdf
- [268] R. Létienne, B. Vié, A. Puech, S. Vieu, B. Le Grand, G. W. John, *Naunyn-Schmiedeberg's Arch. Pharmacol.* **2001**, 363, 464.
- [269] F. Flenner, F. W. Friedrich, N. Ungeheuer, T. Christ, B. Geertz, S. Reischmann, S. Wagner, K. Stathopoulou, K. D. Söhren, F. Weinberger, E. Schwedhelm, F. Cuello, L. S. Maier, T. Eschenhagen, L. Carrier, *Cardiovasc. Res.* **2016**, 109, 90.
- [270] N. Fillmore, G. D. Lopaschuk, *Biochim. Biophys. Acta Mol. Cell Res.* **2013**, 1833, 857.
- [271] M. S. Mito, J. Constantin, C. V. De Castro, N. S. Yamamoto, A. Bracht, *Mol. Cell Biochem.* **2010**, 345, 35.
- [272] H. Tolunay, *Clin. Ther.* **2020**, 42, 374.
- [273] M. K. Davies, *Heart* **2002**, 88, 3-a.
- [274] M. J. Eisenberg, A. Brox, A. N. Bestawros, *Am. J. Med.* **2004**, 116, 35.
- [275] S. Fahie, M. Cassagnol, *StatPearls [Internet]*, StatPearls Publishing, **2021**.
- [276] W. Sawicki, *Eur. J. Pharm. Biopharm.* **2002**, 53, 29.
- [277] S. R. Hamann, R. A. Blouin, R. G. McAllister, *Clin. Pharmacokinet.* **1984**, 9, 26.
- [278] K. Hla, J. Henry, A. Latham, *Br. J. Clin. Pharmacol.* **1987**, 24, 661.
- [279] D. L. Keefe, Y. G. Yee, R. E. Kates, *Clin. Pharmacol. Ther.* **1981**, 29, 21.
- [280] N. Morel, V. Buryi, O. Feron, J. P. Gomez, M. O. Christen, T. Godfraind, *Br. J. Pharmacol.* **1998**, 125, 1005.
- [281] G. R. Mirams, Y. Cui, A. Sher, M. Fink, J. Cooper, B. M. Heath, N. C. McMahon, D. J. Gavaghan, D. Noble, *Cardiovasc. Res.* **2011**, 91, 53.
- [282] J. Kurokawa, S. Adachi-Akahane, T. Nagao, *Eur. J. Pharmacol.* **1997**, 325, 229.
- [283] S. Matsuoka, T. Nawada, I. Hisatome, J. Miyamoto, J. Hasegawa, H. Kotake, H. Mashiba, *General Pharm. Vasc. Syst.* **1991**, 22, 87.
- [284] B. Balasubramanian, J. P. Imredy, D. Kim, J. Penniman, A. Lagrutta, J. J. Salata, *J. Pharmacol. Toxicol. Methods* **2009**, 59, 62.
- [285] A. A. Fossa, T. Wisialowski, E. Wolfgang, E. Wang, M. Avery, D. L. Raunig, B. Fermini, *Eur. J. Pharmacol.* **2004**, 486, 209.
- [286] P. Champeroux, A. Ouillé, E. Martel, J. S. L. Fowler, A. Maurin, S. Richard, J. Y. Le Guennec, *J. Pharmacol. Toxicol. Methods* **2011**, 63, 269.
- [287] S. Dei, M. N. Romanelli, S. Scapecchi, E. Teodori, F. Gualtieri, A. Chiarini, W. Voigt, H. Lemoine, *J. Med. Chem.* **1993**, 36, 439.
- [288] B. Wiśniowska, A. Mendyk, K. Fijorek, A. Glinka, S. Polak, *J. Appl. Toxicol.* **2012**, 32, 858.
- [289] B. Fermini, D. S. Ramirez, S. Sun, A. Bassyouni, M. Hemkens, T. Wisialowski, S. Jenkinson, *J. Pharmacol. Toxicol. Methods* **2017**, 84, 86.
- [290] B. N. Singh, G. Ellrodt, C. T. Peter, *Drugs* **1978**, 15, 169.
- [291] A. Dhainaut, G. Regnier, A. Tizot, A. Pierre, S. Leonce, N. Guilbaud, L. Kraus-Berthier, G. Atassi, *J. Med. Chem.* **1996**, 39, 4099.
- [292] B. Tarabova, L. Lacinova, J. Engel, *Eur. J. Pharmacol.* **2007**, 573, 39.
- [293] P. Bergson, G. Lipkind, S. P. Lee, M. E. Duban, D. A. Hanck, *Mol. Pharmacol.* **2011**, 79, 411.
- [294] T. Kuga, J. Sadoshima, H. Tomoike, H. Kanaide, N. Akaike, M. Nakamura, *Circ. Res.* **1990**, 67, 469.

- [295] C. Arnoult, M. Villaz, H. M. Florman, *Mol. Pharmacol.* **1998**, *53*, 1104.
- [296] E. Perez-Reyes, A. L. Van Deusen, I. Vitko, *J. Pharmacol. Exp. Ther.* **2009**, *328*, 621.
- [297] Y. A. Kuryshv, A. M. Brown, E. Duzic, G. E. Kirsch, *Assay Drug Dev. Technol.* **2014**, *12*, 110.
- [298] D. Dobrev, A. S. Milde, K. Andreas, U. Ravens, *Br. J. Pharmacol.* **1999**, *127*, 576.
- [299] P. Tfelt-Hansen, J. Tfelt-Hansen, *Headache J. Head Face Pain* **2009**, *49*, 117.
- [300] H. Ishibashi, A. Yatani, N. Akaike, *Brain Res.* **1995**, *695*, 88.
- [301] J. Kramer, C. A. Obejero-Paz, G. Myatt, Y. A. Kuryshv, A. Bruening-Wright, J. S. Verducci, A. M. Brown, *Sci. Rep.* **2013**, *3*, 2100.
- [302] S. Roger, J. Y. L. Guennec, P. Besson, *Br. J. Pharmacol.* **2004**, *141*, 610.
- [303] M. Wu, P. N. Tran, J. Sheng, A. L. Randolph, W. W. Wu, *J. Pharmacol. Toxicol. Methods* **2019**, *100*, 106605.
- [304] S. Zhang, Z. Zhou, Q. Gong, J. C. Makielski, C. T. January, *Circ. Res.* **1999**, *84*, 989.
- [305] C. G. Milross, K. A. Mason, N. R. Hunter, W. K. Chung, L. J. Peters, L. Milas, *J. Natl. Cancer Inst.* **1996**, *88*, 1308.
- [306] G. Ermondi, S. Visentin, G. Caron, *Eur. J. Med. Chem.* **2009**, *44*, 1926.
- [307] R. Rajamani, B. A. Tounge, J. Li, C. H. Reynolds, *Bioorg. Med. Chem. Lett.* **2005**, *15*, 1737.
- [308] A. Cavalli, E. Poluzzi, F. De Ponti, M. Recanatini, *J. Med. Chem.* **2002**, *45*, 3844.
- [309] R. A. Pearlstein, R. J. Vaz, J. Kang, X. L. Chen, M. Preobrazhenskaya, A. E. Shchekotikhin, A. M. Korolev, L. N. Lysenkova, O. V. Miroshnikova, J. Hendrix, D. Rampe, *Bioorg. Med. Chem. Lett.* **2003**, *13*, 1829.
- [310] G. M. Keserü, *Bioorg. Med. Chem. Lett.* **2003**, *13*, 2773.
- [311] L. Jia, H. Sun, *Bioorg. Med. Chem.* **2008**, *16*, 6252.
- [312] S. Waldegger, G. Niemeyer, K. Mörike, C. A. Wagner, H. Suessbrich, A. E. Busch, F. Lang, M. Eichelbaum, *Cell Physiol. Biochem.* **1999**, *9*, 81.
- [313] W. G. Ding, A. Tano, X. Mi, A. Kojima, T. Seto, H. Matsuura, *Cell Physiol. Biochem.* **2019**, *52*, 302.
- [314] M. Madeja, V. Müller, U. Mußhoff, E. J. Speckmann, *Neuropharmacology* **2000**, *39*, 202.
- [315] W. Nguyen, B. L. Howard, D. P. Jenkins, H. Wulff, P. E. Thompson, D. T. Manallack, *Bioorg. Med. Chem. Lett.* **2012**, *22*, 7106.
- [316] A. K. Diesch, S. Grissmer, *Cell Physiol. Biochem.* **2017**, *44*, 172.
- [317] R. J. Robe, S. Grissmer, *Br. J. Pharmacol.* **2000**, *131*, 1275.
- [318] H. Rauer, S. Grissmer, *Br. J. Pharmacol.* **1999**, *127*, 1065.
- [319] L. Xu, C. Huang, J. Chen, X. Jiang, X. Li, G. C. Bett, R. L. Rasmusson, S. Wang, *Pharmazie* **2008**, *63*, 475.
- [320] H. Chen, D. Zhang, J. Hua Ren, S. Ping Chao, *Iran. J. Pharm. Res.* **2013**, *12*, 855.
- [321] T. Ninomiya, M. Takano, T. Haruna, Y. Kono, M. Horie, *J. Cardiovasc. Pharmacol.* **2003**, *42*, 161.
- [322] H. J. Motulsky, M. D. Snavely, R. J. Hughes, P. A. Insel, *Circ. Res.* **1983**, *52*, 226.
- [323] D. Staneva-Stoytcheva, N. Dantchev, P. Popov, *General Pharmacol. Vasc. Syst.* **1992**, *23*, 61.
- [324] M. Galinier, J. M. Senard, P. Valet, B. Boneu, F. Galinier, J. L. Montastruc, *Arch. Int. Pharmacodyn. Ther.* **1989**, *301*, 30.
- [325] DrugMatrix/ToxFX, **2023**. <https://ntp.niehs.nih.gov/data/drugmatrix/>
- [326] K. Shibata, A. Hirasawa, R. Foglar, S. Ogawa, G. Tsujimoto, *Circulation* **1998**, *97*, 1227.
- [327] R. D. Feldman, G. D. Park, C. Y. Lai, *Circulation* **1985**, *72*, 547.
- [328] B. Xu, S. L. Zhang, R. X. Chen, *Zhongguo yao li xue bao Acta Pharmacol. Sin.* **1998**, *19*, 148.
- [329] D. Staneva-Stoytcheva, J. Popova, V. Mutafova-Yambolieva, P. Alov, *General Pharmacol. Vasc. Syst.* **1990**, *21*, 149.
- [330] M. D. Drici, Y. Jacomet, P. Iacono, P. Lapalus, *Int. J. Clin. Pharmacol. Ther. Toxicol.* **1993**, *31*, 27.
- [331] H. Affolter, W. P. Burkard, A. Pletscher, *Eur. J. Pharmacol.* **1985**, *108*, 157.
- [332] J. E. Taylor, F. V. Defeudis, *Eur. J. Pharmacol.* **1984**, *106*, 215.
- [333] H. Adachi, T. Shoji, *Jpn. J. Pharmacol.* **1986**, *41*, 431.
- [334] M. Goppelt-Struebe, M. Stroebel, *Naunyn-Schmiedeberg's Arch. Pharmacol.* **1997**, *356*, 240.
- [335] E. O. Okoro, *J. Pharm. Pharmacol.* **2010**, *51*, 953.
- [336] E. Glusa, J. Bevan, S. Heptinstall, *Thromb. Res.* **1989**, *55*, 239.
- [337] J. Popova, D. Staneva-Stoytcheva, E. Ivanova, T. Tosheva, *Gen. Pharmacol. Vasc. Syst.* **1991**, *22*, 1147.
- [338] A. Tamura, T. Ogura, H. Uemura, Y. Reien, T. Kishimoto, T. Nagai, I. Komuro, M. Miyazaki, H. Nakaya, *J. Pharmacol. Sci.* **2009**, *110*, 150.
- [339] J. S. Karliner, H. J. Motulsky, J. Dunlap, J. H. Brown, P. A. Insel, *J. Cardiovasc. Pharmacol.* **1982**, *4*, 515.
- [340] S. Katayama, S. Kito, R. Miyoshi, H. Matsubayashi, *Brain Res.* **1987**, *422*, 168.
- [341] M. Sitges, A. Reyes, *J. Neurosci. Res.* **1995**, *40*, 613.
- [342] D. Staneva-Stoytcheva, N. Danchev, P. Popov, *Gen. Pharmacol. Vasc. Syst.* **1991**, *22*, 1151.
- [343] C. Almansa, J. M. Vela, *Future Med. Chem.* **2014**, *6*, 1179.
- [344] P. Orvos, Z. Kohajda, J. Szlovák, P. Gazdag, T. Árpádfy-Lovas, D. Tóth, A. Geramipour, L. Tálosi, N. Jost, A. Varró, L. Virág, *Toxicol. Sci.* **2019**, *168*, 365.
- [345] L. Johannesen, J. Vicente, J. W. Mason, C. Sanabria, K. Waite-Labott, M. Hong, P. Guo, J. Lin, J. S. Sørensen, L. Galeotti, J. Florian, M. Ugander, N. Stockbridge, D. G. Strauss, *Clin. Pharm. Ther.* **2014**, *96*, 549.

How to cite this article: G. V. Mokrov, *Arch. Pharm.* **2023**, e2300196. <https://doi.org/10.1002/ardp.202300196>